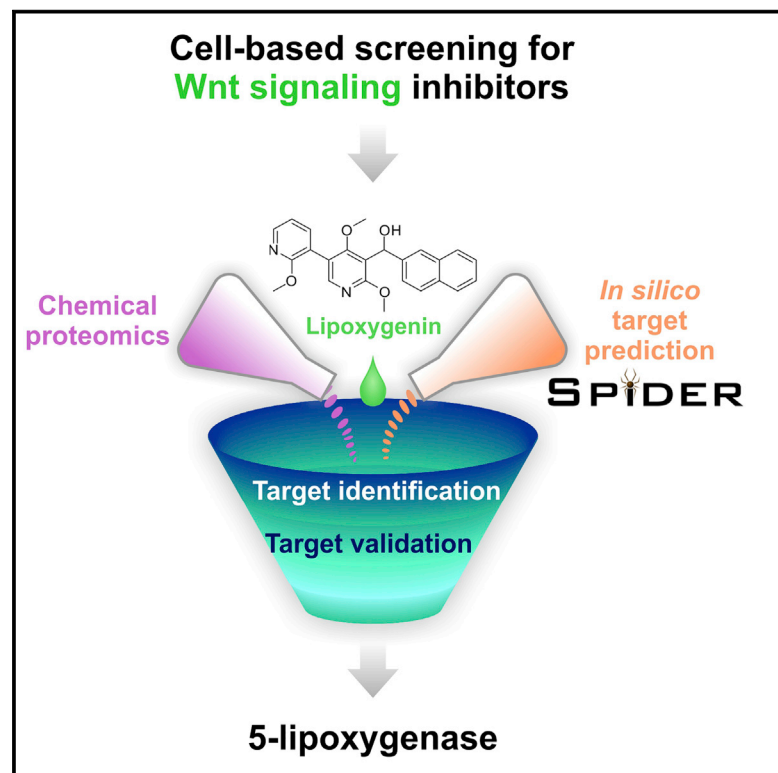


Cell Chemical Biology

Combined Proteomic and *In Silico* Target Identification Reveal a Role for 5-Lipoxygenase in Developmental Signaling Pathways

Graphical Abstract



Authors

Silke Brand, Sayantani Roy, Peter Schröder, ..., Kamal Kumar, Slava Ziegler, Herbert Waldmann

Correspondence

herbert.waldmann@mpi-dortmund.mpg.de

In Brief

Using cell-based screening, Brand et al. identified 3,5-substituted-2,4-dimethoxypyridines as inhibitors of Wnt signaling. Combination of chemical proteomics and computational target prediction followed by target validation revealed 5-lipoxygenase as the target.

Highlights

- The 3,5-substituted-2,4-dimethoxypyridine Lipoxygenin inhibits Wnt signaling
- Chemical proteomics and *in silico* prediction identified 5-lipoxygenase as target
- Lipoxygenin is a non-redox type inhibitor of 5-lipoxygenase
- Inhibition of 5-LO impairs also Hedgehog, TGF- β , Activin A, and BMP signaling

Combined Proteomic and *In Silico* Target Identification Reveal a Role for 5-Lipoxygenase in Developmental Signaling Pathways

Silke Brand,^{1,2,12} Sayantani Roy,^{1,8,12} Peter Schröder,^{1,2,9,12} Bernd Rathmer,² Jessica Roos,³ Shobhna Kapoor,^{1,10} Sumersing Patil,¹ Claudia Pommerenke,⁴ Thorsten Maier,^{5,6} Petra Janning,¹ Sonja Eberth,⁴ Dieter Steinhilber,³ Dennis Schade,^{2,11} Gisbert Schneider,⁷ Kamal Kumar,¹ Slava Ziegler,¹ and Herbert Waldmann^{1,2,12,13,*}

¹Max Planck Institut für Molekulare Physiologie, Otto-Hahn-Strasse 11, Dortmund 44227, Germany

²Technische Universität Dortmund, Fakultät für Chemie und Chemische Biologie, Otto-Hahn-Strasse 6, Dortmund 44227, Germany

³Goethe Universität, Institut für Pharmazeutische Chemie, Max-von-Laue-Strasse 9, Frankfurt am Main 60438, Germany

⁴Leibniz-Institut DSMZ-Deutsche Sammlung von Mikroorganismen und Zellkulturen GmbH, Inhoffenstraße 7B, Braunschweig 38124, Germany

⁵Department for Anesthesiology, Intensive Care Medicine and Pain Therapy, University Hospital Frankfurt, Theodor-Stern-Kai 7, Frankfurt 60590, Germany

⁶Aarhus University, Department of Biomedicine, Bartholins Allé 6, Aarhus C 8000, Denmark

⁷ETH Zürich, Institut für Pharmazeutische Wissenschaften, Vladimir-Prelog-Weg 1-5/10, Zürich CH-8093, Switzerland

⁸Present address: School of Bioscience, Sir J. C. Bose Laboratory Complex, Indian Institute of Technology Kharagpur, Kharagpur 721302, India

⁹Present address: Lead Discovery Center of the Max Planck Gesellschaft, Otto-Hahn-Strasse 15, Dortmund 44227, Germany

¹⁰Present address: Department of Chemistry, Indian Institute of Technology Bombay, Powai, Mumbai, Maharashtra 400076, India

¹¹Present address: Ernst-Moritz-Arndt-Universität Greifswald, Institut für Pharmazie, Abteilung Pharmazeutische/Medizinische Chemie, Felix-Hausdorff-Strasse 1, Greifswald 17489, Germany

¹²These authors contributed equally

¹³Lead Contact

*Correspondence: herbert.waldmann@mpi-dortmund.mpg.de

<https://doi.org/10.1016/j.chembiol.2018.05.016>

SUMMARY

Identification and validation of the targets of bioactive small molecules identified in cell-based screening is challenging and often meets with failure, calling for the development of new methodology. We demonstrate that a combination of chemical proteomics with *in silico* target prediction employing the SPiDER method may provide efficient guidance for target candidate selection and prioritization for experimental in-depth evaluation. We identify 5-lipoxygenase (5-LO) as the target of the Wnt pathway inhibitor Lipoxygenin. Lipoxygenin is a non-redox 5-LO inhibitor, modulates the β -catenin-5-LO complex and induces reduction of both β -catenin and 5-LO levels in the nucleus. Lipoxygenin and the structurally unrelated 5-LO inhibitor CJ-13,610 promote cardiac differentiation of human induced pluripotent stem cells and inhibit Hedgehog, TGF- β , BMP, and Activin A signaling, suggesting an unexpected and yet unknown role of 5-LO in these developmental pathways.

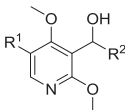
INTRODUCTION

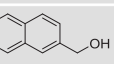
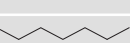
Cell-based screening for modulators of disease-relevant signaling pathways is a powerful strategy to identify novel agents and

targets for chemical biology and drug discovery research. Since, in general, an observed phenotype cannot be directly linked to a biological target, the molecular targets and mode of action of active small molecules are typically characterized *post hoc*. The probably most powerful and widely applied approach to identify cellular targets of small molecules is chemical proteomics (Kapoor et al., 2016; Ziegler et al., 2013), i.e., the affinity-based enrichment of proteins that subsequently needs to be assessed by means of a variety of techniques (Kapoor et al., 2016; Ziegler et al., 2013; Niphakis and Cravatt, 2014; Rix and Superti-Furga, 2009). Despite the proven validity and power of this approach, not infrequently it fails to yield targets that can be validated. In addition, affinity isolation usually yields several target candidates, and prioritization for validation is not obvious, leading to devalidation of false-positive targets in a time-, cost-, and labor-intensive process before the true target is identified. Thus, there is a major need for new approaches that can improve and accelerate target identification and validation and that enable efficient bridging of the chemotype-phenotype-target gap. To this end, efficient guidance for subsequent experimental validation could be provided if the target(s) could be predicted or at least narrowed down, and, accordingly, several cheminformatics approaches have been developed that meet this demand (Keiser et al., 2009; Reker et al., 2014a, 2014b). Here we demonstrate that the combination of chemical proteomics and cheminformatics may efficiently be applied to focus experimental validation on the most likely target(s) and, thereby accelerate or even enable target identification for phenotypic screening hits.

Wnt signaling influences cell proliferation, cell fate specification, and differentiation during embryonic development (Logan

Table 1. SAR Exploration for the R¹ and R² Substituents



Entry	Compound	R ¹	R ²	IC ₅₀ (μM)
1.	1a			2.0 ± 0.6
2.	1b			2.5 ± 0.1
3.	1c			7.3 ± 3.8
4.	1d			3.7 ± 0.2
5.	1e			3.0 ± 0.8
6.	1f			6.0 ± 2.3
7.	1g			11.6 ± 4.2
8.	1h			12.3 ± 5.2
9.	1i			19.3 ± 3.5
10.	1j			9.8 ± 3.2
11.	1k	Br-		inactive
12.	1l			3.8 ± 1.1
13.	1m			5.3 ± 1.1
14.	1n			7.4 ± 0.6
15.	1o			12.5 ± 2.7
16.	1p			21.6 ± 2.3
17.	1q			8.7 ± 0.3
18.	1r			9.8 ± 3.7

Wnt reporter gene assay. Data are mean values ± SD (n = 3).

and Nusse, 2004). Canonical Wnt signaling regulates the stability of β-catenin which, in the absence of the Wnt ligand, is constantly phosphorylated and targeted for proteasomal degradation. Binding of the Wnt ligand to Frizzled and the low-density lipoprotein receptor-related protein initiates a cascade of events that prevents the proteolytic degradation of β-catenin and culminates in the expression of Wnt target genes (Logan and Nusse, 2004). Aberrant Wnt signaling is linked to type II diabetes, neuronal and cardiovascular diseases, and to cancer development (Moon et al., 2004), in particular colorectal and liver cancers and medulloblastoma (Anastas and Moon, 2013). Several drug candidates targeting Wnt signaling are in clinical trials, but a drug for clinical use has not been approved so far (Kahn, 2014). Therefore, novel agents that inhibit Wnt signaling are in high demand. Here we describe the cell-based target-agnostic identification of the Wnt pathway inhibitor Lipoxygenin, and the identification of its target and mode of action by combination of chemical proteomics and *in silico* target prediction. Lipoxygenin inhibits arachidonate 5-lipoxygenase (5-LO), and its mode of action provides evidence for an interconnection between 5-LO and several developmental pathways, in particular Wnt signaling.

RESULTS

Identification and Characterization of Dimethoxy pyridines as Wnt Signaling Inhibitors

To identify Wnt signaling inhibitors, we screened a library of more than 10,000 compounds for modulation of Wnt-3a-induced reporter gene expression in HEK293-Fz cells using the TOPFlash promoter (Park et al., 2006). Several dimethoxy pyridines were identified as hits that inhibited the expression of the firefly luciferase, while cell viability was not compromised and gene transcription or protein translation were unaffected. For exploration of the structure-activity relationship of the hit class the Wnt reporter gene assay was employed (Lanier et al., 2012). Compounds **1a-b** with an *m,p*-dihydroxyphenyl and *p*-hydroxyphenyl substitutions on the left and 2-naphthyl on the right of the dimethoxy pyridine core inhibited the Wnt-3a-responsive reporter gene expression at low micromolar concentration (entries 1–2, Table 1). An *m*-hydroxyphenyl decoration, however, reduced the potency by half (entry 3). Compound **1d** embodying a 2-methoxyphenyl and a naphthyl ring inhibited the Wnt-3a-responsive reporter gene expression with a half-maximal inhibitory concentration (IC₅₀) of 3.7 ± 0.2 μM (Figures 1A and 1B). Compound **1e** with a 2-methoxyphenyl substitution maintained the activity as that of **1d** (entry 5). While keeping the naphthyl moiety intact on the right side of the core, introduction of dimethoxy pyridine as well as other electron-poor aromatics (entries 6–10) significantly reduced the Wnt inhibitory activity of the compounds. Pyrazol, as smaller heterocycle, offered only mild activity (entry 10). In the absence of an aryl ring as R¹ on to the core (entry 11), no Wnt inhibition was observed.

Further variations on the right side of the dimethoxy pyridine core were planned with a 2-methoxyphenyl as R¹ substitution and preference of having additional nitrogen atom in the compounds. While **1l** with a hydroxymethyl substituted naphthyl ring was as active as **1d**, replacing the naphthyl ring with substituted phenyl and quinolines offered only mild to weak

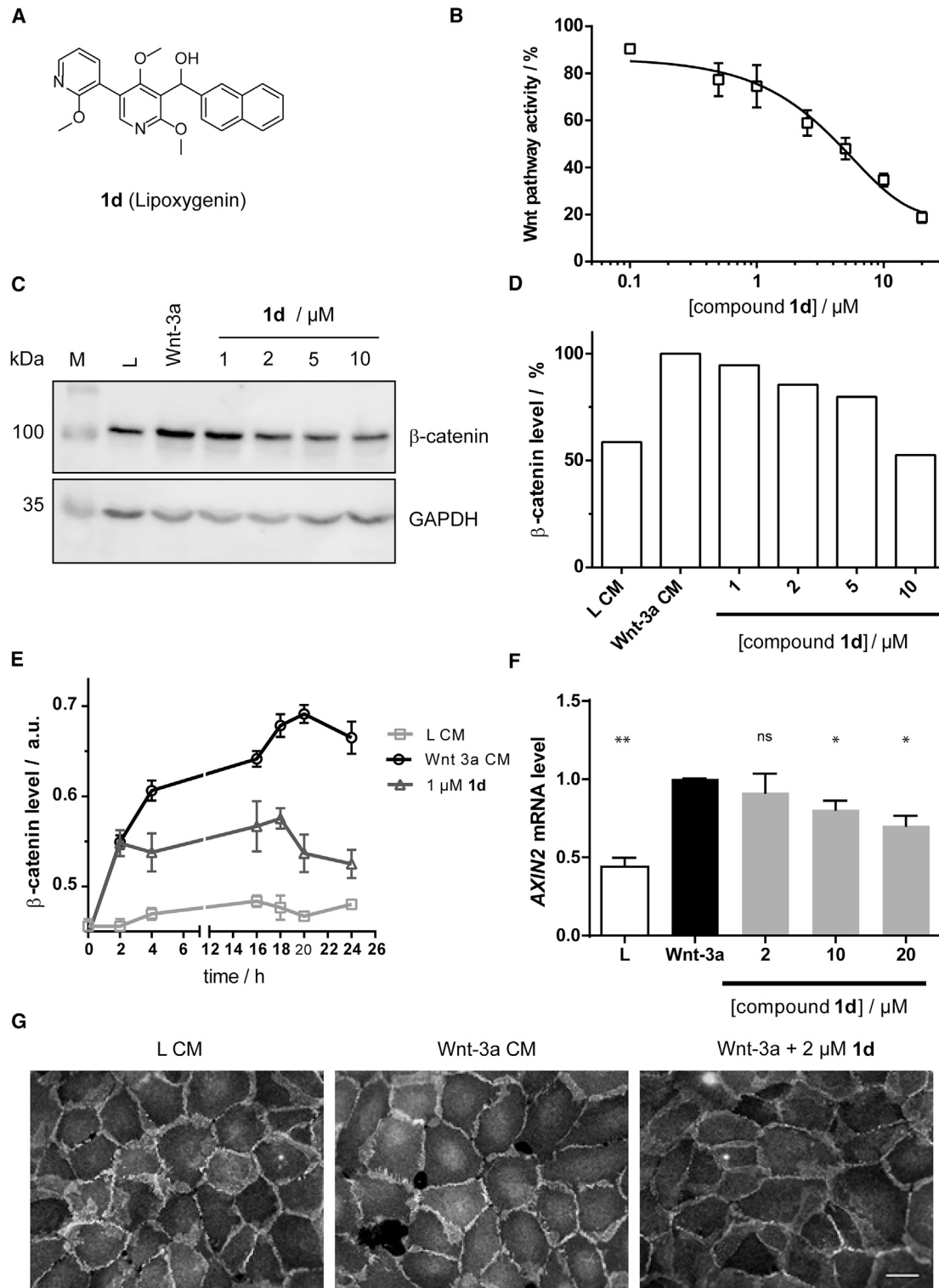


Figure 1. Dimethoxypyridines Inhibit Wnt Signaling

(A) Chemical structure of dimethoxypyridine **1d**.

(B) Compound **1d** inhibits the Wnt-responsive SUPER TOPFlash (STF) promoter in HEK293T cells. Cells were transiently transfected with the STF reporter plasmid and Wnt-3a expression plasmid prior to incubation with the compound for 22 hr. Data are mean values \pm SD (N = 4) and are representative of four biological replicates.

(legend continued on next page)

inhibitors, respectively (entries 13–16). Also, incorporation of cyclic and acyclic alkanes as R² negatively affected the compounds' inhibitory activity (entries 17–18, [Table 1](#)).

Replacement of the hydroxymethyl bridge between the substituted dimethoxypyridine and the naphthyl parts by a ketone yielded ca. 2-fold less active compounds (**1d/2a** and **1a/2b**; [Table S1](#)), indicating that an OH-group is beneficial, probably through interaction with the target through an H-bond. The absolute configuration of the stereocenter modulates inhibitory activity; however, only to a minor extent, with a preference for the (+)-enantiomer (1.8-fold, $p < 0.01$, [Table S1](#)).

Based on these data we selected (*rac*)-**1d** for further biological investigation since the pyridine ring is beneficial for solubility and since the potency of the structurally closely related compounds is comparable.

To explore whether compound **1d** is active upstream or downstream of the destruction complex, we analyzed the cellular levels of total β -catenin. Compound **1d** decreased the levels of β -catenin in HEK293 cells upon stimulation with Wnt-3a ([Figure 1C](#)). In addition, using in-cell western ([Hannoush, 2008](#)), we determined a time-dependent decrease in β -catenin levels in U-2OS cells, and observed reduced amounts of β -catenin as early as 4 hr after addition of compound **1d** at a concentration of 1 μ M ([Figure 1E](#)). Compound **1d** suppressed the expression of the Wnt target gene *AXIN2* in HEK293 cells ([Figure 1F](#)). In addition, reduced levels of β -catenin were detected in the nuclei in the presence of **1d** upon stimulation with Wnt-3a ([Figure 1G](#)). These results indicate that dimethoxypyridine **1d** interferes with Wnt signaling upstream of the destruction complex and leads to reduced cellular and nuclear abundance of β -catenin.

Promotion of Cardiac Differentiation

Temporal modulation of Wnt/ β -catenin signaling is essential and sufficient for efficient cardiac induction in human induced pluripotent stem cells (hiPSCs) ([Lian et al., 2012](#)). Wnt/ β -catenin signaling plays a biphasic role in cardiogenesis: Wnt pathway activation is required for mesoderm formation, while subsequent inhibition of Wnt signaling is necessary for cardiac induction and specification ([Zhang et al., 2015](#)). Wnt inhibitors of different chemotypes are capable of inducing cardiomyocyte formation from progenitor cells ([Schade and Plowright, 2015](#)). This efficacy seems to be independent from their mode of action as to whether they act rather up- or downstream within the pathway. Still, a direct correlation of potency in Wnt reporter gene assays and cardiac differentiation assays has been demonstrated with low-nanomolar Wnt inhibitors promoting cardiogenesis most effectively ([Lanier et al., 2012](#)). In light of the role of Wnt/ β -catenin during cardiomyogenesis, we charac-

terized the Wnt inhibitor **1d** with regard to its ability to promote cardiac differentiation of hiPSCs employing an *in vitro* model system and a cardiac differentiation protocol adapted from [Rao et al. \(2016\)](#) ([Figure 2A](#)). The compound was applied between days 2 and 4 of the differentiation time line, and, at day 10, the cells were examined by microscopy for functional beating cardiomyocyte clusters in the differentiation culture (see [Video S1](#)). We captured beating conditioned medium clusters induced by **1d** and quantified hiPSC-derived cardiomyocytes by flow cytometry upon intracellular immunostaining for the cardiac marker cTnnT ([Figures 2B and 2C](#), see [Video S1](#)). A dose-dependent increase of cardiogenesis was determined with nearly 15-fold over vehicle control at 10 μ M dosing of **1d**. These results confirm the functional perturbation of Wnt/ β -catenin signaling in a complex, developmentally relevant process of human cardiopoietic differentiation.

Affinity-Based Enrichment of Dimethoxypyridine Targets

To identify the cellular target of compound **1d**, we employed a chemical proteomics approach which employs affinity isolation of the putative target protein(s) and subsequent mass spectrometric protein identification. Based on the SAR analysis (see above) we introduced a triethylene glycol linker at C2 of the naphthalene ring to generate affinity probe **3** ([Figure 3A](#)). Control probe **4** embodies only a naphthalene ring but not the bis-pyridine part of the molecule that proved essential for activity ([Figure 3A](#)). Pull-down probe **3** retained biological activity ($IC_{50} = 4.4 \pm 0.3 \mu$ M for inhibition of Wnt reporter activity), but control probe **4** was inactive. Affinity-based enrichment of proteins that bind to immobilized probe **3** and subsequent protein identification by means of mass spectrometry and label-free quantification yielded 14 proteins that selectively bind to probe **3** compared with control probe **4** ([Figure 3B](#); [Table S2](#)).

Faced with the problem of which proteins to select first for validation, we prioritized deoxycytidine kinase (DCK), protein phosphatase 1, and palmitoyl protein thioesterase 1. For DCK, an indirect link to the Wnt pathway has been reported ([Rathe and Largaespada, 2010](#)), palmitoyl protein thioesterase removes palmitates from various proteins, and the Wnt protein is S-palmitoylated ([Willert et al., 2003](#)), and protein phosphatase 1 is involved in regulation of assembly and function of the β -catenin degradation complex ([Luo et al., 2007](#)). However, to our dismay enzymatic assays revealed that compound **1d** did not inhibit the activity of these enzymes (see [Figure S1](#)). These undesired findings clearly demonstrate the challenges to be faced in the target identification and validation selection process when multiple proteins are enriched during the affinity-based purification.

(C) Compound **1d** decreases the levels of total β -catenin. HEK293 cells were treated with L (L) or Wnt-3a (Wnt-3a) conditioned medium (CM) for 24 hr. Where indicated, cells were additionally exposed to the compound. Cell lysates were then subjected to immunoblotting using antibodies against β -catenin or GAPDH as a reference. M, protein standard.

(D) Quantification of the β -catenin levels in (C).

(E) Time-resolved detection of β -catenin levels upon addition of the compound by means of in-cell western. Data are mean values \pm SD and are representative of three biological replicates (N = 4, n = 3).

(F) Influence of compound **1d** on the expression of the Wnt target gene *AXIN2*. The mRNA levels of *AXIN2* or *GAPDH* (reference gene) were quantified by means of qPCR using cDNA as a template and employing the $\Delta\Delta Ct$ approach. Data are mean values \pm SD of three biological replicates. ns, not significant; * $p < 0.05$; ** $p < 0.01$.

(G) Compound **1d** reduces the nuclear localization of β -catenin. U-2OS cells were treated with L or Wnt-3a CM in presence or absence of **1d** for 24 hr prior to staining with β -catenin-specific antibody and a secondary antibody that was coupled to Alexa 594. Scale bar, 25 μ m.

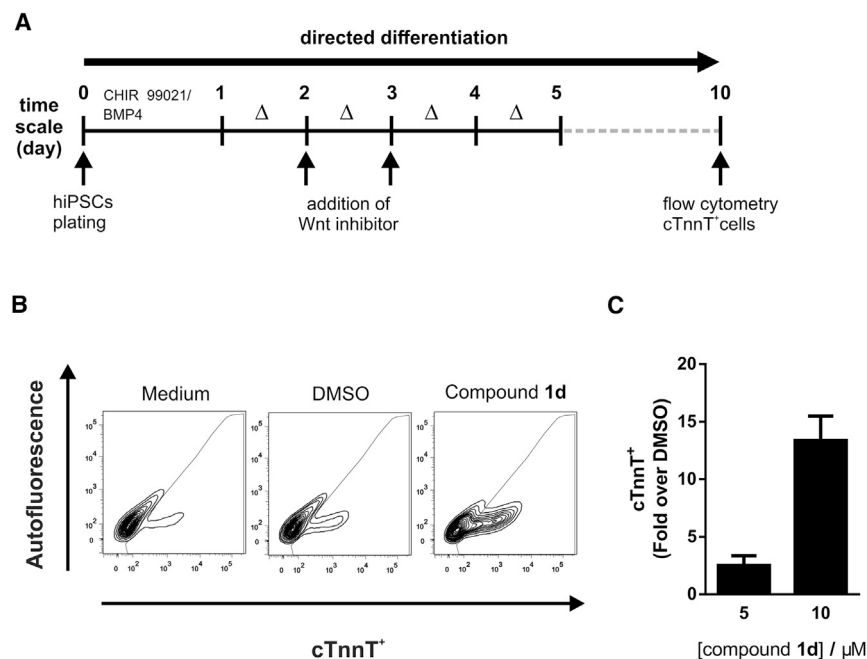


Figure 2. Influence of Dimethoxyppyridine 1d on Cardiomyocyte Differentiation

(A) Scheme of the cardiomyocyte differentiation assay annotated with corresponding timescale and time points of small-molecule application. Δ , ticks indicate media changes.

(B) Representative flow cytometry analysis (as dot plots) of hiPSC-derived cardiomyocytes with typical cTnnT⁺ populations in cells produced from application of compound **1d** (10 μ M) compared with the DMSO vehicle control on day 10 of differentiation.

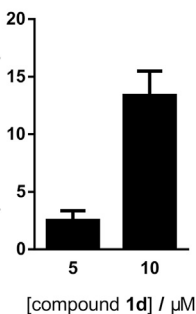
(C) Amount of cTnnT⁺ cells as determined by fluorescence-activated cell sorting analysis after 2 days of treatment with **1d** (day 2–4) on day 10 of differentiation. Data are mean values (N = 2) \pm SD and are representative of five biological replicates.

In Silico Target Prediction

To avoid further laborious target devalidation experiments based on literature precedent or educated guess, and in the absence of further experimental data, we employed *in silico* target prediction using self-organizing maps of drug equivalence relationships (SPIDER method) (Reker et al., 2014b) to prioritize further proteins for target validation. In brief, this computational technique infers potential targets of a given bioactive compound by evaluating the similarity between the query and known bioactive compounds with target annotations. The SPIDER method evaluates similarity in terms of both pharmacophore features and compound properties. It has been successfully applied to the “de-orphaning” of both synthetic compounds and natural products with phenotypic effects (Rodrigues et al., 2016; Schneider et al., 2016; Schneider and Schneider, 2017; Schröder et al., 2015). As a result of the SPIDER run, more than 15 protein families or proteins were predicted to bind to **1d** (Figure 3C; Table S3). Integrating this result with the findings of the chemical proteomics analysis revealed arachidonate 5-LO as the only protein identified by both methodologies. In fact, 5-LO was enriched only by the active probe **3** but not by the control probe **4** (see Table S2).

Inhibition of 5-LO

5-LO catalyzes the oxidation of arachidonic acid to 5(S)-hydroperoxyeicosatetraenoic acid (5-HPETE) and leukotriene A₄ (LTA₄) (Radmark et al., 2007). LTA₄ is further transformed to important mediators of inflammation (e.g., LTB₄, LTC₄). This process occurs on the nuclear membrane and is facilitated by the proteins cytosolic phospholipase A2 and FLAP (Radmark et al., 2007). In its inactive state, 5-LO is localized either in the cytoplasm or inside the nucleus (Radmark et al., 2007). Very recently, 5-LO was independently linked to regulation of Wnt signaling in a model of acute myeloid leukemia (Roos et al., 2014, 2016).



Binding of compound **3** to 5-LO was confirmed by means of immunoblotting after pull-down from lysate, whereas the control probe **4** almost completely failed to enrich the enzyme (Figure 3D). Moreover, addition of excess **1d** reduced binding of 5-LO to the active probe **3** in a concentration-dependent manner (Figure 3D). Similar results were obtained with purified, recombinantly expressed 5-LO (Figure 3E).

To analyze whether compound **1d** inhibits 5-LO, we monitored the activity of the enzyme in intact human granulocytes. Compound **1d** inhibited 5-LO product formation (5-HPETE and LTA₄) with an apparent IC₅₀ of 5 μ M (Figure 4A). If cell homogenates were used instead of intact cells, activity of **1d** was considerably lower (see Figure 4B). When purified recombinant 5-LO was employed, 5-LO inhibition was observed only in the presence of the reducing agent glutathione and glutathione peroxidase (Figure 4C). A similar behavior is documented for non-redox 5-LO inhibitors, e.g., CJ-13,610 (see Figure S2A) (Fischer et al., 2004). These results suggest that compound **1d** acts as a direct, non-redox inhibitor of 5-LO and it was, thus, termed “Lipoxygenin.”

These results suggest that compound **1d** acts as a direct, non-redox inhibitor of 5-LO and it was, thus, termed “Lipoxygenin.”

Wnt Signaling Influences the Subcellular Localization of 5-LO and 5-LO- β -Catenin Complex Formation

5-LO can be targeted to different cellular compartments dependent on the stimuli (Radmark et al., 2007). Thus, we expressed 5-LO in U-2OS to study its subcellular localization. The expression of both FLAG-tagged 5-LO or GFP-tagged 5-LO resulted in nuclear localization of the ectopically introduced protein, which is in line with previous reports (Jones et al., 2003) (Figure S3). We also detected a partial localization of endogenous 5-LO in the nucleus of non-induced U-2OS cells (Figure 5). Upon treatment with Wnt-3a, the nuclear localization of 5-LO was enhanced. Interestingly, Lipoxygenin reversed this influence, as significantly less 5-LO was detected in the nuclei of U-2OS cells upon co-treatment of cells with Wnt-3a and Lipoxygenin (Figures 5A and 5B).

Some of us recently suggested that an interaction of inactive 5-LO and β -catenin hinders β -catenin from entering the nucleus and therefore inhibits Wnt signaling (Roos et al., 2014). Since Lipoxygenin similarly modulates the cellular distribution of both 5-LO and β -catenin (compare Figures 1G and 5A), we

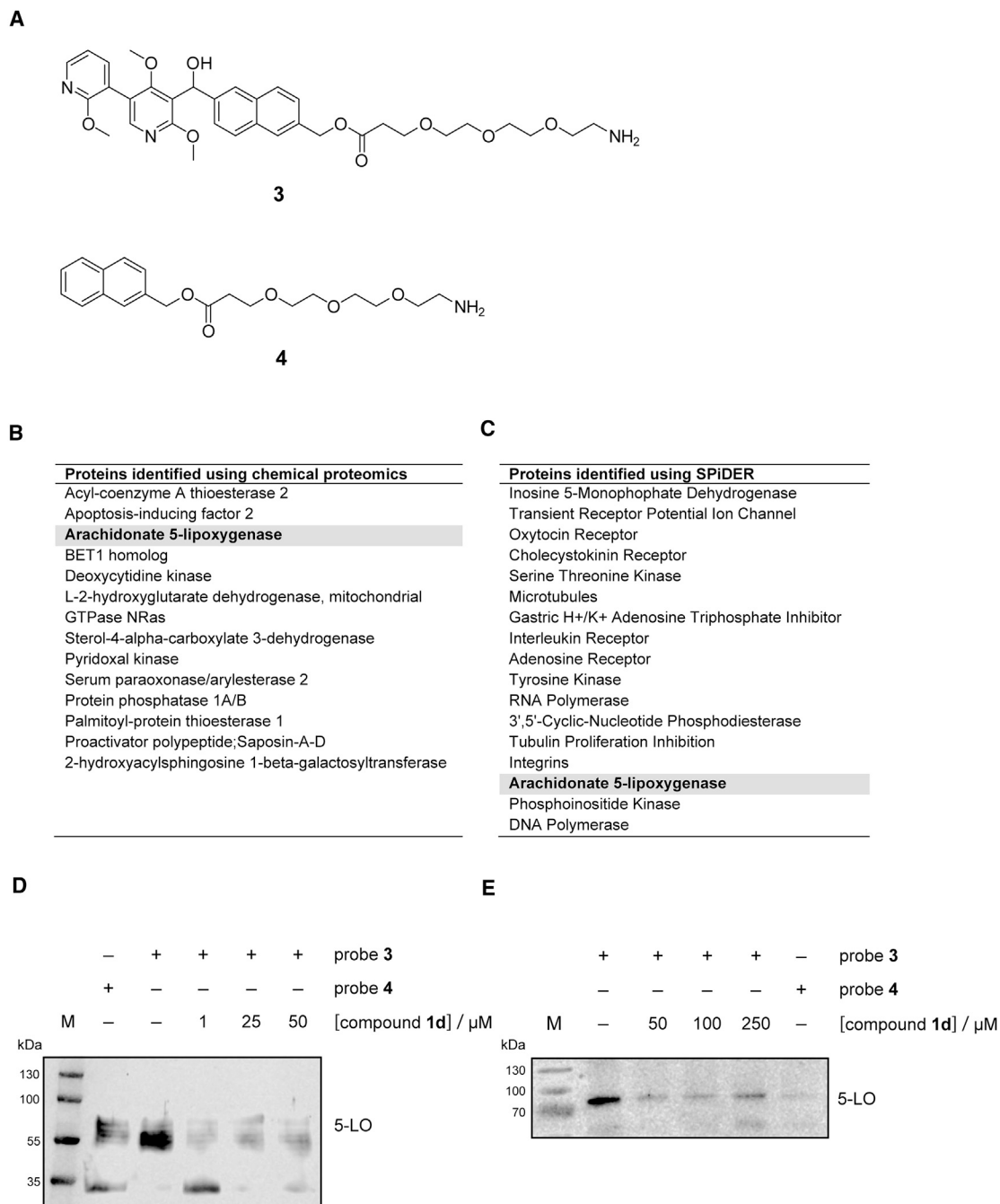


Figure 3. Identification of Arachidonate 5-LO as a Target of 1d

(A) Chemical structures of the active pull-down probe (**3**) and the control probe (**4**).

(B) List of potential target proteins identified by means of chemical proteomics.

(C) List of potential target proteins as predicted by the SPIDER software.

(D) Selective enrichment of 5-LO by the active probe **3** (compared with the control probe **4**) as detected by means of immunoblotting after the pull-down and using an anti-5-LO specific antibody. Where indicated, unmodified compound **1d** was added as a competitor. M, protein standard.

(E) Binding of recombinant 5-LO to probe **3** as detected by means of immunoblotting after affinity enrichment of purified 5-LO protein by probe **3** in comparison with probe **4**. Where indicated, unmodified compound **1d** was added as a competitor. M, protein standard.

See also [Figure S1](#).

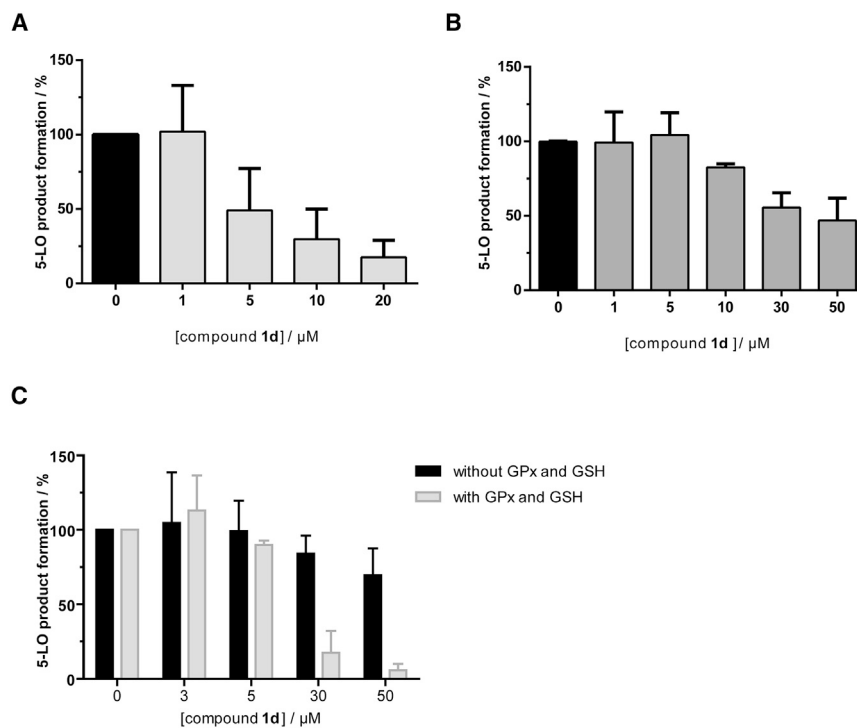


Figure 4. Influence of Compound 1d on 5-LO Activity

Enzymatic activity of 5-LO was monitored in intact human granulocytes (A), cell homogenates (B), or with the purified protein (C) in presence or absence of glutathione peroxidase (GPx) and glutathione (GSH). Data are mean values \pm SD (n = 3). See also Figure S2.

and yet unknown role of 5-LO in these pathways. In fact, 5-LO has been linked so far only to modulation of the Wnt pathway (Roos et al., 2014). Similarly to Lipoxygenin, CJ-13,610 increased cardiomyogenesis (Figure S2C) proving functional impairment of Wnt signaling by this 5-LO inhibitor as well. To the best of our knowledge, no compound or biomolecule involved in all the modulated pathways has been described yet.

DISCUSSION

In light of the high relevance of the Wnt signaling pathway, both in chemical biology and in drug discovery research,

hypothesized that the compound may modulate the 5-LO- β -catenin complex. Indeed, application of the proximity ligation assay (Blokzijl et al., 2010) revealed that 5-LO and β -catenin interact in U-2OS cells (Figures 5C and 5D), and that significantly more interaction sites were observed upon stimulation with Wnt-3a (Figures 5C and 5D). The influence of Wnt-3a was counteracted by Lipoxygenin, as the number of 5-LO- β -catenin interaction spots was reduced upon treatment with Lipoxygenin, which reflects the reduction of β -catenin upon treatment with Lipoxygenin (see above).

5-LO Inhibition Impairs Hedgehog, TGF- β , BMP, and Activin A Signaling

In light of these findings, i.e., the nuclear 5-LO localization, the result of the cardiogenesis experiment described above, and the known convergence of other signaling pathways, which contribute to cardiogenesis during this post-mesoderm stage of differentiation in the nucleus, we investigated whether the compound also modulates the Hedgehog, TGF- β (transforming growth factor β), BMP (bone morphogenetic protein), and Activin A signaling pathways (Figure 6). TGF- β signaling was inhibited by Lipoxygenin to a similar extent as the Wnt pathway (Figure 6A), Hedgehog, BMP, and Activin A signaling were inhibited with slightly lower potency (Figures 6B–6F). Lipoxygenin also inhibited the expression of the Hedgehog target genes *Gli1* and *Ptch1* (Figure 6C). These findings suggest that the mode of action of Lipoxygenin most likely includes a common component of all these signaling pathways. To further validate 5-LO as a target, we examined the influence of the structurally unrelated 5-LO inhibitor CJ-13,610 (Fischer et al., 2004) on these pathways. Similar to Lipoxygenin, CJ-13,610 inhibited Wnt, Hedgehog, TGF- β , BMP and Activin A signaling (Figure S2B), thus suggesting an unexpected

we carried out a cell-based screen for Wnt pathway inhibitors and identified 3,5-substituted-2,4-dimethoxypyridines as inhibitor class. Attempts to identify the cellular target of the compound chosen for in-depth characterization proved to be challenging since several initially prioritized target candidates could not be validated in subsequent experiments (Kapoor et al., 2016; Ziegler et al., 2013). To avoid additional labor-intensive de/validation experiments not guided by additional experimental insights, but mainly based on literature precedent, availability of assay procedures or educated guess, as often practiced in target identification and validation campaigns, and to focus and accelerate the target identification process, we envisioned the combination of two complementary approaches. We sought to combine on the one hand the broadly applied affinity-based chemical proteomics approach that can unravel target proteins, and, on the other hand, *in silico* target prediction, which makes use of the wealth of information available on ligand-target interactions (Koutsoukas et al., 2011). This composite strategy converged exclusively on and revealed arachidonate 5-LO as a potential target. Enzyme inhibition studies provided evidence for a non-redox type of 5-LO inhibition by the inhibitor chosen for in-depth characterization and the small molecule was ultimately termed Lipoxygenin. Lipoxygenin is a non-redox 5-LO inhibitor, targets the β -catenin-5-LO complex, and induces reduction of both β -catenin and 5-LO in the nucleus. In addition to inhibition of the Wnt pathway, Lipoxygenin also inhibits TGF- β , Activin A, Hedgehog, and BMP signaling. This activity is shared by the structurally unrelated, yet mechanistically similar, 5-LO inhibitor CJ-13,610, thus suggesting 5-LO as a common regulator of these developmental pathways. However, apart from Wnt signaling (Roos et al., 2014), currently a clear link between 5-LO and the regulated pathways has not been reported.

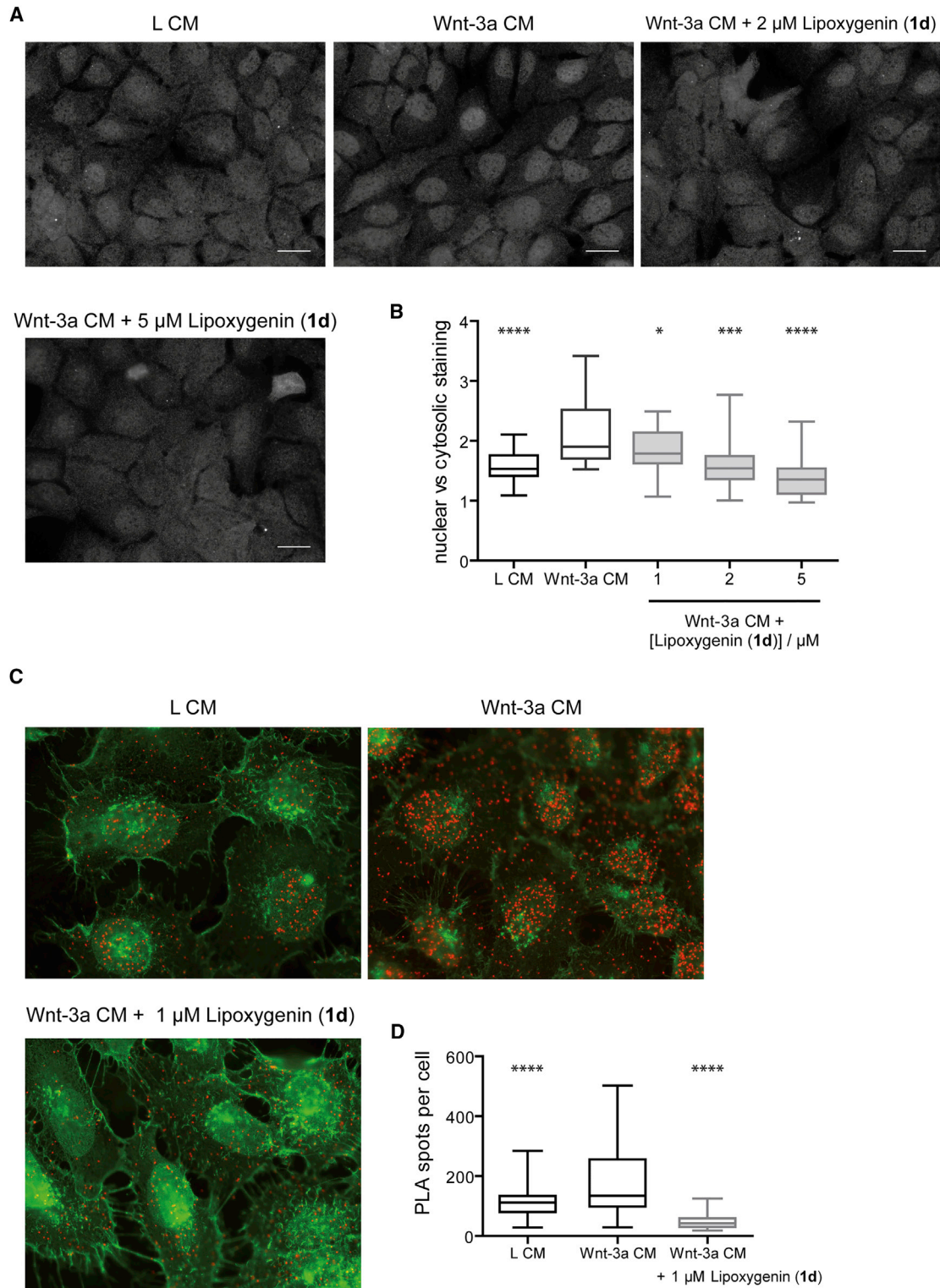


Figure 5. Influence of Lipoxygenin (1d) on the Subcellular Localization of 5-LO and on the 5-LO-β-Catenin interaction

(A) U-2OS cells were incubated with L or Wnt-3a CM for 24 hr. Where indicated, cells were additionally treated with Lipoxygenin. 5-LO was detected upon fixation and staining with anti-5-LO antibody and a secondary antibody that was coupled to Alexa 488. Scale bar, 25 μm.

(B) Quantification of the nuclear to cytosolic distribution of 5-LO in (A). Data are mean values (N = 24) and are representative of more than three biological replicates.

(legend continued on next page)

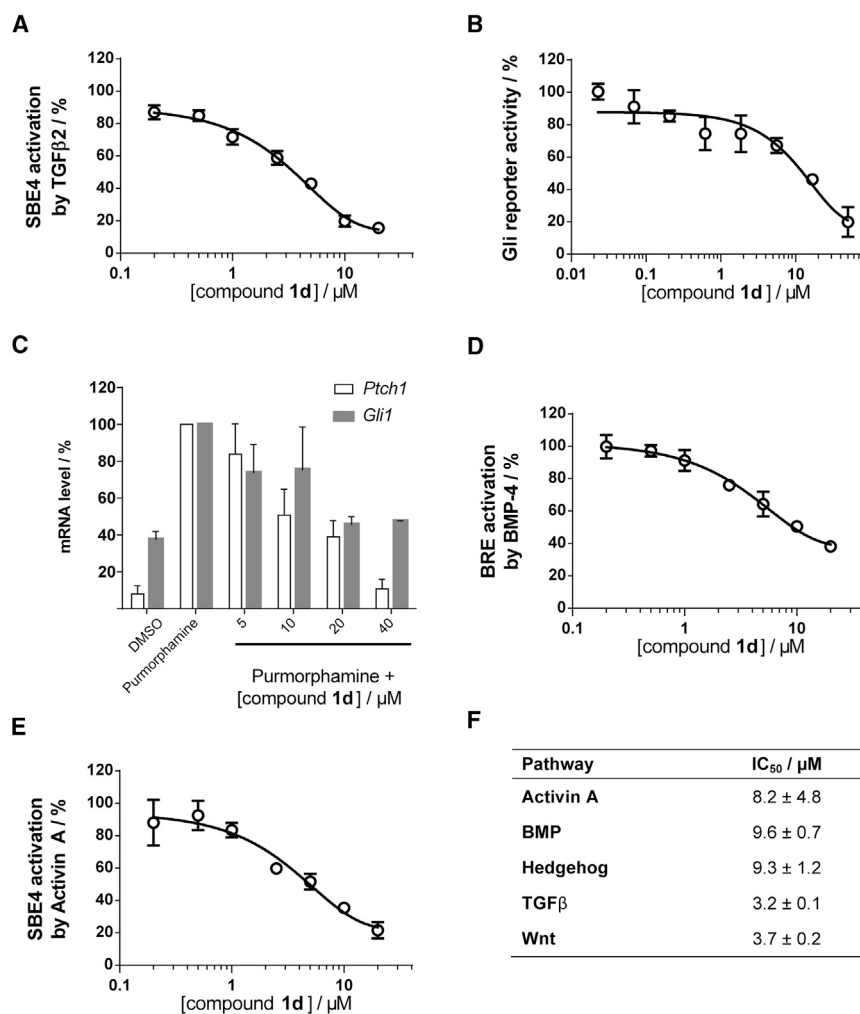


Figure 6. Dimethoxyypyridine 1d Inhibits Several Signaling Pathways

(A) Influence of compound **1d** on TGF-β2-mediated activation of SBE4-responsive reporter gene expression. Pathway activity was monitored by means of an SBE4-responsive reporter gene upon stimulation of HEK293T cells with 10 ng/mL of TGF-β2 ligand and incubation with **1d** for 22 hr.

(B) Influence of compound **1d** on Hedgehog signaling. Hedgehog pathway activity was monitored by means of a Gli-responsive reporter gene expression upon stimulation of Shh-LIGHT2 cells with 2 μM purmorphamine and incubation with **1d** for 48 hr.

(C) Influence of **1d** on the expression of the Hedgehog target genes *Ptch1* and *Gli1*. NIH/3T3 cells were incubated with 2 μM purmorphamine and **1d** for 48 hr prior to detection of the mRNA levels of *Ptch1*, *Gli1*, and *Gapdh*, and employing the ΔΔCt approach. Data are mean values ± SD of three biological replicates (N = 3, n = 3).

(D) Influence of compound **1d** on BMP-4-mediated activation of BMP-responsive element (BRE)-controlled reporter gene expression. Pathway activity was monitored by means of a BRE-responsive reporter gene upon stimulation of HEK293T cells with 10 ng/mL of BMP-4 ligand and incubation with **1d** for 22 hr.

(E) Influence of compound **1d** on Activin A-mediated activation of SBE4-controlled reporter gene expression. Pathway activity was monitored by means of an SBE4-responsive reporter gene upon stimulation of HEK293T cells with 10 ng/mL of Activin A ligand and incubation with **1d** for 22 hr.

(F) Calculated half-maximal inhibitory concentrations (IC₅₀) for inhibition of the assayed signaling pathways. All data are mean values ± SD (N = 3, n = 2–4).

Inhibition of Wnt signaling may be mediated by enzymatically inactive 5-LO, rather than through inhibition of 5-LO-generated lipid mediators (Roos et al., 2014). Interestingly, the localization of 5-LO was modulated by Wnt-3a, since the enzyme was enriched inside the nucleus upon pathway activation. This influence was reverted by Lipoxygenin, suggesting that nuclear 5-LO may positively affect Wnt signaling. Nuclear import of 5-LO is a regulated process that is triggered by different stimuli in-cell-context-dependent manner and nuclear localization often positively correlates with increased leukotriene production (Brock, 2005). The association of 5-LO with the DNA-nuclear fraction (Brock and Healy, 2000) and the inhibition of various signaling pathways regulating gene expression by 5-LO inhibitors may indicate a direct or indirect role for 5-LO in gene regulation, which is supported by the modulation of p53 transcriptional activity by

5-LO (Gilbert et al., 2015). Alternatively, 5-LO may serve as a protein that assists the nucleo-cytoplasmic shuttling of β-catenin. β-Catenin relies on chaperones to enter and exit the nucleus since it lacks nuclear localization (NLS) and nuclear export (NES) signals (Morgan et al., 2014). 5-LO has been reported to contain functional NLS and NES motifs (Luo et al., 2004; Hanaka et al., 2002) and phosphorylation of 5-LO by p38 MAPK causes localization of 5-LO to the nucleoplasm (Flamand et al., 2009). p38 MAPK itself is positively regulated by Wnt signaling, influences Wnt signaling and thus may affect 5-LO localization in Wnt-dependent manner (Bikkavilli et al., 2008; Caverzasio and Manen, 2007). Similar to cytosol-nucleus shuttling proteins (e.g., APC, IRS-1, and FOXM1) (Morgan et al., 2014), 5-LO may promote the translocation of β-catenin to the nucleus. In the absence of Wnt or in the presence of 5-LO inhibitors, such as

(C) U-2OS cells were treated with control conditioned medium (L CM) or Wnt-3a-conditioned medium (Wnt-3a CM) in presence or absence of Lipoxygenin for 24 hr. Proximity ligation assay (PLA) was then carried out using antibodies against 5-LO and β-catenin and secondary antibodies that were coupled to PLA oligonucleotide probes. Sites of interaction (red) were visualized upon rolling circle amplification and hybridization with fluorescently labeled probes. Cells were then stained for DAPI to visualize the nuclei. (C) Microscopic images. Scale bar, 25 μm.

(D) Quantification of PLA spots. Data are representative of seven biological replicates.

*p < 0.05; ***p < 0.001; ****p < 0.0001. See also Figure S3.

Lipoxygenin, 5-LO is retained in the cytoplasm shifting the equilibrium of β -catenin localization from the nucleus to the cytosol, resulting in an increased β -catenin turnover, i.e., degradation. Determination of the exact mode of action of 5-LO in the Wnt pathway may open up new opportunities for the application of 5-LO inhibitors.

Beyond this biological insight our results demonstrate that the combination of experimental techniques for initial identification of small-molecule target candidates with cheminformatic methods for *in silico* small-molecule target prediction may provide efficient guidance for candidate selection and prioritization for experimental in-depth evaluation. Thereby the labor-, time-, and cost-intensive devalidation of false-positive target candidates may be omitted or at least shortened, and efficiency of target identification and validation, in general, may be greatly enhanced.

SIGNIFICANCE

Target-agnostic phenotypic screenings require target deconvolution in a typically challenging, time-consuming, and laborious process. Chemical proteomics is frequently employed for the identification of target proteins of small molecules, but usually identifies several potential targets that need successive (de)validation. Among the available strategies to target identification, *in silico* methods may predict targets for small molecules based on ligand similarity or bioactivity. To make the process of target identification more efficient, i.e., for target prioritization, we combined classical affinity-based enrichment of binding partners with computational target prediction by means of the SPIDER method. This composite strategy was applied to a 3,5-substituted-2,4-dimethoxy-pyridine derivative, termed Lipoxygenin, newly identified as inhibitor of Wnt signaling. Thereby the possible targets were narrowed down to one single protein, 5-lipoxygenase (5-LO). Lipoxygenin was subsequently confirmed as a non-redox type inhibitor of 5-LO. Our study emphasizes the effectiveness of combining experimental and computational approaches to guide target prioritization and generate target hypotheses. We report on a yet unknown link between Wnt signaling and 5-LO, and demonstrate that Wnt signaling triggers nuclear localization of 5-LO, which is counteracted by Lipoxygenin. Furthermore, our findings suggest a role for 5-LO in the regulation of Hedgehog, TGF- β , BMP, and Activin A signaling which may open up novel opportunities for the application of 5-LO inhibitors.

STAR★METHODS

Detailed methods are provided in the online version of this paper and include the following:

- KEY RESOURCES TABLE
- CONTACT FOR REAGENTS AND RESOURCE SHARING
- EXPERIMENTAL MODEL AND SUBJECT DETAILS
- METHOD DETAILS
 - General Information - Chemistry
 - Synthesis of the Compound Collection

- Preparation of Media Containing Wnt-3a Protein
- Reporter Gene Assays
- Target Gene Expression Analysis Using Quantitative PCR
- In-Cell Western
- Human iPS Cell Culture and Cardiac Differentiation
- Flow Cytometry
- Cell Transfection
- Cell Lysate Preparation
- Identification of Proteins Binding to Lipoxygenin
- Cheminformatic Analysis of Protein Targets for Small Molecules
- Immunoblotting
- Purification of PP1 and PP1 Activity Assay
- PPT1 Activity Assay
- DCK Activity Assay
- Purification of 5-LO and 5-LO Activity Assays
- Immunofluorescence
- Proximity Ligation Assay (PLA)

● QUANTIFICATION AND STATISTICAL ANALYSIS

SUPPLEMENTAL INFORMATION

Supplemental Information includes three figures, three tables, one video, and one data file and can be found with this article online at <https://doi.org/10.1016/j.chembiol.2018.05.016>.

ACKNOWLEDGMENTS

H.W. was supported by the European Research Council under the European Union's Seventh Framework Program (FP7/2007–2013; ERC grant 268309 and HEALTH- F2-2009-241498); C.P. was supported by the Wilhelm Sander-Stiftung (2013.061.1); D. Steinhilber was supported by the DFG (SFB1039/A02 and GRK2336/TP4) and the Else Kröner-Fresenius-Stiftung (Else Kröner-Fresenius-Graduiertenkolleg 2014_A187) and D. Schade was supported by the German Federal Ministry of Education and Research (BMBF, grant no. 131605). We thank Anja Vogel, Petra Schneider, Daniel Reker, and Andreas Brockmeyer for technical support.

AUTHOR CONTRIBUTIONS

Conceptualization, H.W.; Formal Analysis, P.J., C.P., and S.E.; Investigation, S.B., S.R., P.S., B.R., J.R., S.K., P.J., and S.P.; Writing – Original Draft, S.B., P.S., S.Z., D. Schade, K.K., and H.W.; Writing – Review & Editing, S.Z. and H.W.; Visualization, S.Z. and B.R.; Supervision, H.W., K.K., S.Z., D. Schade, T.M., G.S., and D. Steinhilber.

DECLARATION OF INTERESTS

G.S. is a co-founder of inSili.com LLC, Zurich and consultant in the life science industry.

Received: October 18, 2017

Revised: February 26, 2018

Accepted: May 22, 2018

Published: June 28, 2018

REFERENCES

- Anastas, J.N., and Moon, R.T. (2013). WNT signalling pathways as therapeutic targets in cancer. *Nat. Rev. Cancer* 13, 11–26.
- Bikkavilli, R.K., Feigin, M.E., and Malbon, C.C. (2008). p38 mitogen-activated protein kinase regulates canonical Wnt-beta-catenin signaling by inactivation of GSK3beta. *J. Cell Sci.* 121, 3598–3607.

- Blokzijl, A., Friedman, M., Ponten, F., and Landegren, U. (2010). Profiling protein expression and interactions: proximity ligation as a tool for personalized medicine. *J. Intern. Med.* *268*, 232–245.
- Brock, T.G. (2005). Regulating leukotriene synthesis: the role of nuclear 5-lipoxygenase. *J. Cell. Biochem.* *96*, 1203–1211.
- Brock, T.G., and Healy, A.M. (2000). Nuclear import of arachidonate 5-lipoxygenase. *Arch. Immunol. Ther. Exp. (Warsz)* *48*, 481–486.
- Caverzasio, J., and Manen, D. (2007). Essential role of Wnt3a-mediated activation of mitogen-activated protein kinase p38 for the stimulation of alkaline phosphatase activity and matrix mineralization in C3H10T1/2 mesenchymal cells. *Endocrinology* *148*, 5323–5330.
- Chen, X.S., and Funk, C.D. (2001). The N-terminal "beta-barrel" domain of 5-lipoxygenase is essential for nuclear membrane translocation. *J. Biol. Chem.* *276*, 811–818.
- Cox, J., and Mann, M. (2008). MaxQuant enables high peptide identification rates, individualized p.p.b.-range mass accuracies and proteome-wide protein quantification. *Nat. Biotechnol.* *26*, 1367–1372.
- Fischer, L., Steinhilber, D., and Werz, O. (2004). Molecular pharmacological profile of the nonredox-type 5-lipoxygenase inhibitor CJ-13,610. *Br. J. Pharmacol.* *142*, 861–868.
- Fischer, L., Szellas, D., Radmark, O., Steinhilber, D., and Werz, O. (2003). Phosphorylation- and stimulus-dependent inhibition of cellular 5-lipoxygenase activity by nonredox-type inhibitors. *FASEB J.* *17*, 949–951.
- Flamand, N., Luo, M., Peters-Golden, M., and Brock, T.G. (2009). Phosphorylation of serine 271 on 5-lipoxygenase and its role in nuclear export. *J. Biol. Chem.* *284*, 306–313.
- Gilbert, B., Ahmad, K., Roos, J., Lehmann, C., Chiba, T., Ulrich-Ruckert, S., Smeenk, L., Van Heeringen, S., Maier, T.J., Groner, B., et al. (2015). 5-Lipoxygenase is a direct p53 target gene in humans. *Biochim. Biophys. Acta* *1849*, 1003–1016.
- Greber, B., Coulon, P., Zhang, M., Moritz, S., Frank, S., Muller-Molina, A.J., Arauzo-Bravo, M.J., Han, D.W., Pape, H.C., and Scholer, H.R. (2011). FGF signalling inhibits neural induction in human embryonic stem cells. *EMBO J.* *30*, 4874–4884.
- Hanaka, H., Shimizu, T., and Izumi, T. (2002). Nuclear-localization-signal-dependent and nuclear-export-signal-dependent mechanisms determine the localization of 5-lipoxygenase. *Biochem. J.* *367*, 505–514.
- Hannoush, R.N. (2008). Kinetics of Wnt-driven beta-catenin stabilization revealed by quantitative and temporal imaging. *PLoS One* *3*, e3498.
- Huangfu, D.W., Maehr, R., Guo, W.J., Eijkelenboom, A., Snitow, M., Chen, A.E., and Melton, D.A. (2008). Induction of pluripotent stem cells by defined factors is greatly improved by small-molecule compounds. *Nat. Biotechnol.* *26*, 795–797.
- Jones, S.M., Luo, M., Peters-Golden, M., and Brock, T.G. (2003). Identification of two novel nuclear import sequences on the 5-lipoxygenase protein. *J. Biol. Chem.* *278*, 10257–10263.
- Kahn, M. (2014). Can we safely target the WNT pathway? *Nat. Rev. Drug Discov.* *13*, 513–532.
- Kapoor, S., Waldmann, H., and Ziegler, S. (2016). Novel approaches to map small molecule-target interactions. *Bioorg. Med. Chem.* *24*, 3232–3245.
- Keiser, M.J., Setola, V., Irwin, J.J., Laggner, C., Abbas, A.I., Hufeisen, S.J., Jensen, N.H., Kujier, M.B., Matos, R.C., Tran, T.B., et al. (2009). Predicting new molecular targets for known drugs. *Nature* *462*, 175–181.
- Korchynski, O., and Ten Dijke, P. (2002). Identification and functional characterization of distinct critically important bone morphogenetic protein-specific response elements in the Id1 promoter. *J. Biol. Chem.* *277*, 4883–4891.
- Koutsoukas, A., Simms, B., Kirchmair, J., Bond, P.J., Whitmore, A.V., Zimmer, S., Young, M.P., Jenkins, J.L., Glick, M., Glen, R.C., et al. (2011). From in silico target prediction to multi-target drug design: current databases, methods and applications. *J. Proteomics* *74*, 2554–2574.
- Lanier, M., Schade, D., Willems, E., Tsuda, M., Spiering, S., Kalsiak, J., Mercola, M., and Cashman, J.R. (2012). Wnt inhibition correlates with human embryonic stem cell cardiomyogenesis: a structure-activity relationship study based on inhibitors for the Wnt response. *J. Med. Chem.* *55*, 697–708.
- Lian, X., Hsiao, C., Wilson, G., Zhu, K., Hazeltine, L.B., Azarin, S.M., Raval, K.K., Zhang, J., Kamp, T.J., and Palecek, S.P. (2012). Robust cardiomyocyte differentiation from human pluripotent stem cells via temporal modulation of canonical Wnt signaling. *Proc. Natl. Acad. Sci. USA* *109*, E1848–E1857.
- Lipinski, R.J., Gipp, J.J., Zhang, J., Doles, J.D., and Bushman, W. (2006). Unique and complimentary activities of the Gli transcription factors in Hedgehog signaling. *Exp. Cell Res.* *312*, 1925–1938.
- Livak, K.J., and Schmittgen, T.D. (2001). Analysis of relative gene expression data using real-time quantitative PCR and the 2- $\Delta\Delta$ CT method. *Methods* *25*, 402–408.
- Logan, C.Y., and Nusse, R. (2004). The Wnt signaling pathway in development and disease. *Annu. Rev. Cell Dev. Biol.* *20*, 781–810.
- Luo, M., Pang, C.W., Gerken, A.E., and Brock, T.G. (2004). Multiple nuclear localization sequences allow modulation of 5-lipoxygenase nuclear import. *Traffic* *5*, 847–854.
- Luo, W., Peterson, A., Garcia, B.A., Coombs, G., Kofahl, B., Heinrich, R., Shabanowitz, J., Hunt, D.F., Yost, H.J., and Virshup, D.M. (2007). Protein phosphatase 1 regulates assembly and function of the beta-catenin degradation complex. *EMBO J.* *26*, 1511–1521.
- Mahshid, Y., Markoutsas, S., Dincbas-Renqvist, V., Surun, D., Christensson, B., Sander, B., Bjorkholm, M., Sorg, B.L., Radmark, O., and Claesson, H.E. (2015). Phosphorylation of serine 523 on 5-lipoxygenase in human B lymphocytes. *Prostaglandins Leukot. Essent. Fatty Acids* *100*, 33–40.
- Moon, R.T., Kohn, A.D., De Ferrari, G.V., and Kaykas, A. (2004). WNT and beta-catenin signalling: diseases and therapies. *Nat. Rev. Genet.* *5*, 691–701.
- Morgan, R.G., Ridsdale, J., Tonks, A., and Darley, R.L. (2014). Factors affecting the nuclear localization of beta-catenin in normal and malignant tissue. *J. Cell. Biochem.* *115*, 1351–1361.
- Niphakis, M.J., and Cravatt, B.F. (2014). Enzyme inhibitor discovery by activity-based protein profiling. *Annu. Rev. Biochem.* *83*, 341–377.
- Park, S., Gwak, J., Cho, M., Song, T., Won, J., Kim, D.E., Shin, J.G., and Oh, S. (2006). Hexachlorophene inhibits Wnt/beta-catenin pathway by promoting Siah-mediated beta-catenin degradation. *Mol. Pharmacol.* *70*, 960–966.
- Radmark, O., Werz, O., Steinhilber, D., and Samuelsson, B. (2007). 5-Lipoxygenase: regulation of expression and enzyme activity. *Trends Biochem. Sci.* *32*, 332–341.
- Rao, J., Pfeiffer, M.J., Frank, S., Adachi, K., Piccini, I., Quaranta, R., Arauzo-Bravo, M., Schwarz, J., Schade, D., Leidel, S., et al. (2016). Stepwise clearance of repressive roadblocks drives cardiac induction in human ESCs. *Cell Stem Cell* *18*, 341–353.
- Rasband, W.S. (1997–2016). ImageJ (U. S. National Institutes of Health). <https://imagej.nih.gov/ij/>.
- Rathe, S.K., and Largaespada, D.A. (2010). Deoxycytidine kinase is downregulated in Ara-C-resistant acute myeloid leukemia murine cell lines. *Leukemia* *24*, 1513–1515.
- Reker, D., Perna, A.M., Rodrigues, T., Schneider, P., Reutlinger, M., Monch, B., Koeberle, A., Lamers, C., Gabler, M., Steinmetz, H., et al. (2014a). Revealing the macromolecular targets of complex natural products. *Nat. Chem.* *6*, 1072–1078.
- Reker, D., Rodrigues, T., Schneider, P., and Schneider, G. (2014b). Identifying the macromolecular targets of de novo-designed chemical entities through self-organizing map consensus. *Proc. Natl. Acad. Sci. USA* *111*, 4067–4072.
- Rix, U., and Superti-Furga, G. (2009). Target profiling of small molecules by chemical proteomics. *Nat. Chem. Biol.* *5*, 616–624.
- Rodrigues, T., Reker, D., Schneider, P., and Schneider, G. (2016). Counting on natural products for drug design. *Nat. Chem.* *8*, 531–541.
- Roos, J., Grösch, S., Werz, O., Schröder, P., Ziegler, S., Fulda, S., Paulus, P., Urbschat, A., Kuehn, B., Maucher, I., et al. (2016). Regulation of tumorigenic Wnt signaling by cyclooxygenase-2, 5-lipoxygenase and their pharmacological inhibitors: a basis for novel drugs targeting cancer cells? *Pharmacol. Ther.* *157*, 43–64.
- Roos, J., Oancea, C., Heinssmann, M., Khan, D., Held, H., Kahnt, A.S., Capelo, R., la Buscato, E., Proschak, E., Puccetti, E., et al. (2014). 5-Lipoxygenase is a

- candidate target for therapeutic management of stem cell-like cells in acute myeloid leukemia. *Cancer Res.* *74*, 5244–5255.
- Sasaki, H., Hui, C.-C., Nakafuku, M., and Kondoh, H. (1997). A binding site for Gli proteins is essential for HNF-3 β floor plate enhancer activity in transgenics and can respond to Shh in vitro. *Development* *124*, 1313–1322.
- Schade, D., Lanier, M., Willems, E., Okolotowicz, K., Bushway, P., Wahlquist, C., Gilley, C., Mercola, M., and Cashman, J.R. (2012). Synthesis and SAR of b-annulated 1,4-dihydropyridines define cardiomyogenic compounds as novel inhibitors of TGF β signaling. *J. Med. Chem.* *55*, 9946–9957.
- Schade, D., and Plowright, A.T. (2015). Medicinal chemistry approaches to heart regeneration. *J. Med. Chem.* *58*, 9451–9479.
- Schneider, G., Reker, D., Chen, T., Hauenstein, K., Schneider, P., and Altmann, K.H. (2016). Deorphaning the macromolecular targets of the natural anticancer compound dolicolide. *Angew. Chem. Int. Ed.* *55*, 12408–12411.
- Schneider, G., and Schneider, P. (2017). Macromolecular target prediction by self-organizing feature maps. *Expert Opin. Drug Discov.* *12*, 271–277.
- Schröder, M., Hafner, A.K., Hofmann, B., Raadmark, O., Tumulka, F., Abele, R., Dotsch, V., and Steinhilber, D. (2014). Stabilisation and characterisation of the isolated regulatory domain of human 5-lipoxygenase. *Biochim. Biophys. Acta* *1841*, 1538–1547.
- Schröder, P., Förster, T., Kleine, S., Becker, C., Richters, A., Ziegler, S., Rauh, D., Kumar, K., and Waldmann, H. (2015). Neuritogenic militarinone-inspired 4-hydroxypyridones target the stress pathway kinase MAP4K4. *Angew. Chem. Int. Ed.* *54*, 12398–12403.
- Taipale, J., Chen, J.K., Cooper, M.K., Wang, B.L., Mann, R.K., Milenkovic, L., Scott, M.P., and Beachy, P.A. (2000). Effects of oncogenic mutations in smoothened and patched can be reversed by cyclopamine. *Nature* *406*, 1005–1009.
- Van Diggelen, O.P., Keulemans, J.L.M., Winchester, B., Hofman, I.L., Vanhanen, S.L., Santavuori, P., and Voznyi, Y.V. (1999). A rapid fluorogenic palmitoyl-protein thioesterase assay: pre- and postnatal diagnosis of INCL. *Mol. Genet. Metab.* *66*, 240–244.
- Veeman, M.T., Slusarski, D.C., Kaykas, A., Louie, S.H., and Moon, R.T. (2003). Zebrafish prickles, a modulator of noncanonical Wnt/Fz signaling, regulates gastrulation movements. *Curr. Biol.* *13*, 85.
- Werz, O., Burkert, E., Samuelsson, B., Radmark, O., and Steinhilber, D. (2002). Activation of 5-lipoxygenase by cell stress is calcium independent in human polymorphonuclear leukocytes. *Blood* *99*, 1044–1052.
- Werz, O., and Steinhilber, D. (1996). Selenium-dependent peroxidases suppress 5-lipoxygenase activity in B-lymphocytes and immature myeloid cells. The presence of peroxidase-insensitive 5-lipoxygenase activity in differentiated myeloid cells. *Eur. J. Biochem.* *242*, 90–97.
- Willems, E., Cabral-Teixeira, J., Schade, D., Cai, W.Q., Reeves, P., Bushway, P.J., Lanier, M., Walsh, C., Kirchhausen, T., Belmonte, J.C.I., et al. (2012). Small molecule-mediated TGF- β type II receptor degradation promotes cardiomyogenesis in embryonic stem cells. *Cell Stem Cell* *11*, 242–252.
- Willert, K., Brown, J.D., Danenberg, E., Duncan, A.W., Weissman, I.L., Reya, T., Yates, J.R., and Nusse, R. (2003). Wnt proteins are lipid-modified and can act as stem cell growth factors. *Nature* *423*, 448–452.
- Zawel, L., Dai, J.L., Buckhaults, P., Zhou, S.B., Kinzler, K.W., Vogelstein, B., and Kern, S.E. (1998). Human Smad3 and Smad4 are sequence-specific transcription activators. *Mol. Cell* *1*, 611–617.
- Zhang, M., Schulte, J.S., Heinick, A., Piccini, I., Rao, J., Quaranta, R., Zeuschner, D., Malan, D., Kim, K.P., Ropke, A., et al. (2015). Universal cardiac induction of human pluripotent stem cells in two and three-dimensional formats: implications for in vitro maturation. *Stem Cells* *33*, 1456–1469.
- Ziegler, S., Pries, V., Hedberg, C., and Waldmann, H. (2013). Target identification for small bioactive molecules: finding the needle in the haystack. *Angew. Chem. Int. Ed.* *52*, 2744–2792.

STAR★METHODS

KEY RESOURCES TABLE

REAGENT or RESOURCE	SOURCE	IDENTIFIER
Antibodies		
Donkey anti-rabbit IRDye 800CW	LI-COR Biosciences	Cat# 926-32213; RRID:AB_621848
Donkey anti-mouse IRDye 680RD	LI-COR Biosciences	Cat# 926-68072; RRID:AB_10953628
Donkey anti-mouse IRDye 800CW	LI-COR Biosciences	Cat# 926-32212; RRID:AB_621847
Donkey anti-rabbit IRDye 680RD	LI-COR Biosciences	Cat# 926-68073; RRID:AB_10954442
Goat anti-mouse Alexa Fluor-488-conjugated	Thermo Fisher Scientific	Cat# A11001; RRID:AB_2534069
Mouse anti-5-lipoxygenase, clone 33	BD Transduction Laboratories	Cat# 610695; RRID:AB_398018
Mouse anti-FLAG M1	Sigma-Aldrich	Cat# F3040; RRID:AB_439712
Mouse anti-GAPDH	Sigma-Aldrich	Cat# G8795; RRID:AB_107899
Mouse anti-troponin T (cTnnT), clone 13-11	Thermo Fisher Scientific	Cat# MA-12960; RRID:AB_11000742
Mouse anti- β -catenin, clone 14	BD Biosciences	Cat# 610154; RRID:AB_397555
Rabbit anti- β -catenin	Millipore	Cat# 06-734; RRID:AB_310231
Bacterial and Virus Strains		
BL21-CodonPlus (DE3)-RILP Competent Cells	Agilent	Cat# 230280
Chemicals, Peptides, and Recombinant Proteins		
2-phospho-ascorbate	Sigma-Aldrich	Cat# 49752
Empore SPE Disks (2215-C18 disks)	Supelco	Cat# 66883-U
4-Methylumbelliferyl 6-thio-Palmitate- β -D-glucopyranoside	Cayman Chemical	Cat# 19524; CAS: 229644-17-1
5-lipoxygenase	(Fischer et al., 2003; Schröder et al., 2014)	N/A
A23187	Sigma-Aldrich	Cat# C7522; CAS:52665-69-7
Accutase	Sigma-Aldrich	Cat# A6964
Activin A	eBioScience	Cat#14-8993
Arachidonic acid	Cayman Chemicals	Cat# 90010.1; CAS:506-32-1
BMP-4	Biotechne	Cat# 314-BP-050
CHIR99021	Selleckchem	Cat# S2924; CAS:1797989-42-4
CJ-13610	Sigma-Aldrich	Cat# SML0187; CAS:179420-17-8
DHP-1	(Willems et al., 2012)	N/A
DMEM medium (high glucose)	PAN Biotech	Cat# P04-03550
DMH-1	Biotechne	Cat# 4126; CAS:1206711-16-1
DRAQ5	Thermo Fisher Scientific	Cat# 62251
Fetal bovine serum	Gibco	Cat# 10500-084
FGF-2	Peprtech	Cat# 100-18B
Geneticin (G418)	Sigma-Aldrich	Cat# 8168
GPx	Sigma-Aldrich	Cat# G6137
GSH	Sigma-Aldrich	Cat# G4251; CAS:70-18-8
HDSF	Santa Cruz Biotech.	Cat# sc-221708; CAS: 86855-26-7
ITS Premix Universal Culture Supplement	BD Corning	Cat# 354350
KnockOUT DMEM	ThermoFisher Scientific	Cat# 10829018
L-Glutamine	PAN Biotech	Cat# P04-80100
Lipofectamine 2000	ThermoFischer Scientific	Cat# 11668027
Matrigel	BD Corning	Cat# 354263
NHS activated magnetic sepharose beads	GE Healthcare	Cat# 28-9513-80

(Continued on next page)

Continued

REAGENT or RESOURCE	SOURCE	IDENTIFIER
Non-essential amino acids	PAN Biotech	Cat# P08-32100
Okadaic acid	Santa Cruz Biotech.	Cat# sc-3513; CAS: 78111-17-8
Opti-MEM	Gibco	Cat# 31985-062
p-Nitrophenyl phosphate	Calbiochem	Cat# 4876; CAS: 4264-83-9
Penicillin-Streptomycin-Glutamine	Thermo Fisher Scientific	Cat# 10378016
Protein phosphatase 1	this paper	
Purmorphamine	Cayman	Cat# Cay10009634; CAS: 483367-10-8
SB-431542	Biotechne	Cat# 1614; CAS:301836-41-9
Sodium pyruvate	PAN Biotech	Cat# P04-43100
Sodium selenite	Sigma-Aldrich	Cat# S5261
TGF- β 2	Sigma-Aldrich	Cat# GF113
Transferrin	Sigma-Aldrich	Cat# T8158
TrypLE	Thermo Fisher Scientific	Cat# 12563011
Vismodegib (GDC-0449)	Seleckchem	Cat# S1082; CAS:879085-55-9
Wheat Germ Agglutinin (WGA) GA-Alexa Fluor 488	Thermo Fisher Scientific	Cat# W11261
Wnt-C59	Biotechne	Cat# 5148; CAS:1243243-89-1
Y-27632	Biotechne	Cat# 1254; CAS:129830-38-2
Zeocin	Invivogen	Cat# ant-zn-1
β -glucosidase	Sigma-Aldrich	Cat# G4511
Critical Commercial Assays		
Cell Line Nucleofector Kit V	Lonza	Cat# VCA-1003
CellTiter-Glo cell viability assay	Promega	Cat# G7570
Dual-Luciferase® Reporter Assay	Promega	Cat# E1960
Duolink PLA Red Kit	Sigma-Aldrich	Cat# DUO92101
FastLane Cell cDNA Kit	Qiagen	Cat# 215011
OneGlo Luciferase assay system	Promega	Cat# E6110
QuantiFast SYBR Green PCR Kit	Qiagen	Cat# 204056
SSO Advanced Universal SYBR Green Supermix	Bio-Rad	Cat# 1725270
Experimental Models: Cell Lines		
HEK293-Fz; TOPflash (female)	(Park et al., 2006)	
HEK293-T cells (female)	DSMZ	Cat#ACC-635; RRID:CVCL_0063
Human foreskin fibroblasts (male)	ATCC	Cat# CRL-2097; RRID:CVCL_2337
Human iPS (male)	(Greber et al., 2011)	N/A
Human PMNL	DRK Blutspendedienst Baden-Württemberg-Hessen, Germany	N/A
L cells (male)	ATCC	Cat# CRL-1.3
L Wnt3a cells (male)	ATCC	Cat# CRL-2647; RRID:CVCL_0635
NIH/3T3 cells (male)	DSMZ	Cat# ACC59; RRID:CVCL_0594
SHH-LIGHT2 cells (male)	(Taipale et al., 2000)	
U-2OS cells (female)	CLS	Cat# 300364; RRID:CVCL_0042
Oligonucleotides		
AXIN2 F AGGGACAGGAATCATTGGGC	Eurofins	N/A
AXIN2 R GTGGACACCTGCCAGTTTCT	Eurofins	N/A

(Continued on next page)

Continued

REAGENT or RESOURCE	SOURCE	IDENTIFIER
<i>Gapdh F</i> CAGTGCCAGCCTCGTC	Eurofins	N/A
<i>GAPDH F</i> TCAGCCGCATCTTCTTTTGCG	Eurofins	N/A
<i>Gapdh R</i> CAATCTCCACTTTGCCACTG	Eurofins	N/A
<i>GAPDH R</i> GGCGCCAATACGACCAA	Eurofins	N/A
<i>Ptch1 F</i> CTCTGGAGCAGATTCCAAGG	(Lipinski et al., 2006) Eurofins	N/A
<i>Ptch1 R</i> TGCCGCAGTTCTTTGAATG	(Lipinski et al., 2006) Eurofins	N/A
Recombinant DNA		
BRE luciferase vector	(Korchynskiy and Ten Dijke, 2002)	Addgene plasmid #45126
M50 Super8×TOPflash reporter vector	(Veeman et al., 2003)	Addgene plasmid #12456
pcDNA3.1-Flag-5-LO	(Mahshid et al., 2015)	N/A
pEGFP-C2-5LO	(Chen and Funk, 2001)	N/A
pET22b-PP1	this paper	
pT3 ALOX 5 wt	(Schröder et al., 2014)	N/A
SBE-4 luciferase vector	(Zawel et al., 1998)	Addgene plasmid #16495
TK-driven <i>Renilla</i> luciferase co-reporter vector	Promega	Cat#E2241
Wnt-3a expressing vector	Upstate Biotech.	Cat# 21-124
Software and Algorithms		
FlowJo		RRID:SCR_008520 https://www.flowjo.com/solutions/flowjo
GraphPadPrism 6.0	GraphPad	RRID:SCR_002798 https://www.graphpad.com/scientific-software/prism/
Image Studio	LI-COR	RRID:SCR_015795 https://www.licor.com/bio/products/software/image_studio/
ImageJ	(Rasband, 1997-2016)	RRID:SCR_003070 https://imagej.nih.gov/ij/
MaxQuant	(Cox and Mann, 2008)	RRID:SCR_014485 http://www.biochem.mpg.de/5111795/maxquant
Quattro/Workflow	quattro researchGmbH	http://www.quattro-research.com/
SPIDER	(Reker et al., 2014a, 2014b)	http://www.cadd.ethz.ch/software/spider.html
Other		
ÄKTA express system	GE Healthcare	https://www.gelifesciences.com/shop/chromatography/chromatography-systems/aktaxpress-p-06166?current=18664501
CFX96 Touch real time PCR detection system	Bio-Rad	https://www.bio-rad.com/en-us/product/cfx96-touch-real-time-pcr-detection-system
Echo520 acoustic dispenser	Labcyte	https://www.labcyte.com/products/liquidhandling/echo-520-liquid-handler

(Continued on next page)

Continued

REAGENT or RESOURCE	SOURCE	IDENTIFIER
Infinite M200 plate reader	Tecan	https://lifesciences.tecan.com/microplate-readers
iQ™5 Real-Time PCR Detection System	Bio-Rad	N/A
LSRII flow cytometer	BD Biosciences	https://www.bdbiosciences.com/us/instruments/research/cell-analyzers/c/744788
Nucleofector	Amaxa / Lonza	https://www.lonza.com/products-services/bio-research/transfection/nucleofector-devices.aspx
Observer Z1 microscope	Zeiss	https://www.zeiss.com/microscopy/int/products/light-microscopes/axio-observer-for-biology.html
Odyssey Fc imaging system	LI-COR	https://www.licor.com/bio/products/imaging_systems/odyssey_fc/
Odyssey®IR Scanner	LI-COR	www.licor.com
Q Exactive™ Hybrid Quadrupole-Orbitrap mass spectrometer equipped with a nano-spray source	Thermo Fisher Scientific	
SpectraMax Paradigm microplate reader	Molecular Devices	https://www.moleculardevices.com/systems/microplate-readers/multi-mode-readers/spectramax-paradigm-multi-mode-microplate-reader
Ultimate™ 3000 RSLC nano-HPLC system	Thermo Fisher Scientific	N/A
Data and Software Availability		N/A

CONTACT FOR REAGENTS AND RESOURCE SHARING

Further information and requests for resources and reagents should be directed to and will be fulfilled by the Lead Contact, Herbert Waldmann (Herbert.waldmann@mpi-dortmund.mpg.de)

EXPERIMENTAL MODEL AND SUBJECT DETAILS

The murine fibroblast cell line NIH/3T3 (male) was cultured in Dulbecco's Modified Eagle's medium (DMEM, high glucose) supplemented with 10 % heat-inactivated fetal calf serum, 2 mM L-glutamine and 1 mM sodium pyruvate. NIH/3T3 cells, stably transfected with a GLI-responsive firefly luciferase reporter plasmid (Sasaki et al., 1997) and a pRL-TK constitutive Renilla-luciferase expression vector (Promega) (SHH-LIGHT2 cells (Taipale et al., 2000)) were cultured in the same culturing medium as the non-transfected cells, additionally supplemented with 400 µg/ml G-418 and 150 µg/ml Zeocin as selecting agents.

The human bone osteosarcoma cell line U-2OS (female) was cultured in DMEM (high glucose) supplemented with 10% fetal bovine serum, 4 mM L-glutamine, 1 mM sodium pyruvate and non-essential amino acids.

The human embryonic kidney cell line HEK293T (female), which constitutively expresses the simian virus 40 (SV40) large T antigen, was cultured in DMEM (high glucose) supplemented with 10% fetal bovine serum, 4 mM L-glutamine, 1 mM sodium pyruvate and non-essential amino acids.

Mouse fibroblast L (L-M(TK-)) cells (male) and L Wnt3a cells (L cells stably expressing Wnt3a protein and delivering it to the medium) were cultured in DMEM (high glucose) supplemented with 10% fetal bovine serum, 4 mM L-glutamine, 1 mM sodium pyruvate and non-essential amino acids. The medium for L Wnt3a cells contained additionally 0.5 mg/ml G-418.

Human foreskin fibroblasts (male) were cultured in KnockOUT DMEM.

All cell lines were maintained at 37°C and 5% CO₂ in humidified atmosphere.

Human polymorphonuclear leukocytes (PMNL) were isolated from buffy coats (anonymous donors, therefore sex unknown) obtained from the German Red Cross (DRK Blood Donation Service Baden-Württemberg-Hessen, Frankfurt am Main, Germany).

METHOD DETAILS

General Information - Chemistry

All commercially available compounds were used as provided without further purifications. Dry solvents (e.g. tetrahydrofuran (THF), dichloromethane (DCM)) were used as commercially available. Solvents for chromatography were laboratory reagent grade or HPLC grade.

Analytical thin-layer chromatography (TLC) was performed on *Merck silica gel aluminium plates* with F-254 indicator. Compounds were visualized by irradiation with UV light or potassium permanganate staining. Column chromatography was performed using *silica gel Acros 60 A* (particle size 0.035-0.070 nm). Solvent mixtures for chromatography are understood as volume/volume.

$^1\text{H-NMR}$ and $^{13}\text{C-NMR}$ were recorded on a *Bruker DRX400* (400 MHz), *Mercury VX 400* (400 MHz), *Bruker DRX500* (500 MHz), *INOVA500* (500 MHz) and *Bruker DRX600* (600 MHz) using CDCl_3 , CD_3OD , acetone- D_6 , DMSO-D_6 as solvents. Data are given in the following order: chemical shift (δ) values are reported in ppm with the solvent resonance as internal standard (CDCl_3 : $\delta = 7.26$ ppm for ^1H , $\delta = 77.16$ ppm for ^{13}C ; CD_3OD : $\delta = 3.31$ ppm for ^1H , $\delta = 49.00$ ppm for ^{13}C ; acetone- D_6 : $\delta = 2.05$ ppm for ^1H , $\delta = 29.84$ ppm for ^{13}C ; DMSO-D_6 : $\delta = 2.50$ ppm for ^1H , $\delta = 39.52$ ppm for ^{13}C); multiplicities are indicated as: brs (broadened singlet), s (singlet), d (doublet), dd (double doublet), t (triplet), q (quartet), m (multiplet); coupling constants are given in Hertz (Hz).

High resolution mass spectra were recorded on a *LTQ Orbitrap* mass spectrometer coupled to an *Accela HPLC-System* (flow injection: 50% (containing 0.1% formic acid) water and 50% (containing 0.1% formic acid) acetonitrile, flow rate: 250 $\mu\text{L}/\text{min}$).

Gas chromatography-mass spectra (GC-MS) were recorded on an *Agilent 7890A GC System* (column: *Agilent DB-5MS*) coupled to an *Agilent 5975 inert XL MSD* mass analyzer using electron impact (70 eV) as ionization method.

Enantiomeric purity for "Lipoxygenin" (**1d**) was determined by HPLC analysis using an *Agilent 1100* system and a chiral stationary phase column (column: *CHIRALPAK IA*, 4.6 x 250 mm; eluent: 20% DCM/EtOH (100/2) / 80% *iso*-hexane, flow rate: 0.5 mL/min).

Optical rotations were determined on a *Schmidt & Haensch Polartronic HH8* polarimeter. Melting points were measured on a *Büchi 530* melting point apparatus.

Preparative HPLC purifications were carried out on an *Agilent HPLC 1100 series* system using a reversed-phase C4 or C18 column (*NUCLEODUR C4* or *C18*, diameter 10 mm, *Macherey & Nagel*).

Method 1 (C4): flow rate 6.0 mL/min, from 10% A to 100% A over 25 min (using B as cosolvent); (A = acetonitrile, B = water).

Method 2 (C18): flow rate 6.0 mL/min, from 25% A to 100% A over 45 min (using B as cosolvent); (A = acetonitrile, B = water).

Method 3 (C18): flow rate 6.0 mL/min, from 10% C to 100% C over 45 min (using D as co-solvent); (C = acetonitrile + 0.1% trifluoroacetic acid, D = water + 0.1% trifluoroacetic acid).

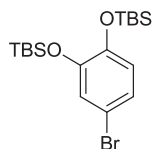
Chiral preparative HPLC purification of "Lipoxygenin" (**1d**) was carried out on a *DIONEX Ultimate 3000* system and a chiral stationary phase column (column: *CHIRALPAK IA*, 10 x 250 mm; eluent: 20% DCM/EtOH (100/2) / 80% *iso*-hexane, flow rate: 2.4 mL/min).

Synthesis of the Compound Collection

The general synthesis strategy for the compounds described herein has already been published by our group (P. Schröder, T. Förster et al., *Angew. Chem. Int. Ed.*, 2015, **54**, 42, 12398-12403).

Synthesis of Building Blocks

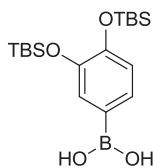
((4-Bromo-1,2-phenylene)bis(oxy))bis(*tert*-butyldimethylsilane) (**5**)



A mixture of 4-bromobenzene-1,2-diol (400 mg, 2.12 mmol) and imidazole (317 mg, 4.66 mmol) in dry dichloromethane (16 mL) was treated dropwise with a solution of *tert*-butylchlorodimethylsilane (703 mg, 4.66 mmol) in dry dichloromethane (2 mL). The mixture was stirred overnight and subsequently water (10 mL) and dichloromethane (20 mL) were added. The organic layer was separated and the aqueous phase was extracted two times with dichloromethane (20 mL). The combined organic layers were washed with brine (20 mL) and dried over MgSO_4 . The solvent was completely removed under reduced pressure and the residue was purified by flash chromatography on silica gel (petroleum ether).

Colorless oil, 79%; R_f : 0.36 (petroleum ether); $^1\text{H-NMR}$ (400 MHz, CDCl_3): $\delta = 0.19$ (s, 6H), 0.20 (s, 6H), 0.97 (s, 9H), 0.98 (s, 9H), 6.69 (d, $^3J = 8.5$ Hz, 1H), 6.92 (dd, $^3,4J = 8.5, 2.5$ Hz, 1H), 6.95 (d, $^4J = 2.4$ Hz, 1H); $^{13}\text{C-NMR}$ (101 MHz, CDCl_3): $\delta = -4.01, -3.97, 18.59, 18.61, 26.03, 26.06, 112.88, 122.32, 124.37, 124.43, 146.55, 148.03$; ESI-MS: m/z 417.13 $[\text{M}+\text{H}]^+$; HRMS (ESI): calculated for $\text{C}_{18}\text{H}_{34}\text{O}_2\text{BrSi}_2$ m/z 417.12752 $[\text{M}+\text{H}]^+$, found m/z 417.12728 $[\text{M}+\text{H}]^+$.

(3,4-Bis(*tert*-butyldimethylsilyloxy)phenyl)boronic acid (**6**)

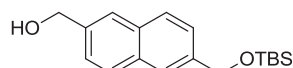


To a solution of ((4-bromo-1,2-phenylene)bis(oxy))bis(*tert*-butyldimethylsilane) (**5**) (460 mg, 1.10 mmol) in dry tetrahydrofuran (3.5 mL) at -78°C was added *n*-BuLi solution (2.5 M in hexane, 530 μL , 1.32 mmol) dropwise and the mixture was stirred for 30 min before triisopropyl borate (510 μL , 2.20 mmol) was added. The resulting solution was stirred for 1 h at -78°C and then for an additional 1 h at ambient temperature. The reaction mixture was quenched by adding hydrochloric acid (1 M, 10 mL) and ethyl acetate (20 mL). The organic layer was separated and the aqueous phase was extracted three times with ethyl acetate (15 mL).

The combined organic layers were washed with brine (20 mL) and dried over Na_2SO_4 . The solvent was completely removed under reduced pressure and the residue was purified by flash chromatography (short column) on silica gel (30% ethyl acetate/petroleum ether).

Glacial gum, 70%; R_f : 0.48 (50% ethyl acetate/petroleum ether); $^1\text{H-NMR}$ (500 MHz, CDCl_3): δ = 0.27 (s, 6H), 0.28 (s, 6H), 1.03 (s, 9H), 1.05 (s, 9H), 6.96 (d, 3J = 7.8 Hz, 1H), 7.64–7.69 (m, 1H), 7.70 (d, 4J = 1.5 Hz, 1H); $^{13}\text{C-NMR}$ (126 MHz, CDCl_3): δ = -3.85, -3.80, 18.63, 18.70, 26.09, 26.18, 120.99, 123.66, 128.04, 129.76, 146.76, 151.32.

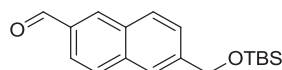
6-(((*tert*-Butyldimethylsilyloxy)methyl)naphthalen-2-yl)methanol (**7**)



To a mixture of naphthalen-2,6-diylmethanol (1.50 g, 8.0 mmol) and imidazole (212 mg, 3.1 mmol) in dry tetrahydrofuran (65 mL) at 0°C was added *tert*-butylchlorodimethylsilane (475 mg, 3.2 mmol) portionwise. The mixture was slowly brought to ambient temperature overnight. The mixture was diluted with brine (30 mL) and extracted four times with a mixture of petroleum ether/diethyl ether (4:1, 4 x 30 mL). The combined organic layers were washed with brine (30 mL) and dried over MgSO_4 . The solvent was completely removed under reduced pressure and the residue was purified by flash chromatography on silica gel (30% ethyl acetate/petroleum ether).

Colorless solid, 62%; mp $68\text{--}69^\circ\text{C}$; R_f : 0.35 (33% ethyl acetate/petroleum ether); $^1\text{H-NMR}$ (500 MHz, CDCl_3): δ = 0.14 (s, 6H), 0.98 (s, 9H), 4.85 (s, 2H), 4.90 (s, 2H), 7.42–7.49 (m, 2H), 7.76–7.85 (m, 4H); $^{13}\text{C-NMR}$ (126 MHz, CDCl_3): δ = -5.03, 18.64, 26.14, 65.29, 65.70, 124.38, 125.15, 125.44, 125.48, 128.01, 128.45, 132.78, 133.06, 138.10, 139.22; ESI-MS: m/z 285.17 $[(\text{M}-\text{H}_2\text{O})+\text{H}]^+$; HRMS (ESI): calculated for $\text{C}_{18}\text{H}_{25}\text{OSi}$ m/z 285.16692 $[(\text{M}-\text{H}_2\text{O})+\text{H}]^+$, found m/z 285.16732 $[(\text{M}-\text{H}_2\text{O})+\text{H}]^+$.

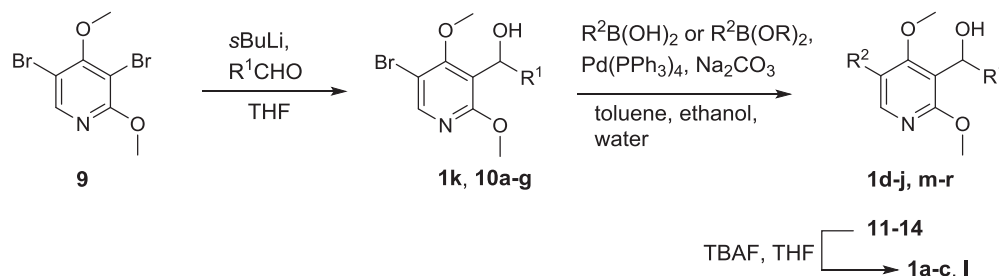
6-(((*tert*-Butyldimethylsilyloxy)methyl)-2-naphthaldehyde (**8**)



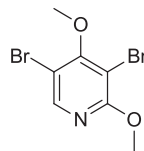
DMP solution (15wt% in dichloromethane, 3.8 mL, 1.8 mmol) was added dropwise to a solution of alcohol **7** (300 mg, 990 μmol) in dry dichloromethane (12 mL) at ambient temperature. The mixture was stirred for 1 h before sat. NaHCO_3 solution (15 mL), ethyl acetate (40 mL) and sodium thiosulfate (1.5 g, 9.5 mmol) were added. The heterogeneous mixture was stirred until both phases became clear. The organic layer was separated and the aqueous phase was extracted with ethyl acetate (20 mL). The combined organic layers were washed with brine (15 mL) and dried over MgSO_4 . The solvent was completely removed under reduced pressure and the residue was purified by flash chromatography on silica gel (5% ethyl acetate/petroleum ether).

Colorless wax, 89%; R_f : 0.39 (10% ethyl acetate/petroleum ether); $^1\text{H-NMR}$ (500 MHz, CDCl_3): δ = 0.15 (s, 6H), 0.99 (s, 9H), 4.93 (s, 2H), 7.54 (d, 3J = 8.3 Hz, 1H), 7.85 (s, 1H), 7.90–7.99 (m, 3H), 8.32 (s, 1H), 10.15 (s, 1H); $^{13}\text{C-NMR}$ (126 MHz, CDCl_3): δ = -5.07, 18.62, 26.11, 65.02, 123.17, 124.46, 125.81, 129.15, 129.61, 132.02, 134.01, 134.43, 136.72, 142.96, 192.38; GC-MS: m/z 300.3 $[\text{M}]^+$; HRMS (ESI): calculated for $\text{C}_{18}\text{H}_{25}\text{O}_2\text{Si}$ m/z 301.16183 $[\text{M}+\text{H}]^+$, found m/z 301.16226 $[\text{M}+\text{H}]^+$.

Synthesis of the Compound Collection of Substituted Pyridines



3,5-dibromo-2,4-dimethoxy pyridine (**9**)

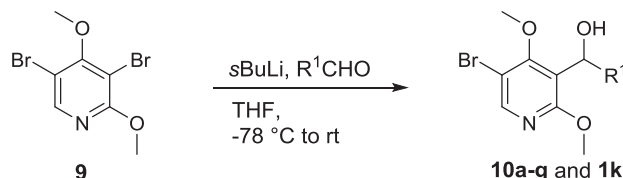


3,5-Dibromo-2,4-dimethoxy pyridine (**9**) was synthesized according to a published procedure (N. R. Irlapati, R. M. Adlington, A. Conte, G. J. Pritchard, R. Marquez, J. E. Baldwin, *Tetrahedron* 2004, 60, 9307-9317). To a cooled (0°C) solution of 2,4-dihydroxypyridine (4.0 g, 36.0 mmol) in 47% aqueous hydrobromic acid (45 mL) was added bromine (4.1 mL, 79.3 mmol) under constant stirring. The resulting mixture was allowed to come to room-temperature and stirred for 1 h. The reaction mixture was diluted with water (120 mL), and stirred for further 30 min at room temperature. The solid product was then filtered, washed with water (80 mL), and dried under vacuum. The crude residue was recrystallized from 95% ethanol to afford 5.3 g (56%) of the known 3,5-dibromo-2,4-dihydroxypyridine as a colorless solid.

To a suspension of 3,5-dibromo-2,4-dihydroxypyridine (5.82 g, 21.7 mmol) and silver carbonate (11.9 g, 43.4 mmol) in dry dichloromethane (450 mL) was added methyl iodide (13.3 mL, 217 mmol). The resulting mixture was stirred for 5 days under light exclusion and then filtered through a pad of celite. The filtrate was completely concentrated under reduced pressure and the residue was purified by flash chromatography on silica gel (2% ethyl acetate/petroleum ether) to give 3,5-Dibromo-2,4-dimethoxypyridine (**9**) as colorless solid.

Colorless solid; R_f : 0.28 (2% ethyl acetate/petroleum ether); $^1\text{H-NMR}$ (400 MHz, CDCl_3): δ = 3.95 (s, 3H), 3.99 (s, 3H), 8.14 (s, 1H); $^{13}\text{C-NMR}$ (101 MHz, CDCl_3): δ = 55.19, 60.90, 102.49, 107.92, 147.29, 161.53, 162.55.

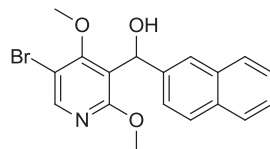
General Procedure 1 (GP 1): Regioselective Lithiation/Addition Reaction Using 3,5-dibromo-2,4-dimethoxypyridine 9.



A 0.1 M solution of 3,5-dibromo-2,4-dimethoxypyridine (1.0 eq.) in dry tetrahydrofuran was cooled to -78°C and *sec*-BuLi solution (1.4 M in cyclohexane, 0.9 eq.) was added dropwise over a duration of 10 min. The mixture was stirred for 1 h at the same temperature before adding a tetrahydrofuran (dry) solution (1.2 M) of the aldehyde (2.5 eq.) dropwise. The mixture was stirred for an additional hour at -78°C before warming up to ambient temperature with continued stirring overnight. The mixture was quenched with a 1:1 mixture of sat. NH_4Cl solution and water and extracted three times with ethyl acetate. The combined organic phases were washed with brine and dried over MgSO_4 . The solvent was completely removed under reduced pressure and the residue was purified by flash chromatography on silica gel (ethyl acetate/petroleum ether).

Representative example:

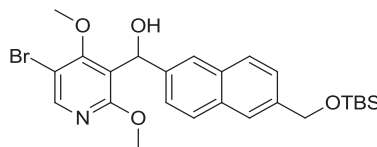
(±)-(5-Bromo-2,4-dimethoxypyridin-3-yl)(naphthalen-2-yl)methanol (**1k**)



Pyridine **9** (300 mg, 1.01 mmol) was dissolved in dry tetrahydrofuran (10 mL), the solution was cooled to -78°C and *sec*-BuLi solution (1.4 M in cyclohexane, 660 μL , 918 μmol) was added dropwise at the same temperature. The solution was stirred for 1 h at -78°C before a solution of 2-naphthaldehyde (394 mg, 2.52 mmol) in dry tetrahydrofuran (2 mL) was added dropwise. The mixture was stirred for an additional hour at -78°C before warming up to ambient temperature with continued stirring overnight. The mixture was quenched by adding water (4 mL), sat. NH_4Cl solution (4 mL) and ethyl acetate (30 mL). The aqueous layer was separated and extracted two times with ethyl acetate (15 mL). The combined organic phases were washed with brine (15 mL) and dried over MgSO_4 . The solvent was completely removed under reduced pressure and the residue was purified by flash chromatography on silica gel (10-20% ethyl acetate/petroleum ether).

Colorless oil, 78%; R_f : 0.29 (20% ethyl acetate/petroleum ether); $^1\text{H-NMR}$ (400 MHz, CDCl_3): δ = 3.74 (s, 3H), 3.92 (s, 3H), 6.35 (s, 1H), 7.42-7.50 (m, 3H), 7.76-7.84 (m, 4H), 8.24 (s, 1H); $^{13}\text{C-NMR}$ (101 MHz, CDCl_3): δ = 54.38, 61.73, 68.55, 107.96, 120.65, 123.85, 124.20, 125.95, 126.24, 127.70, 128.13, 132.77, 133.27, 140.76, 148.81, 162.14, 162.70; ESI-MS: m/z 374.00 $[\text{M}+\text{H}]^+$; HRMS (ESI): calculated for $\text{C}_{18}\text{H}_{17}\text{O}_3\text{NBr}$ m/z 374.03863 $[\text{M}+\text{H}]^+$, found m/z 374.03987 $[\text{M}+\text{H}]^+$.

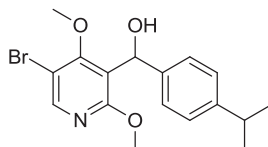
(±)-(5-Bromo-2,4-dimethoxy-pyridin-3-yl)(6-(((*tert*-butyldimethylsilyloxy)-methyl)naphthalen-2-yl)methanol (**10a**)



Deviating from GP I, pyridine **9** (150 mg, 505 μ mol) was dissolved in dry tetrahydrofuran (5 mL). The solution was cooled to -78°C and *sec*-BuLi solution (1.4 M in cyclohexane, 330 μ L, 459 μ mol) was added dropwise at the same temperature. The solution was stirred for 45 min at -78°C before a solution of aldehyde **8** (225 mg, 750 μ mol) in dry tetrahydrofuran (1 mL) was added dropwise. The mixture was stirred for an additional hour at -78°C before warming up to ambient temperature with continued stirring overnight. The mixture was quenched by adding water (4 mL), sat. NH_4Cl solution (4 mL) and ethyl acetate (30 mL). The organic layer was separated and the aqueous layer was extracted two times with ethyl acetate (15 mL). The combined organic phases were washed with brine (15 mL) and dried over MgSO_4 . The solvent was completely removed under reduced pressure and the residue was purified by flash chromatography on silica gel (10% ethyl acetate/petroleum ether).

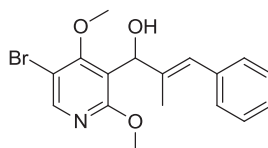
Colorless oil, 76%; R_f : 0.34 (20% ethyl acetate/petroleum ether); $^1\text{H-NMR}$ (600 MHz, CDCl_3): δ = 0.14 (s, 6H), 0.98 (s, 9H), 3.73 (s, 3H), 3.92 (s, 3H), 4.90 (s, 2H), 6.34 (s, 1H), 7.42-7.46 (m, 2H), 7.76 (s, 2H), 7.78 (dd, $^3J = 8.5, 3.1$ Hz, 2H), 8.24 (s, 1H); $^{13}\text{C-NMR}$ (151 MHz, CDCl_3): δ = -5.06, 18.60, 26.11, 54.37, 61.71, 65.24, 68.57, 107.97, 120.75, 123.70, 124.25, 124.31, 125.08, 128.09, 128.13, 132.54, 132.72, 139.14, 140.43, 148.79, 162.15, 162.71; ESI-MS: m/z 518.15 $[\text{M}+\text{H}]^+$; HRMS (ESI): calculated for $\text{C}_{25}\text{H}_{33}\text{O}_4\text{NBrSi}$ m/z 518.13567 $[\text{M}+\text{H}]^+$, found m/z 518.13637 $[\text{M}+\text{H}]^+$.

(±)-(5-Bromo-2,4-dimethoxy-pyridin-3-yl)(4-isopropylphenyl)methanol (**10b**)



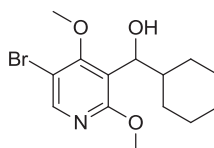
Colorless oil, 73%; R_f : 0.27 (20% ethyl acetate/petroleum ether); $^1\text{H-NMR}$ (600 MHz, CDCl_3): δ = 1.23 (d, $^3J = 6.9$ Hz, 6H), 2.84-2.92 (m, 1H), 3.74 (s, 3H), 3.92 (s, 3H), 6.15 (s, 1H), 7.17 (d, $^3J = 8.2$ Hz, 2H), 7.25 (d, $^3J = 8.1$ Hz, 2H), 8.19 (s, 1H); $^{13}\text{C-NMR}$ (151 MHz, CDCl_3): δ = 24.05, 33.79, 54.25, 61.59, 68.40, 107.91, 120.87, 125.60, 126.36, 140.61, 147.93, 148.48, 162.06, 162.49; ESI-MS: m/z 366.13 $[\text{M}+\text{H}]^+$; HRMS (ESI): calculated for $\text{C}_{17}\text{H}_{21}\text{O}_3\text{NBr}$ m/z 366.06993 $[\text{M}+\text{H}]^+$, found m/z 366.07070 $[\text{M}+\text{H}]^+$.

(±)-(E)-1-(5-Bromo-2,4-dimethoxy-pyridin-3-yl)-2-methyl-3-phenylprop-2-en-1-ol (**10c**)



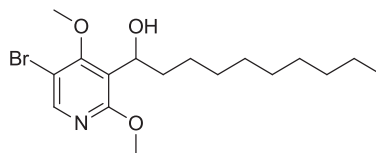
Colorless oil, 80%; R_f : 0.28 (20% ethyl acetate/petroleum ether); $^1\text{H-NMR}$ (500 MHz, CDCl_3): δ = 1.85 (s, 3H), 3.76 (bs, 1H), 3.96 (s, 3H), 3.99 (s, 3H), 5.58 (s, 1H), 6.58 (s, 1H), 7.21-7.29 (m, 3H), 7.35 (t, $^3J = 7.6$ Hz, 2H), 8.23 (s, 1H); $^{13}\text{C-NMR}$ (126 MHz, CDCl_3): δ = 15.45, 54.31, 61.84, 71.24, 107.99, 119.51, 124.22, 126.52, 128.23, 129.05, 137.77, 138.77, 148.55, 162.27, 162.81; ESI-MS: m/z 364.01 $[\text{M}+\text{H}]^+$; HRMS (ESI): calculated for $\text{C}_{17}\text{H}_{19}\text{O}_3\text{NBr}$ m/z 364.05428 $[\text{M}+\text{H}]^+$, found m/z 364.05459 $[\text{M}+\text{H}]^+$.

(±)-(5-Bromo-2,4-dimethoxy-pyridin-3-yl)(cyclohexyl)methanol (**10d**)



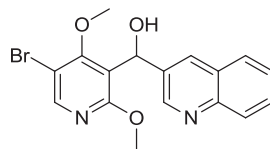
Colorless oil, 63%; R_f : 0.15 (10% ethyl acetate/petroleum ether); $^1\text{H-NMR}$ (400 MHz, CDCl_3): δ = 0.83-1.29 (m, 6H), 1.57-1.66 (m, 2H), 1.69-1.82 (m, 2H), 2.13-2.21 (m, 1H), 3.03 (bs, 1H), 3.90 (s, 3H), 3.94 (s, 3H), 4.58 (d, $^3J = 9.1$ Hz, 1H), 8.11 (s, 1H); $^{13}\text{C-NMR}$ (101 MHz, CDCl_3): δ = 26.01, 26.10, 26.47, 29.62, 30.07, 43.55, 54.12, 61.67, 72.59, 107.97, 120.31, 147.85, 162.15, 162.56; ESI-MS: m/z 330.17 $[\text{M}+\text{H}]^+$; HRMS (ESI): calculated for $\text{C}_{14}\text{H}_{21}\text{O}_3\text{NBr}$ m/z 330.06993 $[\text{M}+\text{H}]^+$, found m/z 330.07043 $[\text{M}+\text{H}]^+$.

(±)-1-(5-Bromo-2,4-dimethoxyphenyl)decan-1-ol (**10e**)



Colorless oil, 68%; R_f : 0.16 (10% ethyl acetate/petroleum ether); $^1\text{H-NMR}$ (400 MHz, CDCl_3): δ = 0.87 (t, 3J = 6.9 Hz, 3H), 1.20-1.34 (m, 13H), 1.43-1.53 (m, 1H), 1.61-1.72 (m, 1H), 1.84-1.94 (m, 1H), 3.91 (s, 3H), 3.97 (s, 3H), 4.90-4.96 (m, 1H), 8.13 (s, 1H); $^{13}\text{C-NMR}$ (101 MHz, CDCl_3): δ = 14.24, 22.81, 26.28, 29.44, 29.56, 29.68, 29.69, 32.02, 37.35, 54.17, 61.83, 67.89, 108.13, 121.40, 147.78, 162.05, 162.18; ESI-MS: m/z 374.24 $[\text{M}+\text{H}]^+$; HRMS (ESI): calculated for $\text{C}_{17}\text{H}_{29}\text{O}_3\text{NBr}$ m/z 374.13253 $[\text{M}+\text{H}]^+$, found m/z 374.13370 $[\text{M}+\text{H}]^+$.

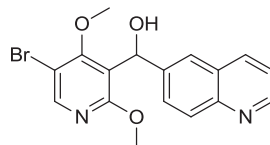
(±)-5-(5-Bromo-2,4-dimethoxyphenyl)(quinolin-3-yl)methanol (**10f**)



Deviating from general procedure I, the reaction mixture was stirred for 1 h at -78°C after the addition of the aldehyde and then the mixture was brought to ambient temperature and stirred for an additional hour (not overnight!). The work up follows the same way as described above.

Colorless wax, 65%; R_f : 0.18 (50% ethyl acetate/petroleum ether); $^1\text{H-NMR}$ (500 MHz, CDCl_3): δ = 3.80 (s, 3H), 3.86 (s, 3H), 4.38 (bs, 1H), 6.39 (s, 1H), 7.52 (t, 3J = 7.5 Hz, 1H), 7.67 (t, 3J = 7.6 Hz, 1H), 7.78 (d, 3J = 8.2 Hz, 1H), 8.05-8.10 (m, 2H), 8.21 (s, 1H), 8.89 (s, 1H); $^{13}\text{C-NMR}$ (126 MHz, CDCl_3): δ = 54.41, 61.89, 66.71, 107.85, 119.44, 127.01, 127.71, 127.94, 129.01, 129.52, 132.31, 136.07, 147.17, 149.04, 149.32, 161.92, 162.77; ESI-MS: m/z 375.18 $[\text{M}+\text{H}]^+$; HRMS (ESI): calculated for $\text{C}_{17}\text{H}_{16}\text{O}_3\text{N}_2\text{Br}$ m/z 375.03388 $[\text{M}+\text{H}]^+$, found m/z 375.03556 $[\text{M}+\text{H}]^+$.

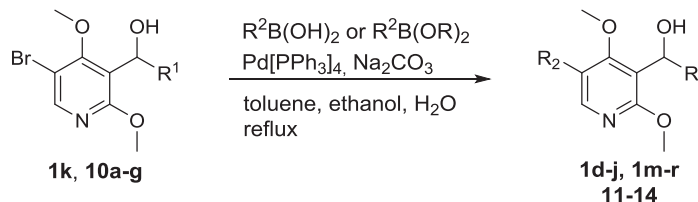
(±)-5-(5-Bromo-2,4-dimethoxyphenyl)(quinolin-6-yl)methanol (**10g**)



Deviating from general procedure I, the reaction mixture was stirred for 1 h at -78°C after the addition of the aldehyde and then the mixture was brought to ambient temperature and stirred for an additional hour (not overnight!). The work up follows the same way as described above.

Colorless wax, 48%; R_f : 0.34 (50% ethyl acetate/petroleum ether); $^1\text{H-NMR}$ (400 MHz, CDCl_3): δ = 3.72 (s, 3H), 3.84 (s, 3H), 6.34 (s, 1H), 7.34 (dd, 3J = 8.3, 4.3 Hz, 1H), 7.64 (dd, 3,4J = 8.8, 2.0 Hz, 1H), 7.77 (s, 1H), 8.01 (d, 3J = 8.8 Hz, 1H), 8.09 (t, 3J = 8.4 Hz, 1H), 8.18 (s, 1H), 8.81 (dd, 3,4J = 4.2, 1.6 Hz, 1H); $^{13}\text{C-NMR}$ (101 MHz, CDCl_3): δ = 54.31, 61.68, 67.93, 107.86, 120.34, 121.34, 123.64, 127.79, 127.98, 129.21, 136.35, 141.80, 147.42, 148.96, 150.16, 161.99, 162.75; ESI-MS: m/z 375.20 $[\text{M}+\text{H}]^+$; HRMS (ESI): calculated for $\text{C}_{17}\text{H}_{16}\text{O}_3\text{N}_2\text{Br}$ m/z 375.03388 $[\text{M}+\text{H}]^+$, found m/z 375.03443 $[\text{M}+\text{H}]^+$.

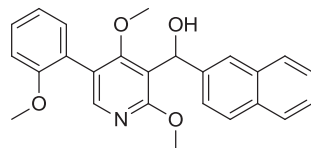
General Procedure II (GP II): Suzuki-Coupling Employing 5-bromopyridines.



A solution of the corresponding 5-bromopyridine (**1k**, **10a-g**, 1.0 eq.), boronic acid/boronic acid pinacol ester (1.8–2.0 eq.) and tetrakis(triphenyl)phosphine palladium(0) (6 mol%) in a 4:1 mixture of toluene/ethanol (0.05 M corresponding to the 5-bromopyridine) was treated with aqueous Na_2CO_3 solution (2 M, 70 percent of volume of the organic solvent). The reaction mixture was degassed and refluxed for 14-20 h. Ethyl acetate was added and the organic phase was separated and washed with water and brine. The phase was dried over MgSO_4 and filtered through a small pad of celite. The solvent was completely removed under reduced pressure and the residue was purified by flash chromatography on silica gel or by HPLC (see general information above).

Representative example:

(±)-(2,4-Dimethoxy-5-(2-methoxyphenyl)pyridin-3-yl)(naphthalen-2-yl)methanol (**1e**)

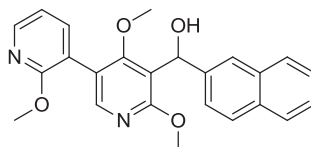


1k (50 mg, 133,6 μ mol), 2-methoxyphenyl boronic acid (36.5mg, 240.5 μ mol) and tetrakis triphenylphosphine palladium(0) (9.3 mg, 8.02 μ mol) were dissolved in a 4:1 mixture of toluene/ethanol (2.6 mL) and treated with Na_2CO_3 solution (2 M, 1.9 mL). The resulting mixture was degassed and refluxed for 20 h. After cooling to ambient temperature, ethyl acetate (40 mL) was added and the organic phase was separated and washed with water (15 mL) and brine (15 mL). The organic phase was dried over MgSO_4 and filtered through a small pad of celite. The filtrate was concentrated under reduced pressure and the residue was purified by flash chromatography on silica gel (30% ethyl acetate/petroleum ether).

Colorless oil, 90%; R_f : 0.22 (30% ethyl acetate/petroleum ether); $^1\text{H-NMR}$ (600 MHz, CDCl_3): δ = 3.22 (s, 3H), 3.81 (s, 3H), 4.00 (s, 3H), 4.28 (d, 3J = 11.7 Hz, 1H), 6.44 (d, 3J = 11.5 Hz, 1H), 6.99 (d, 3J = 8.2 Hz, 1H), 7.03 (td, $^3,^4J$ = 7.5, 1.0 Hz, 1H), 7.30 (dd, $^3,^4J$ = 7.5, 1.7 Hz, 1H), 7.35-7.39 (m, 1H), 7.42-7.48 (m, 2H), 7.55 (dd, $^3,^4J$ = 8.6, 1.7 Hz, 1H), 7.79-7.84 (m, 3H), 7.85 (s, 1H), 8.03 (s, 1H); $^{13}\text{C-NMR}$ (151 MHz, CDCl_3): δ = 54.02, 55.75, 60.53, 68.57, 111.17, 116.98, 120.82, 121.27, 123.87, 124.59, 124.65, 125.71, 126.05, 127.69, 127.90, 128.14, 129.60, 131.49, 132.70, 133.36, 141.76, 148.93, 157.19, 161.89, 164.25; ESI-MS: m/z 402.17 $[\text{M}+\text{H}]^+$; HRMS (ESI): calculated for $\text{C}_{25}\text{H}_{24}\text{O}_4\text{N}$ m/z 402.16998 $[\text{M}+\text{H}]^+$, found m/z 402.16943 $[\text{M}+\text{H}]^+$.

(To ensure that no palladium impurity remains with the molecule and influences the biological investigation, compound **1e** (48 mg) was dissolved in ethyl acetate (12 mL) and palladium scavenger SMOPEX 111 resin (250 mg) was added. The heterogeneous mixture was stirred at 50°C for 1 h and then an additional hour at ambient temperature. The mixture was then filtered and the filtrate was completely concentrated under reduced pressure. The residue was purified again by flash chromatography on silica gel as described above.)

(±)-Naphthalen-2-yl(2',4,6-trimethoxy-[3,3'-bipyridin]-5-yl)methanol (**1d**), "Lipoxygenin"



Colorless oil, 88%; R_f : 0.20 (33% ethyl acetate/petroleum ether); $^1\text{H-NMR}$ (600 MHz, CDCl_3): δ = 3.23 (s, 3H), 3.96 (s, 3H), 4.00 (s, 3H), 6.42 (s, 1H), 6.97 (dd, 3J = 7.3, 5.0 Hz, 1H), 7.42-7.48 (m, 2H), 7.52 (dd, $^3,^4J$ = 8.6, 1.7 Hz, 1H), 7.62 (dd, $^3,^4J$ = 7.3, 1.9 Hz, 1H), 7.78-7.85 (m, 4H), 8.07 (s, 1H), 8.22 (dd, $^3,^4J$ = 5.0, 1.9 Hz, 1H); $^{13}\text{C-NMR}$ (151 MHz, CDCl_3): δ = 54.01, 54.42, 61.02, 68.55, 117.06, 117.71, 118.67, 119.99, 123.97, 124.56, 125.92, 126.24, 127.80, 128.10, 128.23, 132.82, 133.43, 139.93, 141.51, 146.90, 148.71, 161.50, 162.30, 164.43; ESI-MS: m/z 403.44 $[\text{M}+\text{H}]^+$; HRMS (ESI): calculated for $\text{C}_{24}\text{H}_{23}\text{O}_4\text{N}_2$ m/z 403.16523 $[\text{M}+\text{H}]^+$, found m/z 403.16396 $[\text{M}+\text{H}]^+$.

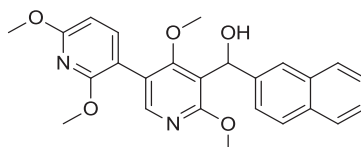
The pure enantiomers were separated by chiral HPLC (see general information).

(-)-enantiomer: α_D^{RT} = - 132.5 (c = 0.60 in CHCl_3).

(+)-enantiomer: α_D^{RT} = + 126.7 (c = 0.60 in CHCl_3).

(To ensure that no palladium impurity remains with the molecule and influence the biological investigation, compound **1d** (38 mg) was dissolved in ethyl acetate (10 mL) and palladium scavenger SMOPEX 111 resin (200 mg) was added. The heterogeneous mixture was stirred at 50°C for 1 h and then an additional hour at ambient temperature. The mixture was then filtered and the filtrate was completely concentrated under reduced pressure. The residue was purified again by flash chromatography on silica gel as described above.)

(±)-Naphthalen-2-yl(2',4,6,6'-tetramethoxy-[3,3'-bipyridin]-5-yl)methanol (**1f**)

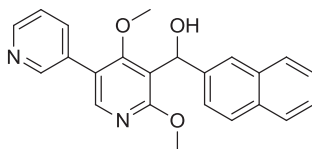


Colorless oil, 91%; R_f : 0.40 (30% ethyl acetate/petroleum ether); $^1\text{H-NMR}$ (600 MHz, CDCl_3): δ = 3.24 (s, 3H), 3.94 (s, 3H), 3.97 (s, 3H), 3.99 (s, 3H), 4.24 (d, 3J = 11.5 Hz, 1H), 6.38-6.44 (m, 2H), 7.42-7.48 (m, 2H), 7.51-7.55 (m, 2H), 7.78-7.85 (m, 4H), 8.06 (s, 1H); $^{13}\text{C-NMR}$ (151 MHz, CDCl_3): δ = 53.68, 53.70, 54.06, 60.63, 68.53, 101.22, 109.04, 117.48, 119.95, 123.87, 124.53,

125.75, 126.08, 127.68, 127.94, 128.13, 132.70, 133.34, 141.63, 142.46, 149.10, 159.91, 161.87, 163.00, 164.26; ESI-MS: m/z 433.17 [M+H]⁺; HRMS (ESI): calculated for C₂₅H₂₅O₅N₂ m/z 433.17580 [M+H]⁺, found m/z 433.17543 [M+H]⁺.

(To ensure that no palladium impurity remains with the molecule and influence the biological investigation, compound **1f** (62 mg) was dissolved in ethyl acetate (14 mL) and palladium scavenger SMOPEX 111 resin (300 mg) was added. The heterogeneous mixture was stirred at ambient temperature for 4 h. The mixture was then filtered and the filtrate was completely concentrated under reduced pressure. The residue was purified again by flash chromatography on silica gel as described above.)

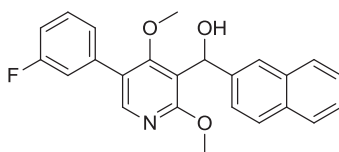
(±)-(4,6-Dimethoxy-[3,3'-bipyridin]-5-yl)(naphthalen-2-yl)methanol (**1g**)



The crude product was purified by HPLC (method 2).

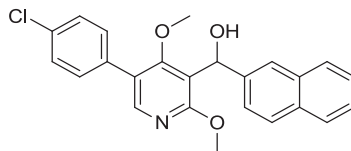
Colorless oil, 43%; R_f: 0.17 (3% methanol/dichloromethane); ¹H-NMR (600 MHz, CDCl₃): δ = 3.20 (s, 3H), 4.00 (s, 3H), 4.16 (d, ³J = 11.6 Hz, 1H), 6.43 (d, ³J = 11.6 Hz, 1H), 7.37 (ddd, ^{3,4}J = 7.9, 4.8, 0.8 Hz, 1H), 7.43-7.48 (m, 2H), 7.50 (dd, ^{3,4}J = 8.5, 1.7 Hz, 1H), 7.79-7.83 (m, 4H), 7.85-7.89 (m, 1H), 8.11 (s, 1H), 8.62 (dd, ^{3,4}J = 4.8, 1.7 Hz, 1H), 8.78 (dd, ⁴J = 2.2, 0.7 Hz, 1H); ¹³C-NMR (151 MHz, CDCl₃): δ = 54.31, 61.30, 68.41, 118.68, 122.10, 123.67, 123.89, 124.36, 125.93, 126.24, 127.74, 128.14, 128.15, 131.23, 132.77, 133.33, 136.24, 141.24, 147.88, 149.09, 149.49, 162.76, 163.99; ESI-MS: m/z 373.20 [M+H]⁺; HRMS (ESI): calculated for C₂₃H₂₁O₃N₂ m/z 373.15468 [M+H]⁺, found m/z 373.15468 [M+H]⁺.

(±)-(5-(3-Fluorophenyl)-2,4-dimethoxypyridin-3-yl)(naphthalen-2-yl)methanol (**1h**)



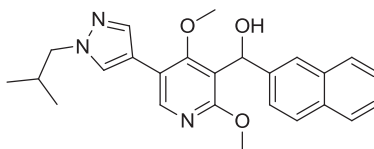
Colorless oil, 71%; R_f: 0.14 (20% ethyl acetate/petroleum ether); ¹H-NMR (400 MHz, CDCl₃): δ = 3.21 (s, 3H), 4.00 (s, 3H), 4.20 (bs, 1H), 6.44 (s, 1H), 7.04-7.10 (m, 1H), 7.24-7.32 (m, 2H), 7.37-7.49 (m, 3H), 7.52 (dd, ^{3,4}J = 8.4, 1.5 Hz, 1H), 7.78-7.85 (m, 4H), 8.10 (s, 1H); ¹³C-NMR (101 MHz, CDCl₃): δ = 54.24, 61.04, 68.47, 114.72 (d, ²J_{C,F} = 21.0 Hz), 115.83 (d, ²J_{C,F} = 22.0 Hz), 118.33, 123.84, 124.18 (d, ⁴J_{C,F} = 2.1 Hz), 124.37, 124.56 (⁴J_{C,F} = 2.9 Hz), 125.87, 126.19, 127.71, 128.08, 128.14, 130.39 (d, ³J_{C,F} = 8.4 Hz), 132.75, 133.33, 137.48 (d, ³J_{C,F} = 8.1 Hz), 141.38, 147.91, 162.35, 163.06 (d, ¹J_{C,F} = 246.4 Hz), 163.80; ESI-MS: m/z 390.20 [M+H]⁺; HRMS (ESI): calculated for C₂₄H₂₁O₃NF m/z 390.15000 [M+H]⁺, found m/z 390.15173 [M+H]⁺.

(±)-(5-(4-Chlorophenyl)-2,4-dimethoxypyridin-3-yl)(naphthalen-2-yl)methanol (**1i**)



Colorless oil, 78%; R_f: 0.15 (20% ethyl acetate/petroleum ether); ¹H-NMR (400 MHz, CDCl₃): δ = 3.19 (s, 3H), 4.00 (s, 3H), 4.23 (bs, 1H), 6.44 (s, 1H), 7.38-7.49 (m, 6H), 7.50-7.54 (m, 1H), 7.77-7.86 (m, 4H), 8.08 (s, 1H); ¹³C-NMR (101 MHz, CDCl₃): δ = 54.20, 60.97, 68.43, 118.33, 123.82, 124.17, 124.35, 125.85, 126.17, 127.69, 128.05, 128.11, 129.09, 130.11, 132.71, 133.31, 133.74, 133.88, 141.34, 147.80, 162.24, 163.77; ESI-MS: m/z 406.26 [M+H]⁺; HRMS (ESI): calculated for C₂₄H₂₁O₃NCl m/z 406.12045 [M+H]⁺, found m/z 406.12008 [M+H]⁺.

(±)-(5-(1-Isobutyl-1H-pyrazol-4-yl)-2,4-dimethoxypyridin-3-yl)(naphthalen-2-yl)-methanol (**1j**)

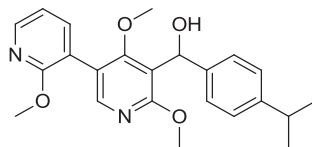


The crude product was purified by HPLC (method 1).

Colorless oil, 45%; R_f: 0.19 (50% ethyl acetate/petroleum ether); ¹H-NMR (400 MHz, CDCl₃): δ = 0.93 (d, ³J = 6.7 Hz, 6H), 2.18-2.29 (m, 1H), 3.41 (s, 3H), 3.93-3.97 (m, 5H), 6.38 (s, 1H), 7.42-7.47 (m, 2H), 7.50 (dd, ^{3,4}J = 8.5, 1.8 Hz, 1H), 7.67 (s, 1H), 7.77-7.83 (m, 5H), 8.21 (s, 1H); ¹³C-NMR (101 MHz, CDCl₃): δ = 20.03, 29.82, 54.11, 60.02, 60.72, 68.45, 114.84, 117.67, 118.67, 123.96, 124.52, 125.87,

126.17, 127.72, 128.06, 128.17, 128.35, 132.76, 133.33, 137.83, 141.38, 146.08, 161.58, 163.15; ESI-MS: m/z 418.19 $[M+H]^+$; HRMS (ESI): calculated for $C_{25}H_{28}O_3N_3$ m/z 418.21252 $[M+H]^+$, found m/z 418.21209 $[M+H]^+$.

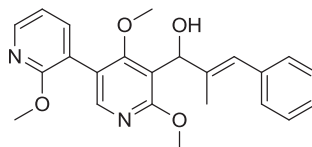
(±)-(4-Isopropylphenyl)(2',4,6-trimethoxy-[3,3'-bipyridin]-5-yl)methanol (**1m**)



Colorless oil, 47%; R_f : 0.15 (20% ethyl acetate/petroleum ether); 1H -NMR (500 MHz, $CDCl_3$): δ = 1.23 (d, 3J = 6.9 Hz, 6H), 2.84-2.92 (m, 1H), 3.24 (s, 3H), 3.94 (s, 3H), 3.98 (s, 3H), 4.08 (d, 3J = 11.8 Hz, 1H), 6.22 (d, 3J = 11.6 Hz, 1H), 6.96 (dd, 3J = 7.2, 5.0 Hz, 1H), 7.18 (d, 3J = 8.2 Hz, 2H), 7.30 (d, 3J = 8.0 Hz, 2H), 7.60 (dd, 3,4J = 7.3, 1.9 Hz, 1H), 8.02 (s, 1H), 8.20 (dd, 3,4J = 5.0, 1.9 Hz, 1H); ^{13}C -NMR (126 MHz, $CDCl_3$): δ = 24.14, 33.86, 53.79, 54.06, 60.85, 68.41, 116.94, 117.75, 118.68, 119.86, 125.77, 126.34, 139.80, 141.32, 146.81, 147.73, 148.56, 161.47, 162.25, 164.02; ESI-MS: m/z 395.17 $[M+H]^+$; HRMS (ESI): calculated for $C_{23}H_{27}O_4N_2$ m/z 395.19653 $[M+H]^+$, found m/z 395.19516 $[M+H]^+$.

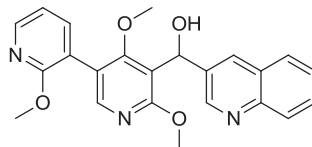
(To ensure that no palladium impurity remains with the molecule and influence the biological investigation, compound **1m** (33 mg) was dissolved in ethyl acetate (8 mL) and palladium scavenger SMOPEX 111 resin (165 mg) was added. The heterogeneous mixture was stirred at ambient temperature for 4 h. The mixture was then filtered and the filtrate was completely concentrated under reduced pressure. The residue was purified again by flash chromatography on silica gel as described above.)

(±)-(E)-2-Methyl-3-phenyl-1-(2',4,6-trimethoxy-[3,3'-bipyridin]-5-yl)prop-2-en-1-ol (**1n**)



Colorless oil, 85%; R_f : 0.21 (30% ethyl acetate/petroleum ether); 1H -NMR (500 MHz, $CDCl_3$): δ = 1.88 (s, 3H), 3.41 (s, 3H), 3.89-3.96 (m, 4H), 4.03 (s, 3H), 5.64 (d, 3J = 10.0 Hz, 1H), 6.58 (s, 1H), 6.98 (dd, 3J = 7.2, 5.1 Hz, 1H), 7.20 (t, 3J = 7.3 Hz, 1H), 7.23-7.27 (m, 2H), 7.32 (t, 3J = 7.6 Hz, 2H), 7.60 (dd, 3,4J = 7.2, 1.7 Hz, 1H), 8.03 (s, 1H), 8.22 (dd, 3,4J = 5.0, 1.6 Hz, 1H); ^{13}C -NMR (126 MHz, $CDCl_3$): δ = 15.39, 53.80, 54.07, 61.03, 71.32, 116.37, 116.95, 118.70, 119.97, 123.97, 126.41, 128.22, 129.12, 138.17, 139.46, 139.79, 146.87, 148.57, 161.54, 162.47, 164.40; ESI-MS: m/z 393.20 $[M+H]^+$; HRMS (ESI): calculated for $C_{23}H_{25}O_4N_2$ m/z 393.18088 $[M+H]^+$, found m/z 393.17957 $[M+H]^+$.

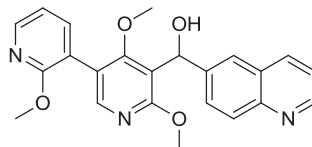
(±)-Quinolin-3-yl(2',4,6-trimethoxy-[3,3'-bipyridin]-5-yl)methanol (**1o**)



The crude product was purified by HPLC (method 3). The resulting trifluoroacetate salt was partitioned between ethyl acetate and aqueous 2M Na_2CO_3 solution (2:1 ratio v/v). The heterogeneous mixture was rapidly stirred at ambient temperature for 30 min. The organic layer was separated, washed with brine and dried over $MgSO_4$. The solvent was removed under reduced pressure to give the title product.

Colorless oil, 60%; R_f : 0.19 (3% methanol/dichloromethane); 1H -NMR (600 MHz, $CDCl_3$): δ = 3.28 (s, 3H), 3.93 (s, 3H), 3.95 (s, 3H), 4.34 (bs, 1H), 6.47 (s, 1H), 6.95 (dd, 3J = 7.3, 5.0 Hz, 1H), 7.52 (t, 3J = 7.5 Hz, 1H), 7.56-7.59 (m, 1H), 7.65-7.59 (m, 1H), 7.80 (d, 3J = 8.2 Hz, 1H), 8.03 (s, 1H), 8.09 (d, 3J = 8.5 Hz, 1H), 8.15 (s, 1H), 8.19-8.21 (m, 1H), 8.94 (s, 1H); ^{13}C -NMR (151 MHz, $CDCl_3$): δ = 53.83, 54.18, 60.91, 66.75, 116.10, 116.94, 118.51, 119.68, 126.92, 127.84, 127.95, 129.04, 129.38, 132.23, 136.79, 139.67, 146.99, 147.14, 149.37, 161.42, 162.04, 164.02; ESI-MS: m/z 404.19 $[M+H]^+$; HRMS (ESI): calculated for $C_{23}H_{22}O_4N_3$ m/z 404.16048 $[M+H]^+$, found m/z 404.15974 $[M+H]^+$.

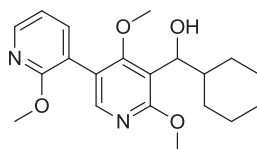
(±)-Quinolin-6-yl(2',4,6-trimethoxy-[3,3'-bipyridin]-5-yl)methanol (**1p**)



The crude product was purified by HPLC (method 3). The resulting trifluoroacetate salt was partitioned between ethyl acetate and aqueous 2M Na₂CO₃ solution (2:1 ratio v/v). The heterogeneous mixture was rapidly stirred at ambient temperature for 30 min. The organic layer was separated, washed with brine and dried over MgSO₄. The solvent was removed under reduced pressure to give the title product.

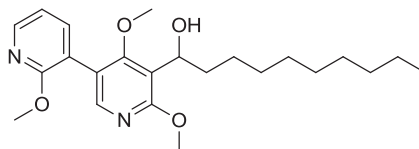
Colorless oil, 59%; R_f: 0.24 (2% methanol/dichloromethane); ¹H-NMR (600 MHz, CDCl₃): δ = 3.23 (s, 3H), 3.94 (s, 3H), 3.97 (s, 3H), 6.42 (s, 1H), 6.94-6.98 (m, 1H), 7.40 (dd, ³J = 8.2, 4.2 Hz, 1H), 7.59-7.61 (m, 1H), 7.74 (d, ³J = 8.8 Hz, 1H), 7.85 (s, 1H), 8.04 (s, 1H), 8.08 (d, ³J = 8.8 Hz, 1H), 8.16 (d, ³J = 8.2 Hz, 1H), 8.20 (d, ³J = 4.2 Hz, 1H), 8.87 (d, ⁴J = 3.8 Hz, 1H); ¹³C-NMR (151 MHz, CDCl₃): δ = 53.81, 54.15, 60.88, 68.10, 116.96, 117.06, 118.52, 119.85, 121.34, 123.70, 128.14, 128.29, 129.06, 136.67, 139.72, 142.71, 146.96, 147.27, 149.11, 149.94, 161.43, 162.18, 164.15; ESI-MS: *m/z* 404.23 [M+H]⁺; HRMS (ESI): calculated for C₂₃H₂₂O₄N₃ *m/z* 404.16048 [M+H]⁺, found *m/z* 404.15876 [M+H]⁺.

(±)-Cyclohexyl(2',4,6-trimethoxy-[3,3'-bipyridin]-5-yl)methanol (**1q**)



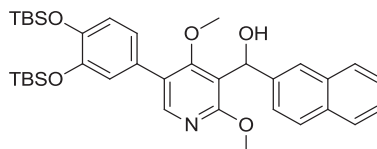
Colorless oil, 28%; R_f: 0.38 (50% ethyl acetate/petroleum ether); ¹H-NMR (400 MHz, CDCl₃): δ = 0.94-1.35 (m, 6H), 1.60-1.70 (m, 2H), 1.72-1.84 (m, 2H), 2.21 (d, ³J = 12.9 Hz, 1H), 3.28 (bs, 1H), 3.38 (s, 3H), 3.92 (s, 3H), 4.01 (s, 3H), 4.70 (d, ³J = 8.3 Hz, 1H), 6.96 (dd, ³J = 7.2, 5.0 Hz, 1H), 7.57 (dd, ^{3,4}J = 7.3, 1.9 Hz, 1H), 7.95 (s, 1H), 8.20 (dd, ^{3,4}J = 5.0, 1.9 Hz, 1H); ¹³C-NMR (101 MHz, CDCl₃): δ = 26.17, 26.34, 26.63, 29.70, 30.08, 43.96, 53.77, 53.91, 60.88, 72.33, 116.92, 117.16, 119.03, 119.68, 139.75, 146.74, 147.87, 161.54, 162.37, 164.20; ESI-MS: *m/z* 359.21 [M+H]⁺; HRMS (ESI): calculated for C₂₀H₂₇O₄N₂ *m/z* 359.19653 [M+H]⁺, found *m/z* 359.19672 [M+H]⁺.

(±)-1-(2',4,6-Trimethoxy-[3,3'-bipyridin]-5-yl)decan-1-ol (**1r**)



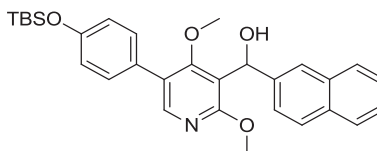
Colorless oil, 71%; R_f: 0.25 (30% ethyl acetate/petroleum ether); ¹H-NMR (500 MHz, CDCl₃): δ = 0.87 (t, ³J = 6.9 Hz, 3H), 1.20-1.37 (m, 13H), 1.46-1.57 (m, 1H), 1.68-1.76 (m, 1H), 1.87-1.96 (m, 1H), 3.36 (d, ³J = 10.3 Hz, 1H), 3.41 (s, 3H), 3.93 (s, 3H), 4.02 (s, 3H), 4.98-5.06 (m, 1H), 6.96 (dd, ³J = 7.2, 5.0 Hz, 1H), 7.57 (dd, ^{3,4}J = 7.3, 1.9 Hz, 1H), 7.96 (s, 1H), 8.20 (dd, ^{3,4}J = 5.0, 1.9 Hz, 1H); ¹³C-NMR (126 MHz, CDCl₃): δ = 14.25, 22.82, 26.37, 29.48, 29.66, 29.74, 29.79, 32.05, 37.69, 53.78, 53.91, 61.04, 67.70, 116.92, 118.34, 118.87, 119.89, 139.83, 146.75, 147.81, 161.53, 162.34, 163.62; ESI-MS: *m/z* 403.27 [M+H]⁺; HRMS (ESI): calculated for C₂₃H₃₅O₄N₂ *m/z* 403.25913 [M+H]⁺, found *m/z* 403.25559 [M+H]⁺.

(±)-(5-(3,4-Bis(*tert*-butyldimethylsilyloxy)phenyl)-2,4-dimethoxy-pyridin-3-yl)-(naphthalen-2-yl)methanol (**11**)



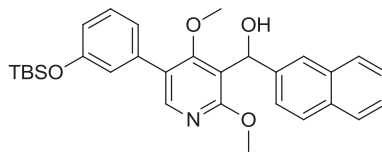
Colorless oil, 98%; R_f: 0.29 (20% ethyl acetate/petroleum ether); ¹H-NMR (400 MHz, CDCl₃): δ = 0.23 (s, 6H), 0.24 (s, 6H), 1.00 (s, 9H), 1.01 (s, 9H), 3.19 (s, 3H), 3.99 (s, 3H), 4.25 (d, ³J = 11.7 Hz, 1H), 6.43 (d, ³J = 11.4 Hz, 1H), 6.89 (d, ³J = 8.2 Hz, 1H), 6.95 (dd, ^{3,4}J = 6.8, 2.2 Hz, 1H), 7.00 (d, ⁴J = 2.1 Hz, 1H), 7.41-7.49 (m, 2H), 7.52 (dd, ^{3,4}J = 8.6, 1.6 Hz, 1H), 7.77-7.85 (m, 4H), 8.06 (s, 1H); ¹³C-NMR (101 MHz, CDCl₃): δ = -3.92, -3.90, 18.62, 26.07, 54.09, 60.58, 68.57, 118.03, 121.39, 121.72, 122.03, 123.85, 124.48, 125.09, 125.80, 126.14, 127.71, 128.00, 128.15, 128.44, 132.73, 133.36, 141.70, 146.82, 147.17, 147.77, 161.68, 163.82; ESI-MS: *m/z* 632.66 [M+H]⁺; HRMS (ESI): calculated for C₃₆H₅₀O₅NSi₂ *m/z* 632.32220 [M+H]⁺, found *m/z* 632.32227 [M+H]⁺.

(±)-(5-(4-(*tert*-Butyldimethylsilyloxy)phenyl)-2,4-dimethoxy-pyridin-3-yl)-(naphthalen-2-yl)methanol (**12**)



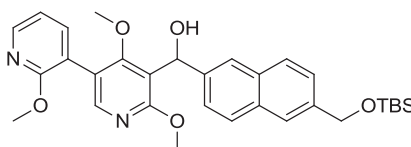
Colorless oil, 94%; R_f : 0.13 (10% ethyl acetate/petroleum ether); $^1\text{H-NMR}$ (500 MHz, CDCl_3): δ = 0.23 (s, 6H), 1.01 (s, 9H), 3.17 (s, 3H), 3.99 (s, 3H), 4.21 (d, 3J = 11.6 Hz, 1H), 6.42 (d, 3J = 11.2 Hz, 1H), 6.91 (d, 3J = 8.6 Hz, 1H), 7.37 (d, 3J = 8.6 Hz, 2H), 7.41–7.48 (m, 2H), 7.51 (dd, 3,4J = 8.5, 1.4 Hz, 1H), 7.77–7.84 (m, 4H), 8.07 (s, 1H); $^{13}\text{C-NMR}$ (126 MHz, CDCl_3): δ = -4.22, 18.40, 25.83, 54.09, 60.64, 68.61, 118.06, 120.52, 123.88, 124.51, 125.08, 125.81, 126.14, 127.73, 128.02, 128.17, 128.27, 130.05, 132.76, 133.40, 141.74, 147.83, 155.58, 161.77, 163.86; ESI-MS: m/z 502.21 $[\text{M}+\text{H}]^+$; HRMS (ESI): calculated for $\text{C}_{30}\text{H}_{35}\text{O}_4\text{NSi}$ m/z 502.24081 $[\text{M}+\text{H}]^+$, found m/z 502.24055 $[\text{M}+\text{H}]^+$.

(±)-(5-(3-((*tert*-Butyldimethylsilyloxy)phenyl)-2,4-dimethoxypyridin-3-yl)(naphthalen-2-yl)methanol (**13**)



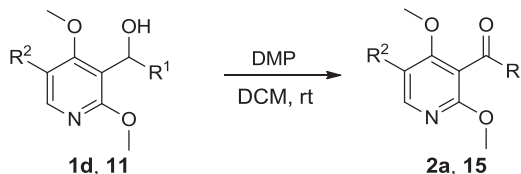
Colorless oil, 91%; R_f : 0.21 (15% ethyl acetate/petroleum ether); $^1\text{H-NMR}$ (400 MHz, CDCl_3): δ = 0.23 (s, 6H), 1.02 (s, 9H), 3.21 (s, 3H), 4.01 (s, 3H), 4.26 (bs, 1H), 6.45 (d, 3J = 8.2 Hz, 1H), 6.86–6.89 (m, 1H), 7.01–7.03 (m, 1H), 7.09–7.13 (m, 1H), 7.30 (t, 3J = 7.9 Hz, 1H), 7.42–7.50 (m, 2H), 7.53 (dd, 3,4J = 8.6, 1.8 Hz, 1H), 7.78–7.88 (m, 4H), 8.10 (s, 1H); $^{13}\text{C-NMR}$ (101 MHz, CDCl_3): δ = -4.25, 18.37, 25.82, 54.13, 60.79, 68.51, 118.04, 119.61, 120.65, 122.00, 123.83, 124.45, 125.05, 125.80, 126.13, 127.70, 128.01, 128.13, 129.84, 132.72, 133.34, 136.67, 141.60, 147.96, 156.05, 162.00, 163.84; ESI-MS: m/z 502.33 $[\text{M}+\text{H}]^+$; HRMS (ESI): calculated for $\text{C}_{30}\text{H}_{36}\text{O}_4\text{NSi}$ m/z 502.24081 $[\text{M}+\text{H}]^+$, found m/z 502.23993 $[\text{M}+\text{H}]^+$.

(±)-(6-(((*tert*-Butyldimethylsilyloxy)methyl)naphthalen-2-yl)(2',4,6-trimethoxy-[3,3'-bipyridin]-5-yl)methanol (**14**)



Pyridine **10a** (98 mg, 189 μmol), (4-((*tert*-butyldimethylsilyloxy)phenyl)boronic acid (60 mg, 390 μmol) and tetrakis triphenylphosphine palladium(0) (14 mg, 12 μmol , 6 mol%) were dissolved in a 4:1 mixture of toluene/ethanol (3.8 mL) and treated with Na_2CO_3 solution (2 M, 2.6 mL). The resulting mixture was degassed and refluxed for 14 h. After cooling to ambient temperature, ethyl acetate (50 mL) was added and the organic phase was separated and washed with water (10 mL) and brine (15 mL). The phase was dried over MgSO_4 and filtered through a small pad of celite. The filtrate was concentrated under reduced pressure and the residue was purified by flash chromatography on silica gel (30% ethyl acetate/petroleum ether).

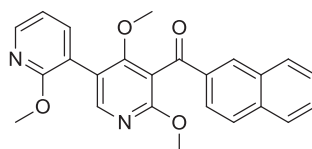
Colorless oil, 62%; R_f : 0.25 (33% ethyl acetate/petroleum ether); $^1\text{H-NMR}$ (600 MHz, CDCl_3): δ = 0.13 (s, 6H), 0.96 (s, 9H), 3.21 (s, 3H), 3.95 (s, 3H), 3.99 (s, 3H), 4.17 (bs, 1H), 4.88 (s, 2H), 6.40 (s, 1H), 6.97 (dd, 3J = 6.7, 5.5 Hz, 1H), 7.42 (d, 3J = 8.4 Hz, 1H), 7.50 (d, 3J = 8.6 Hz, 1H), 7.61 (d, 3J = 7.2 Hz, 1H), 7.74 (s, 1H), 7.78 (dd, 3,4J = 8.5, 3.9 Hz, 2H), 7.80 (s, 1H), 8.06 (s, 1H), 8.21 (d, 3J = 4.8 Hz, 1H); $^{13}\text{C-NMR}$ (151 MHz, CDCl_3): δ = -5.05, 18.62, 26.12, 53.87, 54.22, 60.91, 65.29, 68.51, 116.96, 117.64, 118.62, 119.93, 123.74, 124.28, 124.59, 124.99, 127.96, 128.14, 132.62, 132.68, 138.97, 139.80, 141.12, 146.85, 148.73, 161.46, 162.28, 164.26; ESI-MS: m/z 547.25 $[\text{M}+\text{H}]^+$; HRMS (ESI): calculated for $\text{C}_{31}\text{H}_{39}\text{O}_5\text{N}_2\text{Si}$ m/z 547.26228 $[\text{M}+\text{H}]^+$, found m/z 547.26193 $[\text{M}+\text{H}]^+$. *General Procedure III (GP III): Oxidation of Secondary Alcohols Using Dess-Martin-Periodinane (DMP).*



The secondary alcohol (1.0 eq.) was dissolved in dry dichloromethane (0.02–0.03 M) and DMP solution (15wt% in dichloromethane, 2.0–2.7 eq.) was added dropwise. The solution was stirred at ambient temperature for 1–2 h and quenched with sat. NaHCO_3 solution and ethyl acetate. The biphasic mixture was treated with solid $\text{Na}_2\text{S}_2\text{O}_3$ (75 mg/100 μL of DMP solution used) and stirred until both phases became clear. The aqueous phase was separated and extracted with ethyl acetate again. The combined organic phases were dried over MgSO_4 and the solvent was completely removed under reduced pressure. The product was isolated using flash chromatography on silica gel (ethyl acetate/petroleum ether).

Representative example:

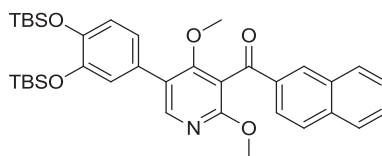
Naphthalen-2-yl(2',4,6-trimethoxy-[3,3'-bipyridin]-5-yl)methanone (**2a**)



1d (26 mg, 63.9 μmol) was dissolved in dry dichloromethane (2.6 mL) and DMP solution (15wt% in dichloromethane, 280 μL , 135 μmol) was added dropwise. The solution was stirred at ambient temperature for 1–2 h and quenched with sat. NaHCO_3 solution (10 mL) and ethyl acetate (30 mL). The biphasic mixture was treated with solid $\text{Na}_2\text{S}_2\text{O}_3$ (200 mg) and stirred until both phases became clear. The aqueous phase was separated and extracted with ethyl acetate (20 mL) again. The combined organic phases were dried over MgSO_4 and the solvent was completely removed under reduced pressure. The product was isolated using flash chromatography on silica gel (20% ethyl acetate/petroleum ether).

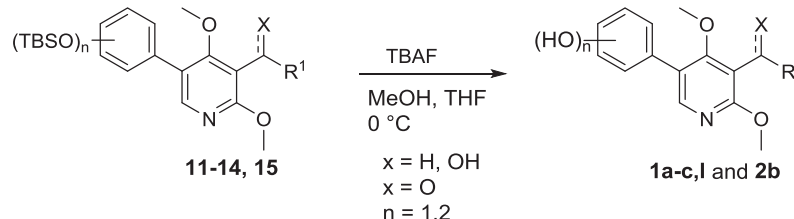
Colorless oil, 84%; R_f : 0.32 (33% ethyl acetate/petroleum ether); $^1\text{H-NMR}$ (500 MHz, CDCl_3): δ = 3.46 (s, 3H), 3.89 (s, 3H), 3.97 (s, 3H), 6.98 (dd, 3J = 7.2, 5.2 Hz, 1H), 7.52–7.57 (m, 1H), 7.59–7.64 (m, 2H), 7.90 (d, 3J = 8.2 Hz, 1H), 7.92–7.97 (m, 2H), 8.08 (dd, 3,4J = 8.6, 1.5 Hz, 1H), 8.15 (s, 1H), 8.21 (dd, 3,4J = 5.0, 1.9 Hz, 1H), 8.35 (s, 1H); $^{13}\text{C-NMR}$ (126 MHz, CDCl_3): δ = 53.82, 54.24, 60.93, 113.61, 116.91, 118.52, 119.48, 124.49, 126.94, 128.01, 128.74, 128.97, 129.94, 132.35, 132.77, 135.00, 136.19, 139.79, 146.79, 149.68, 161.65, 162.26, 163.87, 193.95; ESI-MS: m/z 401.52 $[\text{M}+\text{H}]^+$; HRMS (ESI): calculated for $\text{C}_{24}\text{H}_{21}\text{O}_4\text{N}_2$ m/z 401.14958 $[\text{M}+\text{H}]^+$, found m/z 401.14825 $[\text{M}+\text{H}]^+$.

(5-(3,4-Bis(*tert*-butyldimethylsilyloxy)phenyl)-2,4-dimethoxypyridin-3-yl)(naphthalen-2-yl)methanone (**15**)



Colorless oil, 84%; R_f : 0.20 (5% ethyl acetate/petroleum ether); $^1\text{H-NMR}$ (500 MHz, CDCl_3): δ = 0.22 (s, 6H), 0.24 (s, 6H), 1.00 (s, 9H), 1.01 (s, 9H), 3.42 (s, 3H), 3.89 (s, 3H), 6.90 (d, 3J = 8.2 Hz, 1H), 6.99 (dd, 3,4J = 8.2, 2.1 Hz, 1H), 7.03 (d, 4J = 2.0 Hz, 1H), 7.54 (t, 3J = 7.5 Hz, 1H), 7.61 (t, 3J = 7.5 Hz, 1H), 7.90 (d, 3J = 8.2 Hz, 1H), 7.93 (d, 3J = 8.5 Hz, 2H), 8.07 (dd, 3,4J = 8.6, 1.4 Hz, 1H), 8.19 (s, 1H), 8.32 (s, 1H); $^{13}\text{C-NMR}$ (126 MHz, CDCl_3): δ = -3.90, 18.63, 26.09, 54.17, 60.95, 114.89, 121.27, 122.02, 122.24, 124.41, 124.55, 126.91, 128.00, 128.12, 128.70, 128.91, 129.94, 132.25, 132.77, 135.04, 136.19, 146.91, 147.07, 149.04, 161.48, 163.57, 193.95; ESI-MS: m/z 630.72 $[\text{M}+\text{H}]^+$; HRMS (ESI): calculated for $\text{C}_{36}\text{H}_{48}\text{O}_5\text{NSi}_2$ m/z 630.30655 $[\text{M}+\text{H}]^+$, found m/z 630.30677 $[\text{M}+\text{H}]^+$.

General Procedure IV (GP IV): Removal of O-tert-Butyldimethylsilyl Group.

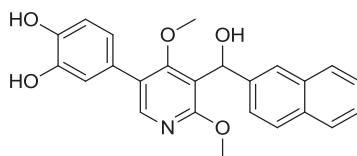


The *tert*-butyldimethylsilyl protected phenol (1.0 eq.) was dissolved in tetrahydrofuran (0.01–0.02 M) containing 1% methanol. The solution was cooled to 0°C and tetra-*n*-butylammonium fluoride solution (1 M in tetrahydrofuran, 2.0–3.0 eq.) was added. The mixture was stirred for 30–45 min (TLC control) at 0°C and quenched by addition of equal amounts of brine and NaHCO_3 solution (5%). The mixture was extracted two times with ethyl acetate and the combined organic phases were washed with brine and dried over MgSO_4 . The solvent was completely removed under reduced pressure and the residue was purified by flash chromatography on silica gel (methanol/dichloromethane).

For mono-protected phenols 2.0 eq. of tetra-*n*-butylammonium fluoride were used and 3.0 eq. for double protected phenols.

Representative example:

(±)-4-(5-(Hydroxy(naphthalen-2-yl)methyl)-4,6-dimethoxypyridin-3-yl)benzen-1,2-diol (**1a**)

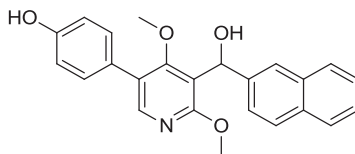


Pyridine **11** (20 mg, 32 μmol) was dissolved in tetrahydrofuran (3 mL) containing 1% methanol. The solution was cooled to 0°C and tetra-*n*-butylammonium fluoride solution (1 M in tetrahydrofuran, 96 μL , 96 μmol) was added. The mixture was stirred for 30 min (TLC control) and quenched by addition of brine (1.5 mL) and NaHCO_3 solution (5%, 1.5 mL). The mixture was extracted two times with ethyl acetate (15 mL) and the combined organic phases were washed with brine (10 mL) and dried over MgSO_4 . The solvent was completely removed under reduced pressure and the residue was purified by flash chromatography on silica gel (4% methanol/dichloromethane).

Colorless oil, 84%; R_f : 0.20 (4% methanol/dichloromethane); $^1\text{H-NMR}$ (600 MHz, CDCl_3): δ = 3.19 (s, 3H), 4.02 (s, 3H), 4.33 (bs, 1H), 6.43 (s, 1H), 6.89–6.94 (m, 2H), 6.99 (d, 4J = 1.9 Hz, 1H), 7.42–7.49 (m, 3H), 7.77–7.82 (m, 4H), 8.05 (s, 1H); $^{13}\text{C-NMR}$ (151 MHz, CDCl_3): δ = 54.68, 60.79, 68.61, 115.68, 115.72, 118.20, 121.58, 123.84, 124.28, 125.21, 125.97, 126.28, 127.44, 127.75, 128.16, 132.77,

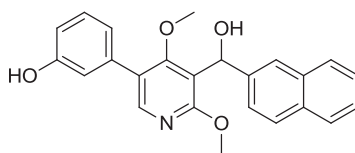
133.33, 141.09, 144.15, 144.34, 147.49, 161.64, 164.22; ESI-MS: m/z 404.52 [M+H]⁺; HRMS (ESI): calculated for C₂₄H₂₂O₅N m/z 404.14925 [M+H]⁺, found m/z 404.14817 [M+H]⁺.

(±)-4-(5-(Hydroxy(naphthalen-2-yl)methyl)-4,6-dimethoxy-pyridin-3-yl)phenol (**1b**)



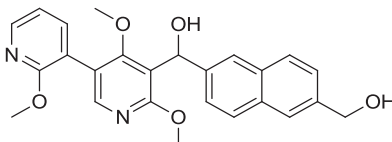
Colorless oil, 86%; R_f: 0.13 (2% methanol/dichloromethane); ¹H-NMR (500 MHz, CDCl₃): δ = 3.19 (s, 3H), 3.99 (s, 3H), 4.25 (d, ³J = 11.6 Hz, 1H), 5.40 (bs, 1H), 6.42 (d, ³J = 11.2 Hz, 1H), 6.90 (d, ³J = 8.6 Hz, 2H), 7.37 (d, ³J = 8.6 Hz, 2H), 7.41-7.48 (m, 2H), 7.51 (d, ³J = 8.6 Hz, 1H), 7.77-7.84 (m, 4H), 8.06 (s, 1H); ¹³C-NMR (126 MHz, CDCl₃): δ = 54.20, 60.72, 68.65, 115.88, 118.09, 123.90, 124.47, 125.01, 125.87, 126.19, 127.66, 127.74, 128.08, 128.18, 130.27, 132.79, 133.39, 141.55, 147.77, 155.62, 161.77, 163.90; ESI-MS: m/z 388.10 [M+H]⁺; HRMS (ESI): calculated for C₂₄H₂₂O₄N m/z 388.15433 [M+H]⁺, found m/z 388.15449 [M+H]⁺.

(±)-3-(5-(Hydroxy(naphthalen-2-yl)methyl)-4,6-dimethoxy-pyridin-3-yl)phenol (**1c**)



Colorless oil, 98%; R_f: 0.18 (3% methanol/dichloromethane); ¹H-NMR (400 MHz, CDCl₃): δ = 3.14 (s, 3H), 3.94 (s, 3H), 4.21 (bs, 1H), 6.07 (bs, 1H), 6.37 (s, 1H), 6.76-6.81 (m, 1H), 6.90-6.93 (m, 1H), 6.95-7.00 (m, 1H), 7.22 (t, ³J = 7.8 Hz, 1H), 7.35-7.45 (m, 3H), 7.70-7.77 (m, 4H), 8.02 (s, 1H); ¹³C-NMR (101 MHz, CDCl₃): δ = 54.42, 60.95, 68.58, 115.04, 115.77, 118.10, 121.21, 123.86, 124.38, 125.04, 125.90, 126.22, 127.74, 128.11, 128.16, 130.18, 132.76, 133.35, 136.75, 141.32, 147.84, 156.40, 162.05, 164.00; ESI-MS: m/z 388.20 [M+H]⁺; HRMS (ESI): calculated for C₂₄H₂₂O₄N m/z 388.15433 [M+H]⁺, found m/z 388.15499 [M+H]⁺.

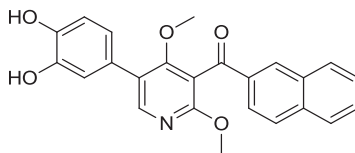
(±)-6-(6-(Hydroxymethyl)naphthalen-2-yl)(2',4,6-trimethoxy-[3,3'-bipyridin]-5-yl)-methanol (**11**)



To a solution of **14** (61 mg, 112 μmol) in dry tetrahydrofuran (7.6 mL, containing 1 Vol% methanol) at 0°C was added dropwise a solution of tetra-*n*-butyl ammonium fluoride (1 M in tetrahydrofuran, 222 μL, 222 μmol). The solution was stirred 45 min at 0°C and then at ambient temperature until reaction was completed (TLC control). Brine (2 mL) and NaHCO₃ solution (5%, 2 mL) were added and the mixture was extracted two times with ethyl acetate (2 x 10 mL). The combined organic phases were washed with brine (8 mL) and dried over MgSO₄. The solvent was completely removed under reduced pressure and the residue was purified by flash chromatography on silica gel (3% methanol/dichloromethane).

Colorless oil, 88%; R_f: 0.26 (4% methanol/dichloromethane); ¹H-NMR (600 MHz, CDCl₃): δ = 3.20 (s, 3H), 3.94 (s, 3H), 3.98 (s, 3H), 4.82 (s, 2H), 6.40 (s, 1H), 6.96 (dd, ³J = 7.3, 5.0 Hz, 1H), 7.45 (dd, ^{3,4}J = 8.4, 1.5 Hz, 1H), 7.50 (dd, ^{3,4}J = 8.6, 1.6 Hz, 1H), 7.59 (dd, ^{3,4}J = 7.3, 1.9 Hz, 1H), 7.74-7.82 (m, 4H), 8.04 (s, 1H), 8.21 (dd, ³J = 5.0, 1.9 Hz, 1H); ¹³C-NMR (101 MHz, CDCl₃): δ = 53.88, 54.25, 60.89, 65.49, 68.43, 116.96, 117.54, 118.57, 119.89, 123.71, 124.77, 125.27, 125.51, 127.98, 128.54, 132.65, 132.82, 138.45, 139.80, 141.51, 146.83, 148.72, 161.41, 162.22, 164.27; ESI-MS: m/z 433.19 [M+H]⁺; HRMS (ESI): calculated for C₂₅H₂₅O₅N₂ m/z 433.17580 [M+H]⁺, found m/z 433.17492 [M+H]⁺.

(5-(3,4-Dihydroxyphenyl)-2,4-dimethoxy-pyridin-3-yl)(naphthalen-2-yl)methanone (**2b**)

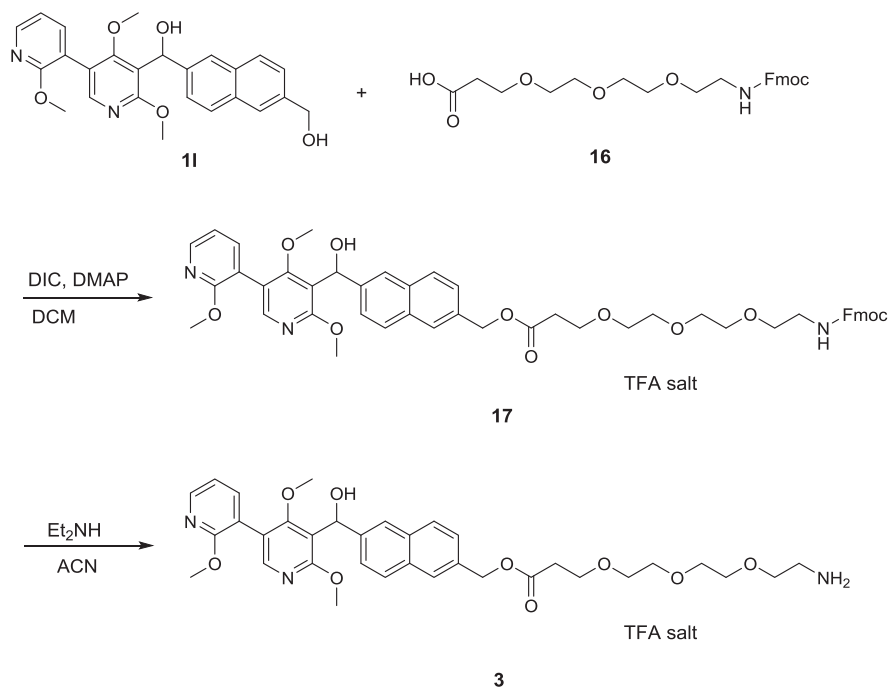


Colorless oil, 83%; R_f: 0.19 (4% methanol/dichloromethane); ¹H-NMR (600 MHz, CDCl₃): δ = 3.45 (s, 3H), 3.94 (s, 3H), 6.92-6.98 (m, 2H), 7.06 (d, ⁴J = 1.5 Hz, 1H), 7.52-7.57 (m, 1H), 7.60-7.65 (m, 1H), 7.90 (d, ³J = 8.0 Hz, 1H), 7.94 (d, ³J = 8.5 Hz, 2H), 8.05 (dd, ^{3,4}J = 8.6, 1.5 Hz, 1H), 8.19 (s, 1H), 8.32 (s, 1H); ¹³C-NMR (126 MHz, CDCl₃): δ = 55.26, 61.19, 114.89, 115.72, 116.17, 121.94, 124.37, 124.74, 126.91, 127.10, 128.05, 128.93, 129.19, 130.01, 132.43, 132.73, 134.74, 136.32, 144.11, 144.41, 147.65, 161.16, 164.30, 193.61; ESI-MS: m/z 402.55 [M+H]⁺; HRMS (ESI): calculated for C₂₄H₂₀O₅N m/z 402.13360 [M+H]⁺, found m/z 402.13252 [M+H]⁺.

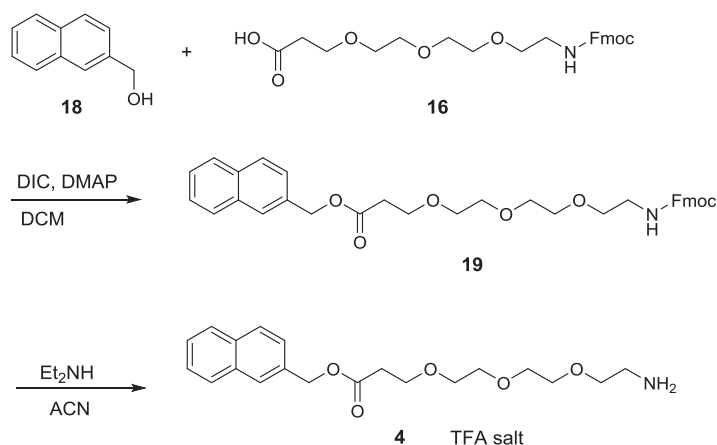
Synthesis of Pulldown Probes

Outline of the Synthesis of Pull Down Probes.

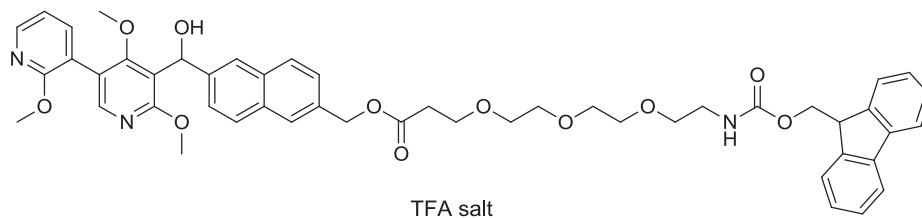
Active probe



Control probe



(±)-(6-(Hydroxy(2',4,6-trimethoxy-[3,3'-bipyridin]-5-yl)methyl)naphthalen-2-yl)methyl 1-(9H-fluoren-9-yl)-3-oxo-2,7,10,13-tetraoxa-4-azahexadecan-16-oate TFA salt (**17**)

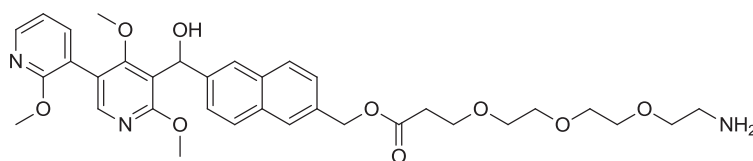


To a solution of pyridine **11** (51 mg, 117 μmol) in dry dichloromethane (4.3 mL), DMAP (3 mg, 24 μmol) and FmocNH-(PEG)-COOH **16** (52 mg, 117 μmol) were added. The solution was cooled to 0°C and treated with diisopropylcarbodiimide (18 μL , 117 μmol). The

mixture was slowly brought to ambient temperature overnight. After addition of dichloromethane (30 mL), the organic phase was washed with sat. NaHCO₃ solution (8 mL) and brine (8 mL) and dried over MgSO₄. The solvent was completely removed under reduced pressure and the crude product was purified by HPLC (method 3).

Colorless oil, 40%; R_f: 0.20 (3% methanol/dichloromethane) as free base; ¹H-NMR (600 MHz, CDCl₃): δ = 2.61-2.70 (m, 2H), 3.22 (s, 3H), 3.33-3.39 (m, 2H), 3.50-3.65 (m, 10H), 3.73-3.82 (m, 2H), 4.03 (s, 3H), 4.09 (s, 3H), 4.17-4.25 (m, 1H), 4.41 (d, ³J = 6.4 Hz, 2H), 5.27 (s, 2H), 5.59 (bs 1H), 6.45 (s, 1H), 7.10 (dd, ³J = 6.7, 5.8 Hz, 1H), 7.29 (t, ³J = 7.2 Hz, 2H), 7.38 (t, ³J = 7.2 Hz, 2H), 7.42-7.49 (m, 2H), 7.58 (d, ³J = 7.1 Hz, 2H), 7.71-7.85 (m, 7H), 8.14 (s, 1H), 8.32 (d, ³J = 5.3 Hz, 1H); ¹³C-NMR (151 MHz, CDCl₃): δ = 35.06, 41.03, 47.29, 55.28, 56.00, 61.36, 66.65, 67.03, 68.21, 68.23, 70.09, 70.30, 70.42, 70.53, 117.47, 118.62, 118.88, 119.68, 120.09, 123.69, 124.46, 125.13, 126.43, 127.22, 127.83, 128.40, 128.58, 132.58, 132.98, 133.55, 140.73, 141.35, 141.44, 143.94, 145.69, 146.55, 157.19, 160.87, 161.76, 165.96, 171.78; ESI-MS: *m/z* 857.86 [M+H]⁺; HRMS (ESI): calculated for C₄₉H₅₂O₁₁N₃ *m/z* 858.35964 [M+H]⁺, found *m/z* 858.36027 [M+H]⁺.

(±)-6-(Hydroxy(2',4,6-trimethoxy-[3,3'-bipyridin]-5-yl)methyl)naphthalen-2-yl)methyl 3-(2-(2-(2-aminoethoxy)ethoxy)ethoxy)propanoate TFA salt (**3**)

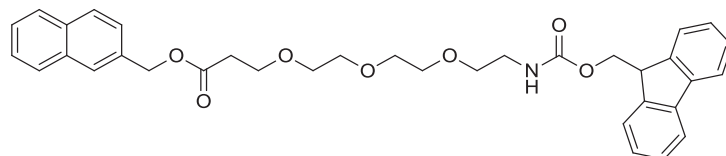


TFA salt

A solution of compound **17** (51 mg, 47 μmol) in dry acetonitrile (3.6 mL) was treated with diethylamine (700 μL) at ambient temperature. The reaction mixture was stirred overnight and then concentrated under reduced pressure (temperature should not exceed ambient temperature!). The crude product was purified by HPLC (method 3).

Colorless oil, 60%; ¹H-NMR (400 MHz, CDCl₃): δ = 2.66 (t, ³J = 5.8 Hz, 2H), 3.07-3.15 (m, 2H), 3.21 (s, 3H), 3.50-3.62 (m, 8H), 3.65-3.77 (m, 4H), 3.94 (s, 3H), 3.97 (s, 3H), 4.52 (bs, 3H), 5.26 (s, 2H), 6.39 (s, 1H), 6.97 (dd, ³J = 7.3, 5.0 Hz, 1H), 7.42 (dd, ^{3,4}J = 8.4, 1.3 Hz, 1H), 7.51 (dd, ^{3,4}J = 8.5, 1.3 Hz, 1H), 7.61 (dd, ^{3,4}J = 7.3, 1.9 Hz, 1H), 7.75-7.84 (m, 4H), 8.01 (bs, 2H), 8.05 (s, 1H), 8.21 (dd, ^{3,4}J = 5.0, 1.9 Hz, 1H); ¹³C-NMR (151 MHz, CDCl₃): δ = 35.00, 39.92, 53.91, 54.24, 60.92, 66.47, 66.95, 67.01, 68.38, 68.41, 70.08, 70.14, 70.30, 117.00, 117.43, 118.60, 119.90, 123.69, 124.99, 126.17, 127.27, 128.11, 128.67, 132.44, 133.03, 133.07, 139.84, 142.13, 146.87, 148.83, 161.44, 162.23, 164.24, 172.64; ESI-MS: *m/z* 636.17 [M+H]⁺; HRMS (ESI): calculated for C₃₄H₄₂O₉N₃ *m/z* 636.29156 [M+H]⁺, found *m/z* 636.29184 [M+H]⁺.

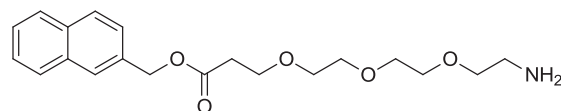
Naphthalen-2-ylmethyl-1-(9H-fluoren-9-yl)-3-oxo-2,7,10,13-tetraoxa-4-azahexadecan-16-ol (**19**)



To a solution of naphthalene-2-ylmethanol (25 mg, 158 μmol) in dry dichloromethane (3.3 mL), DMAP (2 mg, 16 μmol) and FmocNH-(PEG)-COOH **16** (70 mg, 158 μmol) were added. The solution was cooled to 0°C and treated with diisopropylcarbodiimide (24 μL, 158 μmol). The mixture was slowly brought to ambient temperature overnight. After adding dichloromethane (30 mL), the organic phase was washed with sat. NaHCO₃ solution (8 mL) and brine (8 mL) and dried over MgSO₄. The solvent was completely removed under reduced pressure and the residue was purified by flash chromatography on silica gel (50% ethyl acetate/petroleum ether).

Colorless oil, 74%; R_f: 0.20 (2% methanol/dichloromethane); ¹H-NMR (500 MHz, CDCl₃): δ = 2.66 (t, ³J = 6.3 Hz, 2H), 3.34-3.40 (m, 2H), 3.49-3.64 (m, 10H), 3.77 (t, ³J = 6.3 Hz, 2H), 4.21 (t, ³J = 6.7 Hz, 1H), 4.41 (d, ³J = 6.8 Hz, 2H), 5.29 (s, 2H), 5.42 (bs, 1H), 7.31 (t, ³J = 7.4 Hz, 2H), 7.39 (t, ³J = 7.4 Hz, 2H), 7.44 (d, ³J = 8.2 Hz, 1H), 7.46-7.51 (m, 2H), 7.60 (d, ³J = 7.5 Hz, 2H), 7.76 (d, ³J = 7.5 Hz, 2H), 7.79-7.85 (m, 4H); ¹³C-NMR (126 MHz, CDCl₃): δ = 35.23, 41.05, 47.40, 66.54, 66.64, 66.70, 70.12, 70.41, 70.55, 70.64, 120.04, 125.17, 125.95, 126.37, 126.40, 127.12, 127.41, 127.74, 127.79, 128.06, 128.44, 133.20, 133.27, 133.41, 141.41, 144.12, 156.62, 171.53; ESI-MS: *m/z* 584.07 [M+H]⁺; HRMS (ESI): calculated for C₃₅H₃₈O₇N *m/z* 584.26428 [M+H]⁺, found *m/z* 584.26533 [M+H]⁺.

Naphthalen-2-ylmethyl 3-(2-(2-(2-aminoethoxy)ethoxy)ethoxy)propanoate TFA salt (**4**)



CF₃COOH

A solution of compound **19** (39 mg, 67 μmol) in dry acetonitrile (5 mL) was treated with diethylamine (1 mL) at ambient temperature. The reaction mixture was stirred overnight and then concentrated under reduced pressure (temperature should not exceed ambient temperature!). The residue was purified by HPLC (method 3).

Colorless oil, 61%; $^1\text{H-NMR}$ (400 MHz, CDCl_3): δ = 2.68 (t, ^3J = 5.9 Hz, 2H), 3.04-3.16 (m, 2H), 3.49-3.64 (m, 8H), 3.67-3.80 (m, 4H), 5.29 (s, 2H), 7.44 (d, ^3J = 8.4 Hz, 1H), 7.46-7.52 (m, 2H), 7.79-7.88 (m, 4H), 8.06 (bs, 2H); $^{13}\text{C-NMR}$ (101 MHz, CDCl_3): δ = 35.03, 39.91, 66.48, 66.93, 67.03, 70.11, 70.14, 70.27, 125.93, 126.51, 126.52, 127.51, 127.84, 128.11, 128.56, 133.15, 133.24, 133.27, 172.67; ESI-MS: m/z 362.11 $[\text{M}+\text{H}]^+$; HRMS (ESI): calculated for $\text{C}_{20}\text{H}_{28}\text{O}_5\text{N}$ m/z 362.19620 $[\text{M}+\text{H}]^+$, found m/z 362.19671 $[\text{M}+\text{H}]^+$.

Preparation of Media Containing Wnt-3a Protein

To obtain medium containing the Wnt-3a protein (Wnt-3a conditioned medium), 2.5×10^5 L Wnt-3a cells were seeded into a 175cm^2 flask in the absence of selection antibiotic and incubated for four days. The medium was collected and replaced by fresh medium to allow the cells to grow for another three days. The media were combined and filtered through a $0.22\ \mu\text{M}$ filter. L cells were grown to obtain control medium without Wnt-3a protein (L conditioned medium).

Reporter Gene Assays

Screening Assay for Wnt Modulators

Wnt activity was analyzed using a human embryonic kidney cell line (HEK293) stably expressing a luciferase reporter gene under the control of a Wnt-responsive promoter and overexpressing the frizzled receptor (Park et al., 2006). Cells were activated by addition of Wnt conditioned medium which has been harvested from L cells overexpressing the Wnt-3a protein (L Wnt3A) (Willert et al., 2003). Control cells were treated with L-cell medium. 3000 cells per well of a 384 well plate were seeded and incubated with the compounds for 6 h. OneGlo Reagent (Promega) was added and the luminescence signal was read with a Spectramax Paradigm reader (Molecular Devices). As toxic compounds also lead to a decreased luciferase signal, cell viability was always assessed in parallel to the Wnt measurements. Therefore, a commercial reagent which measures the ATP content of the cells was used (Cell TiterGlo (Promega). Shortly, 1000 cells of the HEK293-Fz cell line were seeded per well of a 384-well plate. After 6 h treatment with the compounds, the luminescence signal was measured after addition of Cell Titer Glo Reagent. Dose response analyses were carried out using eight three-fold dilution steps starting from $30\ \mu\text{M}$. Compounds were dispensed using an Echo520 acoustic dispenser (Labcyte Inc.). IC_{50} values were calculated with Quattro/Workflow (quattro research GmbH). All measurements were done in triplicate.

Wnt (TCF/LEF) Reporter Gene Assay

Wnt3a/ β -catenin luciferase reporter gene assay was performed as described by Lanier et al (Lanier et al., 2012). Briefly, 3×10^6 HEK293T cells were transiently co-transfected in batch (T25 flask) using Lipofectamine 2000 (3:1 $[\mu\text{l}/\mu\text{g}$ DNA]) with a Wnt-3a-expressing vector (3 μg) for pathway activation, M50 Super8xTOPflash reporter vector (3 μg M50 Super 8x TOPFlash was a gift from Randall Moon (Addgene plasmid # 12456) (Veeman et al., 2003)), and the TK-driven *Renilla* luciferase co-reporter vector (0.3 μg , Promega, E2241). 8 h post transfection, 25,000 transfected cells were seeded in 96-well plates and treated with the compounds for 22 h. The activity of firefly and *Renilla* luciferase were determined by means of the Dual-Glo Luciferase Assay System (Promega). A derivative of the known Wnt pathway inhibitor IWR analog was employed as a control.

TGF β , Activin A or BMP-4 Inhibition

To measure TGF β or Activin A pathway inhibition, a SMAD-4 binding element (SBE-4)-based transient luciferase reporter gene assay was performed in HEK293T cells as described in detail before (Schade et al., 2012). Except for a different luciferase reporter vector, based on a BMP responsive element (BRE), the measurement of the BMP-4 pathway inhibition was done in the same manner. Here, 3×10^6 cells were co-transfected in batch (T25 flask) using Lipofectamine 2000 (3:1 $[\mu\text{l}/\mu\text{g}$ DNA]) with an SBE-4- or BRE-firefly luciferase (6 μg) and TK-driven *Renilla* luciferase plasmids (0.3 μg) (SBE4-Luc was a gift from Bert Vogelstein (Addgene plasmid # 16495) (Zawel et al., 1998); pGL3 BRE Luciferase was a gift from Martine Roussel & Peter ten Dijke (Addgene plasmid # 45126) (Korchynskyi and Ten Dijke, 2002)). Cells were replated 12 h post transfection to 96 well plates (25,000 per well) prior to induction with either 10 ng/ml TGF- β 2, Activin A or BMP-4 depending on the experimental setup. Compounds were added subsequently and cells were incubated for 22 h. The activity of the luciferase reporters were determined using the Dual-Glo Luciferase Assay System (Promega).

DHP-1 (inhibitor of TGF β) (Willems et al., 2012), SB-431542 (inhibitor of TGF β signaling) or DMH-1 (inhibitor of BMP-4 signaling) were employed as controls. Nonlinear regression analysis and IC_{50} determination was performed by means of the GraphPadPrism software.

GLI Dependent Reporter Gene Assay

3×10^4 SHH-LIGHT2 (Taipale et al., 2000) cells per well were seeded in triplicates in 96-well plates. After incubation overnight, cells were treated with the compounds in presence of $4\ \mu\text{M}$ purmorphamine to induce hedgehog signaling or DMSO as a control for 48h. Firefly and *Renilla* luciferase expression was detected by means of the Dual-Luciferase Reporter Assay System from Promega, using the Infinite $^{\text{M}}$ M200 plate reader (Tecan). The activity of firefly luciferase was normalized to the activity of *Renilla* luciferase in each sample and was then related to the activity of cells that were treated with purmorphamine and DMSO control (set to 100%). Vismodegib was employed as a positive control for Hedgehog pathway inhibition. Nonlinear regression analysis and IC_{50} determination was performed by means of the GraphPadPrism software.

Target Gene Expression Analysis Using Quantitative PCR

To study the expression of the Hedgehog target gene *Ptch1*, 2×10^4 NIH/3T3 cells were seeded per well in 24-well plates. After incubation overnight, cells were treated with the compound or DMSO as a control in presence of $2\ \mu\text{M}$ purmorphamine for 48 h. cDNA was prepared using the FastLane Cell cDNA Kit (Qiagen) following the manufacturer's instructions. The relative mRNA amount of the Hedgehog target gene *Ptch1* and the reference gene *Gapdh* was assessed in triplicates using the QuantiFast

SYBR Green PCR Kit (Qiagen) and the iQ™5 Real-Time PCR Detection System (Bio-Rad, Germany). The following oligonucleotides were used to detect mouse *Ptch1* and *Gapdh*: *Ptch1* (Lipinski et al., 2006): *Ptch1 F* 5'-CTCTGGAGCAGATTCCAAGG-3' / *Ptch1 R* 5'-TGCCGCAGTTCTTTTGAATG-3' and *Gapdh*: *Gapdh F* 5'-CAGTGCCAGCCTCGTC-3' / *Gapdh R* 5'-CAATCTCCACTTTGTC CACTG-3', respectively. The expression levels of *Ptch1* were determined using the $2^{-\Delta\Delta Ct}$ method. Values were normalized to the levels of *Gapdh* and related to the expression level in purmorphamine-activated cells, which was set to 100%.

To study the expression of the Wnt target gene *AXIN2*, HEK293 cells were seeded per well in a 6-well-plate. After overnight incubation, cells were treated with Wnt-3a conditioned medium and the compounds or DMSO as a control. As a negative control, cells were treated with L conditioned medium. After 24 h, cells were lysed and RNA was extracted using the RNeasy Mini Kit (Qiagen). 1 μ g RNA was reverse transcribed using the QuantiTect Reverse Transcriptase Kit (Qiagen). The relative mRNA amount of the Wnt target gene *AXIN2* (oligonucleotides *AXIN2 F* AGGGACAGGAATCATTGCGC and *AXIN2 R* GTGGACACCTGCCAGTTTCT) and the reference gene *GAPDH* (oligonucleotides *GAPDH F* TCAGCCGCATCTTCTTTTGCG) and *GAPDH R* GGCGCCAATACGACCAA) was assessed in triplicates using the SSO Advanced Universal SYBR Green Supermix (Bio-Rad) and the CFX96 Touch real time PCR detection system (Bio-Rad). The expression levels of *AXIN2* were determined using the $2^{-\Delta\Delta Ct}$ (Livak and Schmittgen, 2001). Values were normalized to the levels of *GAPDH* and related to the expression level in Wnt3a-activated cells (set to 100%).

In-Cell Western

The In-cell western was performed according to the previously published report. (Hannoush, 2008) Briefly, U-2OS cells were seeded in 384-well black clear bottomed plates (Corning) and grown overnight in a humidified atmosphere at 37°C and 5% CO₂. Upon compound treatment, cells were washed with phosphate-buffered saline (PBS) followed by 30 min fixation at room temperature with 3.7% paraformaldehyde (PFA) in PBS. Plates were then washed three times with PBS for 5 min prior to permeabilization with 0.1 % Triton X-100 in PBS for 5 min. Subsequently, cells were washed with PBS and blocked with Odyssey Blocking buffer (LI-COR Biosciences) overnight at 4°C. Afterwards plates were incubated with mouse anti- β -catenin antibody diluted at 1:200 in Odyssey Blocking buffer for 2 h at room temperature. Plates were then washed with 0.1% Tween-20 in PBS, and incubated for 1 h with an IRDye-800 CW-conjugated donkey anti-mouse secondary antibody solution (diluted 1:300) containing the DNA stain DRAQ5 (0.5 μ M) dilution. Plates were then washed and scanned using the Odyssey®IR Scanner (LI-COR). Scan settings were medium image quality, 169 μ m resolution, and intensity 7.0 for the 700- and 800-nm channels with a focus offset of 4.0. The normalized β -catenin protein levels were calculated after background subtraction (cells treated with only secondary antibody) by dividing the trimmed mean intensity for the β -catenin fluorescence (800 nm channel; pseudocolor) by the trimmed mean intensity of the DRAQ5 fluorescence (DNA counts) to account for well to well variations (700 nm channel; pseudocolor).

Human iPS Cell Culture and Cardiac Differentiation

The human iPS cell line has been produced from foreskin fibroblasts by following Melton's protocol (Huangfu et al., 2008) with three factors (OCT4, SOX2, and KLF4) and were kindly provided from the Boris Greber (Greber et al., 2011).

The generation of cardiomyocytes from hiPSCs was conducted in adaption to protocol of Rao et al. (2016). The maintenance of hiPSCs took place in monolayer culture in 6-well plate format. After 4 days of culture a fully confluent hiPSC layer was harvested using Accutase (Sigma), centrifuged at 200g for 2 min, resuspended in day 0 differentiation medium and seeded at 500,000 cells/2ml/well of a 24-well plate. Day 0 differentiation medium consisted of KnockOUT DMEM, 1x ITS-Mix (BD Corning), 10 μ M Y-27632 (Biotecne), 1x penicillin/streptomycin/glutamine (Thermo), 20 ng/ml FGF-2 (Peprotech), BMP-4 (Biotecne), and CHIR99021 (Selleckchem). Cardiac differentiation was promoted at 1 ng/ml BMP4 and 2 μ M CHIR99021. To constitute an even cell distribution and optimal attachment, plates were tapped a few times carefully under a stereo microscope and then left standing at room temperature for 20 min.

From day 1 onwards medium was exchanged on a daily basis. The basal differentiation medium consisted of Knockout™ DMEM, 1x TS (transferrin/selenium), 250 nM 2-phospho-ascorbate (Sigma-Aldrich), and 1x penicillin/streptomycin/glutamine. 100x TS stock was prepared in advance by dissolving 55 mg transferrin (Sigma) in 100 ml PBS containing 0.067mg sodium selenite (Sigma). WNT inhibitor Wnt-C59 (Biotecne) was applied at 1 μ M and added on days 2-3 after the initiation of differentiation.

One day prior seeding, the wells of 6-well or 24-well plate were coated with Matrigel™ (BD Corning, for 6-well plates: 1 ml of a 1:75 dilution of the stock, for 24-well plates: 0.5 ml of a 1:450 dilution of stock).

Flow Cytometry

Prior to FACS analysis, hiPSCs were dissociated into single cells using TrypLE™ select (1x) (Thermo Fisher Scientific) for 15-20 min at 37°C, 5% CO₂. Cells were then collected and fixed with 4% paraformaldehyde for 7-10 min at room temperature. Antibodies used were anti-cTnnT (1:200) and Alexa Fluor-488-conjugated goat anti-mouse (1:1000).

Blocking and antibody incubations were performed in Saponin solution (0.5% saponin / 2% FBS in DPBS). Cells were finally resuspended in Saponin solution and analyzed using BD LSRII flow cytometer. Values of cTnnT-positive cells were determined following pre-gating for intact single cells based on appropriate settings for forward and side scatter in FlowJo software.

Cell Transfection

To generate cells that stably express 5-LO U2OS cells were transfected by means of electroporation. For this, 1x10⁶ cells were mixed with 2 μ g pcDNA3.1-5-LO (Mahshid et al., 2015) or with pEGFP-C2-5-LO (Chen and Funk, 2001) and 100 μ l of Nucleofector solution V

(Amaxa Nucleofector Kit V). The cell/DNA suspension was transferred to a cuvette and the cuvette was inserted into the Nucleofector device. Cells were electroporated using Program X-001. Cells were transferred to a 10 cm dish and allowed to grow for two days later. Cells were then reseeded in medium containing 0.5 $\mu\text{g/ml}$ G418 to select for pools of stable transfectants.

Cell Lysate Preparation

Cells were harvested by trypsination and centrifugation. Cells were then washed twice with PBS and incubated in lysis buffer (50 mM PIPES, 50 mM NaCl, 5 mM MgCl_2 , 5 mM EGTA, 0.1% NP-40, 0.1% Triton X-100, 0.1% Tween 20, pH 7.4) at 4°C with frequent mixing for 30 min. Lysates were then passed five times through a 20G needle fitted to a syringe. Finally, centrifugation for 20 min at 18,500 x g was used to remove cell debris.

Identification of Proteins Binding to Lipoxygenin

Pulldown

NHS activated magnetic sepharose beads (GE Healthcare) (25 μl) were washed with 500 μl of 1 mM ice-cold HCl and incubated with 10 μM active (compound **3**) or inactive probe (compound **4**) in coupling buffer (0.15 M triethanolamine, 0.5 M NaCl pH 8.3) for 2 h at room temperature. The beads were blocked alternatively with the blocking buffers A (0.5 M ethanol amine, 0.5 M NaCl, pH 8.3) and B (0.1 M sodium acetate, 0.5 M NaCl, pH 4.0) three times each followed by washing with lysis buffer. Afterwards, beads were incubated for 2 h at 4°C with 2 mg/ml U2OS cell lysate. Beads were then washed once at 4°C for 10 min with PBS containing 75 mM MgCl_2 and two times with PBS at 4°C for 10 min. Afterwards, the beads were incubated for 1 h at room temperature with 100 μl elution buffer 1 (2 M urea in 50 mM Tris (pH 7.5), 1 mM DTT, 5 $\mu\text{g/ml}$ trypsin). Then the beads were washed with 100 μl elution buffer 2 (2 M urea in 50 mM Tris (pH 7.5), 5.5 μM chloroacetamide) for 2 min at RT in thermomixer. Both extracts were combined and incubated overnight at room temperature. Tryptic digest was terminated by adding 2 μl TFA. Each sample was purified using STAGE-tips (C18) (Empore 2215-C18). Briefly, the discs were activated with methanol and equilibrated with an aqueous solution of formic acid (0.1%). After elution of the tryptic peptides from the C18 filter disks and vacuum dry, peptides were separated and analyzed by nano-HPLC/MS/MS.

For detection of target proteins after the pulldown using immunoblotting, the NHS magnetic sepharose beads (25 μl , GE Healthcare) were treated with the probes and blocked as described above. Afterwards, beads were incubated for 1 h with purified 5-LO (10 mg/l) or U-2OS cell lysate and different concentrations of the compound for 2 h at 4°C. Beads were then washed once with PBS containing 75 mM MgCl_2 followed by two wash steps in PBS for 10 min. Proteins were released from the beads by heating at 95°C for 5 min in Laemmli buffer prior immunoblotting.

Mass Spectrometry

After tryptic digestion and purification, the protein fragments were analyzed by nano-HPLC/MS/MS using an Ultimate™ 3000 RSLC nano-HPLC system and a Q Exactive™ Hybrid Quadrupole-Orbitrap mass spectrometer equipped with a nano-spray source (all ThermoFisher Scientific). Briefly, the lyophilized tryptic peptides were dissolved in 20 μl 0.1 % TFA and 3 μl of these samples were injected and enriched onto a C18 PepMap 100 column (5 μm , 100 Å, 300 μm ID * 5 mm, Dionex, Germany) using 0.1 % TFA and a flow rate of 30 $\mu\text{l}/\text{min}$ for 5 min. Subsequently, the peptides were separated on a C18 PepMap 100 column (3 μm , 100 Å, 75 μm ID * 25 cm) using a linear gradient starting with 95 % solvent A/5 % solvent B and increasing to 68.0 % solvent A/32.0 % solvent B in 185 min with a flow rate of 300 nL/min (solvent A: water containing 0.1 % formic acid, solvent B: acetonitril containing 0.1 % formic acid). The nano-HPLC was online coupled to the Q Exactive mass spectrometer using a standard coated Pico Tip emitter (ID 20 μm , Tip-ID 10 μm , New Objective, Woburn, MA, USA). Mass range of m/z 300 to 1650 was acquired with a resolution of 70000 for full scan, followed by up to ten high energy collision dissociation (HCD) MS/MS scans of the most intense at least doubly charged ions with a resolution of 17500.

Protein identification and relative quantification were performed using MaxQuant v.1.3.0.3 (Cox and Mann, 2008) including the Andromeda search algorithm and searching the human reference proteome of the uniprot database. Briefly, a MS/MS ion search was performed for full enzymatic trypsin cleavages allowing two miscleavages. For protein modifications carbamidomethylation was chosen as fixed and oxidation of methionine and acetylation of the N-terminus as variable modifications. The mass accuracy was set to 20 ppm for the first and 6 ppm for the second search. The false discovery rates for peptide and protein identification were set to 0.01. Only proteins for which at least two peptides were quantified were chosen for further validation.

Relative quantification of proteins was carried out using the label-free quantification algorithm implemented in MaxQuant. All experiments were performed in technical quadruplets. Label-free quantification (LFQ) intensities were logarithmized (log2) and samples resulting from affinity purification using the active molecule bound to solid support were grouped together and samples resulting from affinity purification using the inactive control molecule bound to solid support as well. Proteins which were not at least two times quantified in at least one of the groups were filtered off. Missing values were imputed using small normal distributed values (width 0.3, down shift 1.8, imputation was performed separately for each column) and a two-sided t-test ($s_0 = 0$, FDR = 0.05) was performed. Proteins which were statistically significant outliers and enriched in the samples resulting from affinity enrichment using the active molecule bound to the solid support were considered as hits

Cheminformatic Analysis of Protein Targets for Small Molecules

We used the SPIDER (*self-organizing map-based prediction of drug equivalence relationships*) (Reker et al., 2014b) software tool for predicting potential targets of compound **1** (www.cadd.ethz.ch/software/spider.html). The two-dimensional query structure was

used as input without further modification. The resulting target list was sorted according to increasing *p*-values of the predictions, with a maximal *p*-value of 0.05 (5% potential false-positive).

Immunoblotting

Proteins were resolved using SDS polyacryl amide gel electrophoresis (SDS-PAGE) using 10 % gels prior to transfer to PVDF membrane by means of semi-dry blotting. Membranes were then incubated in LI-COR blocking buffer prior to incubation with the primary antibodies (anti- β -catenin, anti-GAPDH) overnight at 4°C followed by exposure to the secondary antibodies (anti-rabbit or anti-mouse IRDye 800CW / 680RD) for 1 h at room temperature. Detection of the secondary antibodies was performed with the LI-COR Odyssey Fc system and Image Studio software (LI-COR).

Purification of PP1 and PP1 Activity Assay

Expression and Purification of Human Recombinant PP1 from *E. coli*

Human protein phosphatase 1A (PP1A) ORF was cloned into pET22b. PP1A was expressed in BL21(DE3)RIL cells. Cells were grown at 37°C before induction with 0.1 mM IPTG and further incubation at 18°C for 20 h. Cells were harvested, lysed, centrifuged prior to loading the supernatant onto Ni-NTA column. Upon washing proteins were eluted with 500 mM imidazol and elution fractions were dialysed using 50 mM Tris (pH 7.5), 200 mM NaCl, 100 μ M MnCl₂, 10% glycerol and 5 mM DTT.

PP1 Activity Assay

Human protein phosphatase 1 (250 μ g/ml) was incubated in assay buffer containing 40 mM Tris (pH 8.1), 30 mM MgCl₂, 20 mM KCl, 0.025% NP40 and freshly added 5 mM DTT) with different concentration of Lipoxygenin or 1 μ M okadaic acid or DMSO as controls for 30 min at 37°C followed by addition of 2 mM *para*-nitrophenylphosphate (*p*-NPP). Relative PP1 inhibition was measured at 405 nm over 30 min kinetic cycle in an Infinite M200 plate reader.

PPT1 Activity Assay

The activity of PPT1 was determined in lysates of U2-OS cells (Van diggelen et al., 1999). Lysates were incubated with the PPT1 substrate 4-methylumbelliferyl-6-thio- β -D-glucopyranoside (MU-6-thio-b-glucoside, 0.64 mM), 0.8 U β -glucosidase in *Mcllvains* phosphate/citric-acid buffer (pH 4) supplemented with 15 mM DTT and 0.38% Triton X100 for 1 h at 37°C. The reaction was terminated by addition of 0.5 M Na₂CO₃/NaHCO₃ containing 0.025% Triton X-100 to release the fluorescent 4-methylumbelliferone, which was detected at ex/em 365/445 nm in an Infinite M200 plate reader. The PPT1 inhibitor HDSF was used as a control.

DCK Activity Assay

The DCK assay was performed by NovoCIB. Briefly, 5mU/ml human recombinant dCK was preincubated with the compound for 15 min at 37°C in a buffer containing 100 mM Tris-HCl, 250 mM KCl, 10 mM MgCl₂, 0.5 mg/ml BSA, 5 mM NAD, 0.5 mM inosine, 30 mU/ml IMPDH. The reaction was initiated by addition of ATP (125 μ M final concentration). Absorbance at 340 nm was monitored every minute for 30 min at 37°C.

Purification of 5-LO and 5-LO Activity Assays

Expression and Purification of Human Recombinant 5-LO from *E. coli*

Human recombinant 5-LO-wt (r5LO-wt) was expressed in *E. coli* BL21-CodonPlus (DE3)-RILP cells using the plasmid pT3-ALOX5 as described previously (Fischer et al., 2003; Schröder et al., 2014). After growing BL21 cells for 5 hours at 37°C, 0.2 mM IPTG (isopropyl-thio- β -D-galactopyranoside) was added and the protein expression occurred for 18 hours at 22°C. Cells were harvested, lysed, homogenized by sonication and centrifuged at 100,000 \times g for 70 minutes at 4°C. The supernatant, containing the enzyme was then purified by ATP affinity chromatography and anion exchange chromatography on an ÄKTA express system (GE Healthcare, Sweden) by loading on an ATP agarose column and eluting with 50 mM phosphate/1 mM EDTA/20 mM ATP pH 7.4. Following this step, the eluate was run through a ResourceQ 1 mL column (GE Healthcare, Sweden) and eluted with 50 mM phosphate/1 mM EDTA/0.5 mM NaCl pH 7.4.

5-LO Activity Assay Using Recombinant Protein

3 μ g of purified 5-LO was added to a solution of PBS/EDTA with 1 mM ATP for a final volume of 1 mL. Samples were supplemented with Glutathion peroxidase (GPx-1, Sigma-Aldrich) (30 mU) and GSH (1 mM) as indicated. The test compound was added to the solution and incubated for 15 minutes on ice, warmed for 30 seconds at 37°C, followed by the addition of 4 arachidonic acid and 2 mM CaCl₂. After 10 minutes, the reaction was stopped with 1 mL ice-cold methanol. The 5-LO product formation was analyzed as in intact cells (see below).

5-LO Activity Assay in Cells

Human polymorphonuclear leukocytes (PMNL) were isolated from buffy coats obtained from the German Red Cross (DRK Blood Donation Service Baden-Württemberg-Hessen, Frankfurt am Main, Germany). PMNL were isolated via dextran sedimentation, centrifugation and hypotonic lysis to separate erythrocytes as described previously (Werz et al., 2002). To measure 5-LO product formation, PMNL (5 \times 10⁶ cells/mL; purity >95%) were suspended in PBS pH 7.4 containing 1 mg/mL glucose and 1 mM CaCl₂ (PGC buffer). Subsequently, cells were incubated with the compounds for 15 min at 37°C. Next, A23187 (2.5 μ M) was added and after 3 min arachidonic acid (AA) was supplemented. The sample was further incubated for 10 min. The addition of 1 mL of ice-cold methanol stopped the reaction and the samples were analyzed via HPLC following solid phase extraction as described previously (Werz and

Steinhilber, 1996). The 5-LO products per 10^6 cells were declared in nanograms and include LTB_4 and 5(S)-hydro(pero)xy-6-trans-8,11,14-cis-eicosatetraenoic acid (5-H(p)ETE).

5-LO Activity Assays in Cell Homogenates

7.5×10^6 PMNL were centrifuged at $900 \times g$ for 20 minutes and the pellets were resuspended in 1 mL of PBS plus 1 mM EDTA. The suspension was sonicated three times for 10 s each on ice and 1 mM ATP was added. This preparation was centrifuged at $10,000 \times g$ for 10 minutes to remove intact cells, mitochondria and nuclei. The test compound was added and incubated on ice for 10 min. Samples were then warmed for 30 s at 37°C before the reaction began because of the addition of $20 \mu\text{M}$ AA and 2 mM CaCl_2 . The reaction was stopped after 10 min with the addition of 1 mL of ice-cold methanol. The 5-LO product formation was measured as described for intact cells.

Immunofluorescence

65,000 U-2OS cells were seeded on cover slips (diameter 12 mm) in 24-well plates. After incubation overnight, cells were treated with inhibitors overnight. Cells were then washed with PBS containing 1 mg/ml glucose and 1 mM calcium chloride (PCG buffer), fixed with 4 % formaldehyde in PCG, washed with PBS and PBS containing 0.3 M glycine, permeabilized with Triton X-100 (0.1 % in PBS), washed with Tween-20 (0.05 % in PBS) and PBS. BSA (2% in PBS, 0.1 % Tween 20) was used for blocking (1 h, room temperature). Incubation with the primary antibody (anti- β -catenin, anti-5-LO or anti-FLAG antibody in 2 % BSA, 0.1 Tween-20 in PBS) was performed overnight at 4°C . After washing, the samples were incubated with the secondary antibody (anti-mouse Alexa Fluor-488) for 1 h at room temperature. Samples were stained in parallel with DAPI and after washing mounted on glass slides using Aqua Poly/Mount (Polysciences Inc.) mounting medium. Images were acquired on a Zeiss Observer Z1 microscope with 63x oil objective and image analysis was performed using ImageJ (Rasband, 1997-2016).

Proximity Ligation Assay (PLA)

To investigate the interaction between 5-LO and β -catenin, the Duolink PLA Red Kit was used. Briefly, 1×10^5 cells were seeded on 12 mm cover slips in a 24-well-plate. After 24 h, cells were treated with L or Wnt-3a conditioned medium and/or inhibitor for another 24 h. Cells were fixed using 4% paraformaldehyde in PBS for 10 min. To stain the cell membranes, samples cells were treated with Alexa488-WGA (final concentration $5 \mu\text{g/ml}$, 10 min) prior to permeabilisation with Triton X-100 (0.1 % in PBS). Blocking was performed using BSA (2% in PBS with 0.1 % tween20) for 1 h at room temperature. Incubation with the primary antibodies was performed overnight at 4°C . Following primary antibodies were used: mouse anti-5-LO (1:1000) and rabbit anti- β -catenin (1:2000).

Binding of PLA probes, ligation and amplification were performed according to the manufacturer's instructions. Cover slips were mounted on glass slides using Aqua Poly/Mount mounting medium (Polysciences Inc.). Images were acquired in a Zeiss Observer Z1 microscope with 63 x oil objective and image analysis was performed using ImageJ. For analysis, cells membranes were marked and the PLA spots counted per cell using a modified "analyze particles" macro. For evaluation, cells were analyzed from at least five images per condition.

QUANTIFICATION AND STATISTICAL ANALYSIS

Data from independent experiments (n) are presented as mean values \pm standard deviation (SD). N is the number of technical replicates and n is the number of biological replicates. Data fitting performed using GraphPad Prism 6.0. Statistical analysis was performed using unpaired t test with Welch's correction (GraphPad Prism 6.0).